Lund University • Sweden
Lund Institute of Technology
Department of Building Science
Report TABK--98/3051

Heat Flows in a Full Scale Room Exposed to Natural Climate

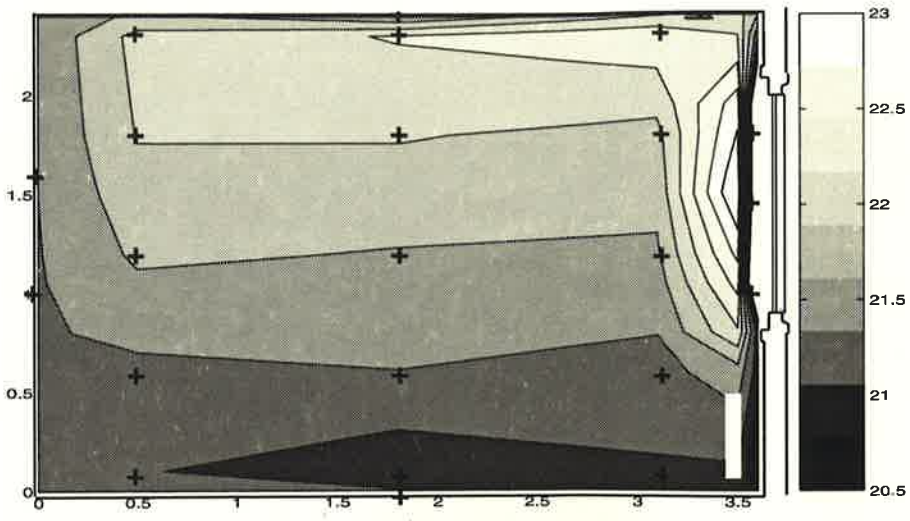

Petter Wallentén

Building Science

Lund University

Lund University, with eight faculties and a number of research centres and specialized institutes, is the largest establishment for research and higher education in Scandinavia. The main part of the University is situated in the small city of Lund which has about 97 600 inhabitants. A number of departments for research and education are, however, located in Malmö. Lund University was founded in 1666 and has today a total staff of 5 850 employees and 38 200 students attending 50 degree programmes and 850 subject courses offered by 170 departments.

Department of Building Science

The Department of Building Science is part of the School of Architecture within the Faculty of Technology. The Department has two professorial chairs, Building Science and Building Services. Research at the Department is concentrated on energy management, climatic control and moisture problems. The main areas of research are:

- design and preformance of new low-energy buildings
- energy conservation in existing buildings
- utilization of solar heat
- climatic control
- climatic control in foreign climates
- moisture research

Heat Flows in a Full Scale Room Exposed to Natural Climate

Petter Wallentén

This report relates to Research grant No 960480-8 from the Swedish Council for Building Research to the Department of Building Science, Lund University, Lund Institute of Technology, Lund, Sweden.

Keywords

convective, heat transfer coefficient, window, wall, measurements, finite difference , frequency analysis, transient, shortwave, longwave, radiation exchange, temperature, building, solar radiation, window model.

Printed by KFS AB, Lund 1998

Report TABK--98/3051
Heat Flows in a Room Exposed to natural Climate

Lund University, Lund Institute of Technology,
Department of Building Science, Lund, Sweden.

ISSN 1103-4467
ISRN LUTADL/TABK--3051--SE

Lund University,
Department of Building Science
P.O. Box 118
SE-221 00 LUND
Sweden

Telephone: + 46 46 222 73 45
Telefax: + 46 46 222 47 19
E-mail: bkl@bkl.lth.se
Homepage: http://www.bkl.lth.se

Contents

Nomenclature

a	in chapter 4 absorbed part of solar radiation	(-)
	else thermal diffusivity $a=\lambda / (\rho\, c_p)$	(m^2/s)
A_i	area or surface nr i	(m^2)
c_p	specific heat at constant pressure	(J/kg K)
C	heat capacity per unit area	(J/m^2K)
d	distance or thickness	(m)
d_{bl}	thickness of thermal boundary layer	(m)
D	diameter of the thermocouple	(m)
f	factor used in comparison with equation (5.10)	(-)
$F_{i,j}$	viewfactor between surface i and j	(-)
F	viewfactor matrix	(-)
g	acceleration due to gravitation	(m/s^2)
g^{ij}_{kl}	complex elements in transfer function matrix	
G^i_j	transfer function between layer i and j	(W/m^2K)
$G^{in}_{hfm,in}$	transfer function from inside to the surface of the heat flow meter	(W/m^2K)
G^{in}_{hfm}	transfer function from inside as measured by the heat flow meter	(W/m^2K)
G_i	total incoming radiation (per unit area)	(W/m^2)
$\mathbf{G}_n(\omega)$	transfer function matrix from layer n to n+1.	
Gr or Gr_H	Grashof number=$g\, \beta\, \Delta\, T\, H^3 / \nu^2$	(-)
h_c	generally the mean convective heat transfer coefficient, except when referring to	

	measured values when it is the local convective heat transfer coefficient	(W/m^2K)
h_c^*	calculated local convective heat transfer coefficient	(W/m^2K)
h_r	heat transfer coefficient for longwave radiation	(W/m^2K)
h_{tot}	total heat transfer coefficient = $h_c + h_r$	(W/m^2K)
$h^{2\text{-}1}{}_c$	convective/conductive heat transfer coefficient between pane 2 and 1	(W/m^2K)
$h^{2\text{-}1}{}_r$	radiation heat transfer coefficient between pane 2 and 1	(W/m^2K)
H_c	convective heat transfer coefficient per meter thermocouple	(W/m K)
H_r	radiation heat transfer coefficient per meter thermocouple	(W/m K)
H	height of wall or window	(m)
J_i	total radiation (per unit area) leaving the surface	(W/m^2)
J	radiation matrix in section 7.2	(W/m^2)
N	number of ..	(-)
Nu^*	local Nusselt number = $q_c(x)x/\Delta T$	(-)
Nu	mean Nusselt number = $q_c H/\Delta T$	(-)
Pr	Prandtl number = $\nu/a = \mu\, c_p/\lambda$	(–)
r	reflected part of solar radiation	(-)
Ra	Rayleigh nember = Gr Pr	(-)
Re	Reynolds number = $\bar{u}H/\nu$	(–)
q	heat transfer	(W/m^2)
q_r	longwave radiation heat transfer	(W/m^2)
q_{cond}	conductive heat transfer in material	(W/m^2)

q_c	convective heat transfer	(W/m^2)
q_{abs}	absorbed shortwave radiation	(W/m^2)
q_{hfm}	heat flow as measured by the heat flow meter (used in calculations)	(W/m^2)
$q_{measured}$	heat flow measured by the heat flow meter	(W/m^2)
Q_i	net heat flow to surface i	(W)
t	time	(s)
t_p	period time	(s)
T	temperature	(K)
T_a	air temperature	(K)
T^a_{in}	amplitude if inner surface variation	(K)
T^a_{out}	amplitude of outer surface variation	(K)
T_{ref}	reference (air) temperature	(K)
T_{surf}	surface temperature	(K)
T_r	surrounding mean radiation temperature	(K)
T_t	thermocouple temperature	(K)
T_{wall}	wall temperature.	(K)
T_w	window pane temperature in section .8.2.4.	(K)
T^+	dimensionless temperature $T^+ = \rho c u_\tau \frac{T_{wall} - T(y)}{q_c}$	(-)
T	"temperature" matrix used in section 7.2	(W/m^2)
u	air velocity	(m/s)
u^+	dimensionless velocity = u/u_τ	(-)
u_τ	friction velocity:	(m/s)
v	air velocity in section 8.2.4	(m/s)
W	width of air gap between the panes	(m)
x	length scale	(m)
y^+	local Reynolds number:	

$$y^+ = \frac{y u_\tau}{\nu} \qquad (-)$$

y	length scale	(m)
α	shortwave absorption coefficient for the metal	(-)
β	thermal expansion coefficient = 1/T (for air)	(K^{-1})
$\delta_{i,j}$	= 0 if $i \neq j$ else 1	
δt	time step in finite difference model	(s)
δh_c	estimated error in convective heat transfer measurement	(W/m^2K)
$\delta\Delta T$	estimated error in temperature measurement	(K)
δq_c	estimated error in convective heat flow measurement	(W/m^2)
δq_r	estimated error in radiation heat flow measurement	(W/m^2)
δq_{cond}	estimated error in convective heat flow measurement	(W/m^2)
Δ_t	sample time in frequency analysis	(s)
ΔT	temperature difference, generally between surface and air	(K)
ε_{surf}	emissivity of the surface.	(-)
ε_{eff}	effective emissivity	(-)
θ	θ factor general finite difference formulation	(-)
λ	thermal conductivity	(W/mK)
μ	dynamic viscosity	(N s / m^2)
$\nu = \mu / \rho$	kinematic viscosity	(m^2 / s)
τ	transmitted part of solar radiation	(-)

ρ	density	(kg/m^3)
σ	Stefan-Boltzmanns constant $5.67\ 10^{-8}$	(W/m^2K^4)
ω	angle frequency	(rad/s)
$\tilde{f}\ (..,\omega)$	Fourier transform of $f\ (..,t)$	(-)

indices

frequency	calculated with the frequency method
FD	calculated with the Finite Difference method

1 Summary

It is, with the thermal models used in today's building simulation programs, possible to calculate the major part of the heat transfer in a room with an ambient outer wall. However, there are some parameters these models calculate with less or unknown accuracy: heat flows in poorly insulated walls or windows, heat flows in a room exposed to strong solar radiation, temperatures on the inside of ambient outer walls and windows.

The reason for these difficulties is mainly that there is a lack of experimental data for the detailed energy transfer in a window exposed to ambient climate and the convective energy transport in a room exposed to ambient climate.

The aim of this study was to investigate the detailed energy transfer at an ambient wall including window. The investigation included both theoretic analysis and measurements performed under conditions close to the real situation with, for example, ambient climate.

The method used in this study was to estimate the heat flow through wall and window from measured solar radiation on the façade and temperatures. The temperatures were measured inside the wall, on the window panes, in the air, at inner surfaces etc. The longwave radiation was calculated from surface temperatures. The convective heat transfer was calculated as the difference between the heat flow through the building element and the longwave radiation. This indirect way of measuring the convective heat transfer was not as accurate as other more direct techniques but it was however a method which permitted measurement under realistic conditions.

The most important conclusions regarding the calculation models and measurement technique used in this study were:

- It is possible to measure the continuous heat flow through a window from temperature sensors and solar radiation measurements. The accuracy at least for low angles of incidence of the solar radiation was estimated to +/- 10%

- The absorption of solar radiation on the thin thermocouples (0.08 mm) glued to the window pane beneath a microscope cover glass was not a problem.

- To measure air temperatures in sunlit places thin (0.08 mm in this case) stripped thermocouples are the only alternative. With the thin thermocouples the measurement error was estimated to less than 0.5°C when exposed to 400 W/m^2 of solar radiation.

- The one-dimensional finite difference model for the heat transfer through the wall was acceptable. It was possible to calculate the heat flow through a wall from temperature sensors but some problems were noticed when the room was heated by a radiator making the surface temperature slowly increase 6°C.

- The one-dimensional dynamic heat transfer model for the window which included shortwave radiation was fairly good except for small temperature differences and high angles of incidence for solar radiation.

Conclusions for the convective heat transfer coefficient were:

- It is possible to continuously measure the convective heat transfer coefficient on the inner surface of a wall or a window. The accuracy is not very good: at best +/-15% for the window and +/- 20% for the wall. Even with this low accuracy the effect of different heating and ventilation strategies on the inside could clearly be detected.

- The presented results show that the importance of the ventilation design and the position of the radiator is crucial. Local convective heat transfer coefficients can be more than 10 times the expected, due to ventilation or position of the radiator.

- It is not obvious how the results of this study should be generalized. But as a rough estimate, we suggest that the following formulae can be used:

$$h_c = f \cdot \begin{cases} 1.34(\Delta T / H)^{1/4} & \Delta T H^3 < 9.5\,\mathrm{m^3K} \\ 1.33\Delta T^{1/3} - 0.474 / H & \Delta T H^3 > 9.5\,\mathrm{m^3K} \end{cases}$$

h_c = the convective heat transfer coefficient ($W/m^2°C$)
ΔT = temperature difference between surface and air (°C)
H = height of the wall or window (m)

Radiator at back wall: f=0.7 for the window and f=1 for the wall.

Radiator below window: f=2.5 for the window with the radiator power on and f=0.7 with the radiator off and f=0.7 for the wall.

Future studies

With the already measured data comfort calculations will be performed. The importance of low U-value windows and comfort will be studied. The experimental setup also allows total heat transfer coefficients to be estimated with a furnished and occupied room.

The presented method was not entirely satisfying due to the low accuracy. Future studies will be focused on investigating the Mayer ladder technique, or more precisely to measure the temperature difference very close to a surface with thermocouple pairs in series. This study suggests that the measurement error of that type of technique could be less than 10% in the convective heat flow.

2 Introduction

2.1 Problem

It is, with the thermal models used in today's building simulation programs, possible to calculate the major part of the heat transfer in a room with an ambient wall. The longwave radiation exchange between surfaces is complicated but possible to analyse. The heat transfer in ambient walls is dominated by conduction which is a well investigated phenomenon etc. Thus one can say that in general there is enough knowledge for rough estimates of hourly heat flows in a room. There are however some parameters which are more difficult to estimate:

1. Heat flows when walls and windows are poorly insulated.

2. Heat flow in a room exposed to strong solar radiation.

3. Temperatures on the inside of ambient walls and windows.

4. Thermal comfort.

The reason for these difficulties is mainly that the following two phenomena are difficult to estimate:

- The detailed energy transfer in a window exposed to ambient climate, including sun.

- The convective energy transport in a room exposed to ambient climate, including sun.

The energy transfer in a window is possible to calculate but it is difficult to measure temperatures and other parameters when the probes are exposed to sunlight. The convective heat transfer is related to the air movement in a room and is very difficult to calculate and then only for simplified models. There is a lack of data for convective heat transfer from experiments in realistic situa-

tions. Most measurements have been made in special environments with, for example, metal coated walls.

2.2 Aim of study

The aim of this study is to investigate the detailed energy transfer at an ambient wall including window. The investigation includes both theoretic analysis and measurements performed under conditions close to the real situation with for example natural ambient climate.

Questions that this study tries to answer:

- Is it possible to accurately measure the continuous heat flow through a window from temperature sensors and solar radiation measurements?
- Is it possible to accurately measure the continuous heat flow through a wall from temperature sensors?
- Is it possible to measure the air temperature with a thermocouple exposed to sunlight?
- If the questions above are satisfactorily answered, can realistic values for the heat transfer coefficient between room and ambient wall be estimated?

2.3 Method

The method used in this study is to estimate the heat flow through wall and window from measured solar radiation on the façade and temperatures. The temperatures are measured inside the wall, on the window panes, in the air, at inner surfaces etc. The longwave radiation is calculated from surface temperatures. The convective heat transfer is calculated as the difference between the heat flow through the building element and the longwave radiation. This indirect way of measuring the convective heat transfer is not as accurate as other more direct techniques but it is however a method which makes for the most realistic measurement.

2.4 Literature survey

One-dimensional heat transfer in window without solar radiation has been studied by many authors (e.g. Arasteh et al 1989 and Klems and Reilly 1989) and are found to be in good agreement with measurements. Calculations with solar radiation has not been verified with measurements to that extent. Shapiro et al (1987) found good agreement with three-dimensional calculations with solar radiation and measurements. The heat transfer in the gap between two panes consists of convective/conductive heat transfer in the gas (e.g. air or argon) and longwave radiation between the panes. The convective transfer is described with the so called Nusselt number. This has been investigated by e.g. ElSherbiny (1982), Wright (1996). The short wave radiation transfer in windows is partly described by Fresnel's formulae (August Jean Fresnel 1788-1827).

Measurements of the realistic convective heat transfer coefficients have been performed by some authors. Hatton and Awbi (1995), Delaforce et al (1993), Khalifa and Marshall (1990), Min et al (1956). Most authors used test situations with reduced longwave exchange, typically by having metal plates on the walls. The agreement between the different authors is not very good. The results differ sometimes with a factor 2 or even more. Most tests were performed without ventilation and only Delaforce et al used natural climate.

3 Method

3.1 Determine the convective heat transfer

The method used in this study is to estimate the heat flow through wall and window from measured temperatures and solar radiation on the façade. The places where the temperature is measured are shown in Figure 3.1. The glass and wall rows are three to four thermocouples positioned in a vertical line through the window and wall respectively.

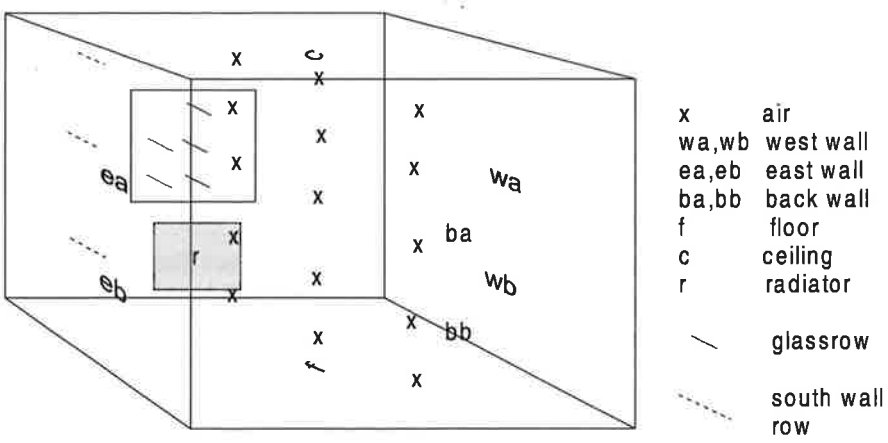

Figure 3.1 Thermocouples on surfaces in the test room.

The temperatures are measured inside the wall, on the window panes, in the air, at inner surfaces etc. From surface temperatures the longwave radiation is calculated: q_r. The conductive heat transfer is calculated from the thermocouple staples in the material: q_{cond}. The convective heat transfer is calculated as the difference between the heat flow through the building element and the longwave radiation.

q_r	longwave radiation heat transfer	(W/m^2)
q_{cond}	conductive heat transfer in material	(W/m^2)

q_c convective heat transfer (W/m^2)

For the inner surface, with q_{cond} positive for conduction from inside to outside, the heat balance gives:

$$q_c = q_{cond} - q_r \quad (W/m^2) \quad (3.1)$$

This indirect way of measuring the convective heat transfer is not as accurate as other more direct techniques but it is however a method which makes for the most realistic measurement.

Equation (3.1) is not valid for window panes exposed to the sun. In that case the solar energy absorbed in the pane, q_{abs}, has to be accounted for:

$$q_c = q_{cond} - q_r - q_{abs} \quad (W/m^2) \quad (3.2)$$

The solar energy absorbed in the pane is calculated from sun angle and global solar radiation on the façade.

The heat transfer coefficient can now be calculated as:

$$h_c = \frac{q_c}{T_{ref} - T_{surf}} \quad (W/m^2K) \quad (3.3)$$

Here T_{ref} is a reference temperature and T_{surf} is the surface temperature of the wall or window. The reference temperature is in this study usually chosen as the mean air temperature at a vertical line in the middle of the room.

3.2 Determine the conductive heat transfer

The conductive heat transfer is calculated from the temperatures in the wall and window. The physical properties of wall and window determine the heat transfer. The actual calculations for the wall was made with a finite difference model and for the window with a lumped capacity model. The accuracy of the model and the assumption of how the wall and window are constructed will of course strongly affect the results.

3.3 Determine the longwave radiation heat transfer

The longwave radiation exchange is easily calculated from: surface temperatures, geometric shape of the surfaces and the emissivity of the surfaces. However, the emissivity is often not known and has to be estimated.

4 Heat flows in a room

4.1 Heat transfer mechanisms

Three basic mechanisms perform the heat transfer in a room:

1.	Conduction	in solids and fluids (gases)
2.	Convection	in fluids (gases)
3.	Radiation (shortwave/longwave)	between surfaces in a transparent or partially transparent medium

Strictly speaking there are two more physical processes that transfer heat in a room:

> Latent heat from phase changing materials, e.g. water.
> Radiation exchange between molecules or particles in a fluid/gas.

Of these the first one might be important in an ambient wall which has been exposed to rain and the strong sun. The second one is only important if the temperature is very high or if the gas is full of particles (from fire etc).

4.1.1 Conduction

Conduction occurs through a material across which there exists a temperature gradient. This is possible for both fluids and solid materials. For isotropic homogeneous materials (fluids or solids), the heat flux density in a direction x is:

$$q = -\lambda(T)\frac{dT}{dx} \qquad (\mathrm{W/m^2}) \qquad (4.1)$$

Here λ (W/mK) is the thermal conductivity for a material. Equation (4.1) is generally called Fourier's law. For non homogeneous materials such as glass wool the heat transfer is a mix of radiation, convection and conduction in gas

and solid. In building applications this is usually approximated as a representative thermal conductivity.

4.1.2 Convection

Convection occurs in non isothermal fluids that are moving. The convective heat flux density parallel to the x-axis, might be described as:

$$q = \rho(T)c_p(T)\cdot u\frac{dT}{dx} \qquad (W/m^2) \qquad (4.2)$$

Here ρ (kg/m^3) is the density, c_p (J/kg K) is the specific at constant pressure and u (m/s) is the speed of flow. Conduction always occurs when there is convection. However, in a moving fluid the convection will usually dominate.

4.1.3 Radiation

The radiation is in building physics traditionally divided into short wave and long wave radiation. The process is the same but this division approximately corresponds to how building materials are affected by radiation of different wavelengths. Short wave radiation is the radiation which is transmitted through a glass pane with the wavelength 0.3-4 μm and longwave has the wavelength >4 μm. Glass, thin metal films, plastic and air are examples of materials which are transparent or partially transparent for short wave radiation. Parts of the radiation will be transmitted, reflected and absorbed. It is necessary to take into account the angle dependency of the radiation and for the materials.

Most building materials are opaque to longwave radiation. The radiation will therefore mainly be absorbed and reflected. Usually it is not necessary to take into account the angle dependency of radiation and materials. The longwave radiation exchange between two surfaces A_1 and A_2 with the temperatures T_1 and T_2 (in Kelvin) is described by:

$$q_{1,2} = \varepsilon_{eff} F_{12} \sigma\left(T_1^4 - T_2^4\right) \qquad (W/m^2) \qquad (4.3)$$

Here is σ Stefan-Boltzmanns constant (5.67 10^{-8} W/m^{2}K^4) , F_{12} a factor that describes the geometry and ε_{eff} the efficient emissivity between the surfaces.

4.2 Heat transfer in a room

The heat transfer in a room with window, radiator and ventilation is summarized in Figure 4.1.

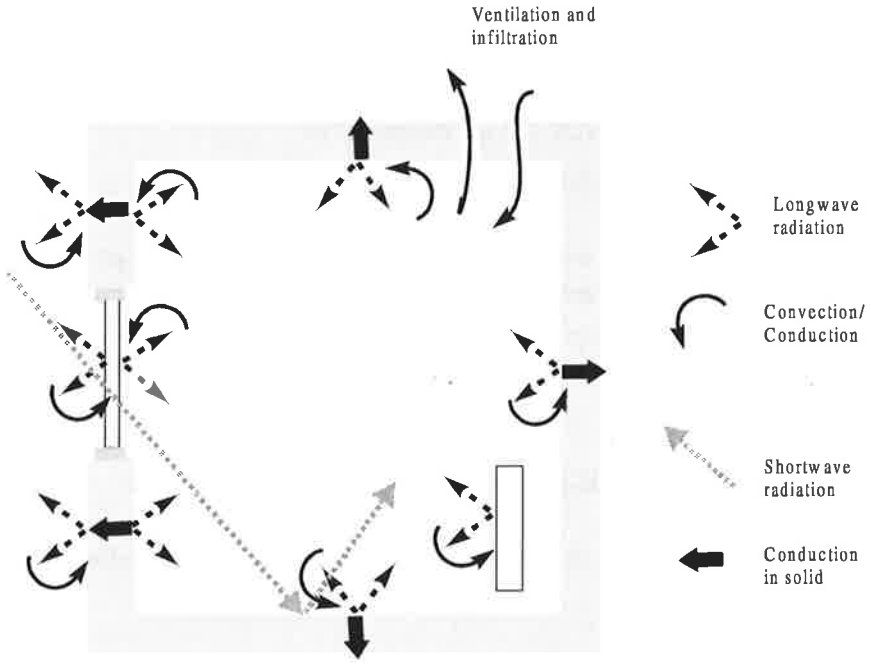

Figure 4.1 *Heat transfer in a section of a room with window, ventilation and radiator.*

The heat transfer in a room with an ambient wall can be summarized as follows:

- Longwave radiation exchange between all surfaces that can "see" each other. In the room: inner walls, floor, ceiling inner window pane and radiator. On the outside: outer wall, outer window pane, sky and surrounding surfaces.
- Convective/conductive exchange between all surfaces exposed to air: inner and outer walls, window panes and radiator.
- Convective/conductive exchange from ventilation and leak air.
- Conduction in all walls.

- Shortwave radiation through the window to inner surfaces. Most of the solar energy is absorbed in the first surface, but some is reflected more or less diffusely to other surfaces.

4.3 Heat transfer in a window

The heat transfer in a window is summarized in Figure 4.2.

- Longwave radiation exchange between all surfaces that can "see" each other : panes , frame surface, sky, inner walls etc.
- Convective/conductive between all surfaces exposed to air: panes and frame.
- Conduction in all solid parts in the window: panes and frame.
- Short wave radiation that hits a glass pane is transmitted, reflected or absorbed.

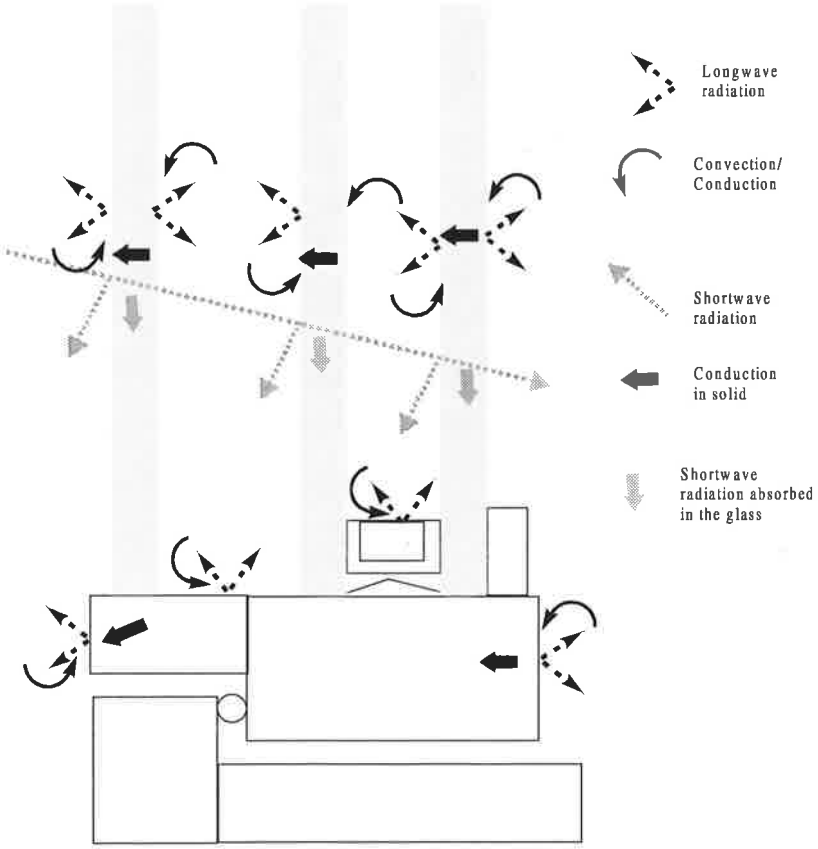

Figure 4.2 Heat transfer in a window

For each pane surface in a window it is true that:

$$\tau + a + r = 1 \qquad (-) \qquad (4.4)$$

Here τ is the transmitted part, a the absorbed and r the reflected part. The transmittance t is the same if the direction of the ray is reversed but a and r might change. The absorbed part heats the window pane. All the variables are angle and wavelength dependent. In building heat transfer calculations the wavelength dependency in the shortwave region is often ignored but the angle dependency has to be accounted for. The conduction in the pane is approximately one-dimensional in the centre area of the pane and two-dimensional at the centre edge and three dimensional close to the corner.

5 Heat transfer coefficients

5.1 Why using heat transfer coefficients?

The heat transfer at a surface comprises of convective/conductive exchange to the air and longwave radiation exchange with the surrounding surfaces. Detailed models of these heat transfer processes are complex as the heat transfer depends of many parameters. A simple and useful approximation is to use heat transfer coefficients that encapsulate the complexity of the problem. The radiation and convection/conduction heat transfer can be treated separately or together. Here they are dealt with separately. The incoming heat flux q to a surface is:

$$q = q_c + q_r \qquad (\mathrm{W/m^2}) \qquad (5.1)$$

Here q_c is the heat flux by convection/conduction and q_r the heat flux from radiation exchange.

The radiation part can be calculated with the basic physical formula:

$$q_r = \varepsilon_{surf}\,\sigma\left(T_r^4 - T_{surf}^4\right) \qquad (\mathrm{W/m^2}) \quad T \text{ in Kelvin} \qquad (5.2)$$

Here T_{surf} is the surface temperature and T_r the surrounding mean radiation temperature and ε_{surf} the emissivity of the surface. A more detailed model is described in chapter 7.2. The heat flow thus depends nonlineary on the temperatures. Equation (5.2) can be linearized as:

$$\begin{aligned} q_r &= h_r\left(T_r - T_{surf}\right) \\ h_r &= \varepsilon_{surf}\,\sigma\left(T_{surf}^2 + T_r^2\right)\left(T_{surf} + T_r\right) \qquad (\mathrm{W/m^2K}) \end{aligned} \qquad (5.3)$$

Here h_r is the heat transfer coefficient for longwave radiation.

The conductive/convective heat transfer is much more complicated. The most detailed approach is to solve Navier-Stoke's equations, which describe the mechanical and thermodynamic behaviour of a fluid. These equations are physically correct for laminar flow but for turbulent flow approximations must be used. The computational task is huge since the discretisation mesh in two or three dimensions must be fine. This particular field of study is called *compu-*

tational fluid dynamics or *CFD*. It is to date not possible to trust a particular numerical solution of a specific fluid flow problem without experimental verification from a similar problem. To circumvent the need for a full CFD, model different simplifications are used. The most common method is to use a convective heat transfer coefficient: h_c, which describes the heat transfer from some fictitious, but representative air temperature to the surface temperature.

$$q_c = h_c(T_s, T_a, H) \cdot (T_a - T_s) \qquad (\mathrm{W/m^2}) \qquad (5.4)$$

The heat transfer coefficient can be determined experimentally or analytically or by a mix of both methods. The air flow is divided in *natural* and *forced* convection. Both types can be laminar or turbulent respectively. If the air flow is due to fans and wind this is called forced convection. If the air flow is produced by density differences of different air packages due to temperature differences this is called natural or buoyancy driven convection. If there is only natural convection, h_c will typically depend on the temperature difference between the surface and the air, the actual geometry and the absolute temperature. If the air flow is forced the fan or wind will readily dominate over the influence from temperature differences. The air flow in a room will hence be a mix of natural and forced convection, with the natural convection often dominant. The exterior air flow is almost exclusively forced. Table 5.1 shows the order of the different coefficients.

Table 5.1 *Typical values for the heat transfer coefficients for winter conditions.*

	Interior	**Exterior**
h_c	1-4 W/m^2K	5-15 W/m^2K
h_r	5 W/m^2K	4 W/m^2K

This study only deals with the interior convective heat transfer coefficient.

5.2 Interior convective heat transfer coefficient

The formulae for the convective heat transfer coefficients can be determined theoretically, experimentally or by a mix of both. The theoretic formulae are derived from boundary layer theory from a vertical heated plane in an undisturbed surrounding. The plane can have either uniform temperature or uniform heat flux. For pure laminar flow analytic or semi-analytic solutions exist. The

formulae from experiments are derived from a wide range of situations. Both scaled experiments in water and full scale experiments with air have been performed. From theoretic analysis it is found that the heat transfer depends on four different dimensionless numbers:

$$\text{Reynolds number} \quad \mathrm{Re} = \frac{u H}{\nu}$$

$$\text{Prandtl number} \quad \mathrm{Pr} = \frac{\nu}{a} = \frac{\mu c_p}{\lambda} \qquad (5.5)$$

$$\text{Grashof number} \quad \mathrm{Gr} = \frac{g \beta \Delta T H^3}{\nu^2}$$

$$\text{Rayleigh number} \quad \mathrm{Ra} = \mathrm{Gr} \cdot \mathrm{Pr}$$

With:

u	free stream velocity	(m / s)
λ	thermal conductivity	(W/mK)
c_p	specific heat at constant pressure	(J/kg K)
g	gravitational gravity	(m/s^2)
H	characteristic dimension, here height	(m)
μ	dynamic viscosity	($N\ s / m^2$)
ρ	density	(kg/m^3)
$\nu = \mu / \rho$	kinematic viscosity	(m^2 / s)
$a=\lambda / (\rho\ c_p)$	thermal diffusivity	(m^2/s)
β = 1/T (for air)	thermal expansion coefficient	(K^{-1})
ΔT	temperature difference	(K)

The convective heat flow to a plane when the fluid flow is parallel to the plane is described by:

$$q_c(x) = h_c^*(x) \cdot \Delta T = \Delta T \frac{\lambda \mathrm{Nu}^*(x)}{x} \qquad (\mathrm{W/m^2}) \qquad (5.6)$$

Here Nu^* is the local Nusselt number, h_c^* the local heat transfer coefficient, x is the length from the edge of the plane in the flow direction. The mean heat flow is described by the mean Nusselt number (Nu) or the mean heat transfer coefficient h_c:

$$q_c = \Delta T h_c(H) = \Delta T \int_0^H h_c^*(x)dx \cdot = \tag{5.7}$$

$$\Delta T \lambda \int_0^H \frac{\mathrm{Nu}^*(x)}{x}dx = \Delta T \frac{\lambda \mathrm{Nu}(H)}{H} \qquad (\mathrm{W/m^2})$$

For laminar natural convection the local and mean Nusselt number is proportional to $Ra_x^{1/4}$. The constants wary somewhat depending on if they are based of theoretical calculations or experiments. (Bejan 1993)

$$\mathrm{Nu}(H) = 0.51\,\mathrm{Ra}_H^{1/4} \qquad Nu^*(x) = 0.39\,\mathrm{Ra}_x^{1/4}$$

or (5.8)

$$h_c(H) = 1.35\left(\frac{\Delta T}{H}\right)^{1/4} \qquad h_c^*(x) = 0.99\left(\frac{\Delta T}{x}\right)^{1/4}$$

If the plate is sufficiently long the flow will become turbulent. This transition occurs where $10^8 < Gr < 10^{10}$ (Bejan 1993). Usually the flow is considered laminar if $Gr<10^9$ and turbulent if $Gr>10^9$. For air this corresponds to $Gr=10^9 \approx Ra_x = 10^9$. For turbulent flow the mean and local Nusselt number is proportional to $Ra_x^{1/3}$(McAdams 1954, Churchill and Chu 1975):

$$\mathrm{Nu}(H) = 0.11\,\mathrm{Ra}_H^{1/3} - 18.5 \qquad \mathrm{Nu}^*(x) = 0.11\,\mathrm{Ra}_x^{1/3}$$

or (5.9)

$$h_c(H) = 1.33\Delta T^{1/3} - 0.474/H \qquad h_c^*(x) = 1.33\Delta T^{1/3}$$

If (5.9) and (5.8) is evaluated for T=15°C we get the following formula:

$$h_c(H) = \begin{cases} 1.34(\Delta T/H)^{1/4} & \Delta T H^3 < 9.5\,\mathrm{m^3K} \\ 1.33\Delta T^{1/3} - 0.474/H & \Delta T H^3 > 9.5\,\mathrm{m^3K} \end{cases} \tag{5.10}$$

This formula is hereafter referred to as Churchill and Chu.

Churchill and Chu derived a formula valid for the whole range (laminar, transition, turbulent):

$$\mathrm{Nu}(H) = (0.825 + 0.324\ \mathrm{Ra}_H^{1/6})^2$$

or (5.11)

$$h_c(H) = 0.017 / x + 0.298 \frac{\Delta T^{1/6}}{x^{1/2}} + 1.27 \Delta T^{1/3}$$

This formula is hereafter referred to as Churchill and Chu 2. Figure 5.1 shows the local and mean heat transfer coefficient h_c and h_c^* when equations (5.8)-(5.11) are used. The transition from laminar to turbulent is set to Ra=10^9 but the transition zone 10^8 < Ra=10^{10} is also indicated. In fact most of the wall is in this transition zone.

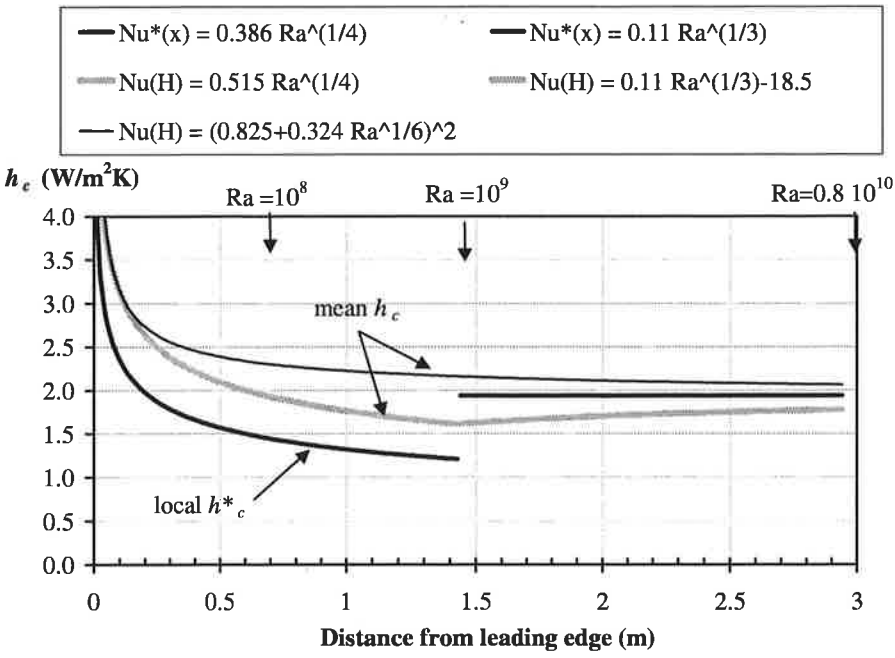

Figure 5.1 *The local and mean convective heat transfer coefficient for air based on equations (5.8)-(5.11). The temperature difference is ΔT=3° C and the mean temperature 20°C.*

Almadari and Hammond (1983) suggested a formula valid for both the laminar and turbulent region:

$$h_c = \left[\left(1.51 \left(\frac{\Delta T}{H} \right)^{1/4} \right)^6 + \left(1.33 \left(\Delta T \right)^{1/3} \right)^6 \right]^{1/6} \quad (\mathrm{W/m^2K}) \qquad (5.12)$$

Formulae based on full scale experiments give in general a slightly higher value than analytic or small scale experiments. Min et al (1956) performed experiments in a test cell with floor areas 3.6 x 7.2 m^2 or 3.6 x 3.6 m^2 and the height 2.4 or 3m. The temperature difference was above 3°C between surface and air. For the floor heating case they got:

$$h_c = 2 \frac{\Delta T^{0.32}}{H^{0.04}} \quad (\mathrm{W/m^2K}) \qquad (5.13)$$

Hatton and Awbi (1995) made full scale experiments in a test cell with the floor area 2.78 x 2.78 m^2 and height 2.3 m. The temperature difference between surface and air was between 5 and 30 °C. The walls were aluminium plated and longwave radiation was taken into account. The heat transfer coefficient was based on heated parts of the test cell. They found the mean convective heat transfer coefficient for the wall to be:

$$h_c = 1.57 \Delta T^{0.31} \quad (\mathrm{W/m^2K}) \qquad (5.14)$$

Khalifa and Marshall (1990) used a test cell with floor area 2.95 x 2.35 m^2 and height 2.05 m and a temperature difference of 0.5 to 3.5 °C. The walls in the test cell were aluminium coated. The longwave radiation exchange was not taken into account. With floor heating they got for the wall.

$$h_c = 2.07 \Delta T^{0.23} \quad (\mathrm{W/m^2K}) \qquad (5.15)$$

With a radiator opposite to the cold wall they got for the wall:

$$h_c = 2.20 \Delta T^{0.22} \quad (\mathrm{W/m^2K}) \qquad (5.16)$$

Radiator opposite to the cold wall, for the glazing:

$$h_c = 7.61 \Delta T^{0.06} \quad (\mathrm{W/m^2K}) \qquad (5.17)$$

With radiator under glazing, for the wall:

$$h_c = 2.35 \Delta T^{0.21} \quad (\mathrm{W/m^2K}) \qquad (5.18)$$

With radiator under window, for the windows:

$$h_c = 8.07 \Delta T^{0.11} \quad (\mathrm{W/m^2K}) \qquad (5.19)$$

Delaforce et al (1993) made measurements in an outside test cell with the floor area 2.03 x 2.03 m^2 and the height 2.33 m. The heat was supplied by an air heating system and the temperature difference was in the range of 0.5-4.0 °C. They did not formulate equations.

In Figure 5.2 the different heat transfer coefficients are shown. The results from Delaforce et al are indicated as black squares. When the formula has 0.25 as an exponent the experiment is predominantly laminar. An exponent of 0.33 indicates a more turbulent situation. The highest value is about 2 times the lowest one. Churchill and Chu gives the lowest values and Min et al gives the highest or close to the highest. These two formulae will subsequently be used to compare with the measured values from this study. Churchill and Chu 2 in gives in this interval the same values as (5.14).

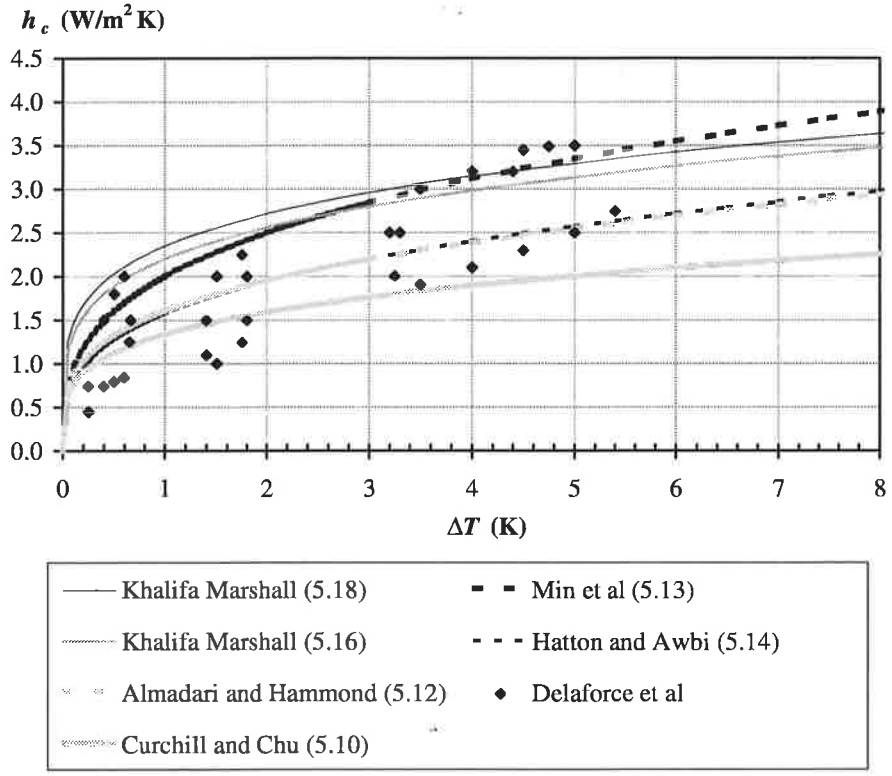

Figure 5.2 *A selection of convective heat transfer coefficients found in the literature. H=2m.*

6 Experimental setup

6.1 Description of test room

The test room was one of seven similar rooms inside a experimental building located in Lund, Sweden (latitude 55.72°, longitude 13.22°): MiniLab. Figure 6.1 shows the outline of the building. The test room was room E. The building was designed so that seven experiments could be performed simultaneously. Room E had the dimensions 3 · 3.6 · 2.4 m. One wall and the roof were exposed to the ambient climate. A window of the dimensions 1m · 1.1 m was placed in this wall, see Figure 6.2. The floor was on top of a basement which held a constant temperature of 18 °C. The temperature in the room E varied between 15 and 35 °C. Room D and F were identical. The house was built with a sandwich construction of lightweight concrete and polystyrene. The interior surfaces were all painted with a matt white colour except for the floor which had a light brown linoleum carpet. The U-values for the building components were:

North wall	0.15		W/m^2K
West wall	0.15		W/m^2K
South wall	0.27		W/m^2K
East wall	0.15		W/m^2K
Window	0.81	or 1.80	W/m^2K
Floor	0.16		W/m^2K
Roof	0.14		W/m^2K
Door	0.5		W/m^2K

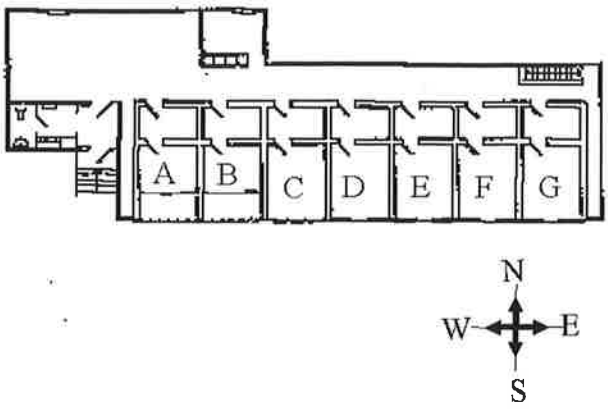

Figure 6.1 *Test building MiniLab.*

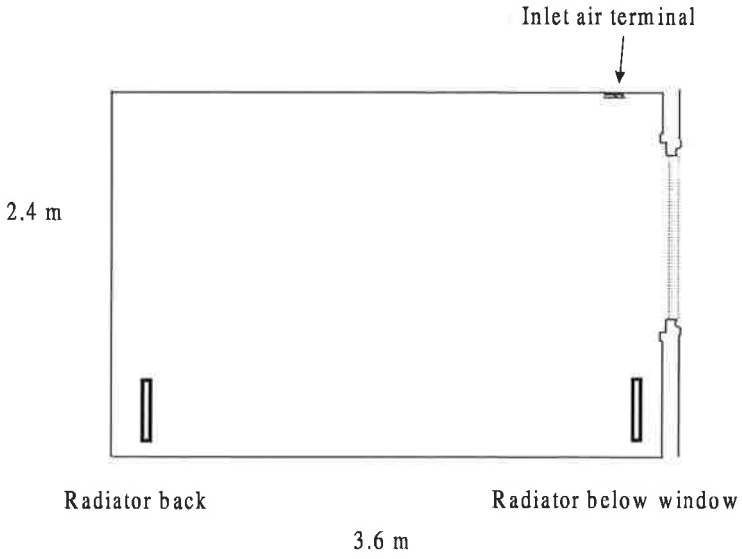

Figure 6.2 *Section of room E with window, radiator positions and inlet air terminal.*

6.1.1 The external wall

The ambient, south wall, was built with a normal non load bearing stud wall. The inner surface was a gypsum board covered with wall paper. The insulation was nominally 95 + 50 mm mineral wool, total 145 mm. Outer surface was a

wooden panel. The inner mineral wool was estimated being compressed to 90 mm. Four thermocouples were positioned in the wall at three heights on the wall as indicated in Figure 6.3.

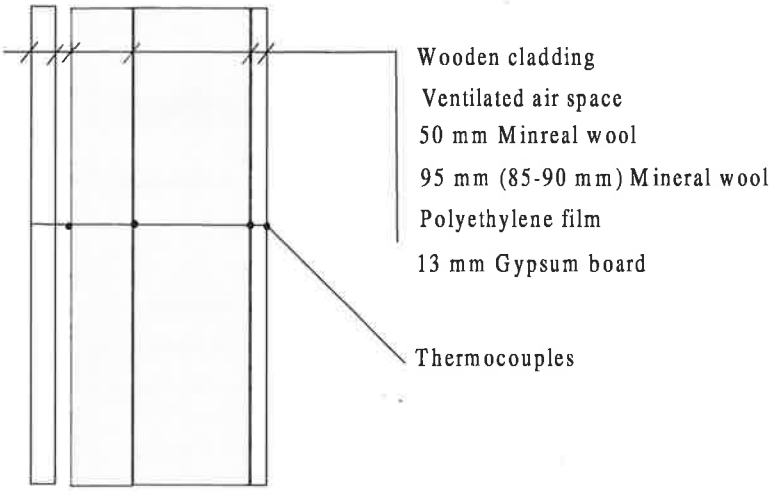

Figure 6.3 The ambient wall with thermocouples.

$\lambda_{gypsum} = 0.22$ W/mK
d_{gypsum}=13 mm
$\lambda_{minwool\ 1}$= 0.036 W/mK
$\rho_{minwool\ 1}$= 20 kg/m^3
$d_{minwool\ 1}$ = 90-95 mm
$\lambda_{minwool\ 2}$ = 0.032 W/mK
$\rho_{minwool\ 2}$= 55 kg/m^3
$d_{minwool\ 2}$=50 mm

6.1.2 Windows

Two windows were investigated: one superinsulated 4-pane window and one "normal" 3-pane window. The superinsulated window had a centre-of-glass U-value of 0.62 W/m^{2}K and a total U-value of 0.81 W/m^{2}K. The normal window had a centre-of-glass U-value of 1.75 W/m^{2}K and a total U-value of 1.80 W/m^{2}K. The description was (from outside to inside):

	4 mm pane (Pilkington Float)
	50 mm air space
IGU	4 mm with low e-coating (LuxGuard) 16 mm argon gas 4 mm pane (Pilkington Float) 16 mm argon gas low-e coating on 4 mm pane (LuxGuard)

The glass area was 1.1 m^2. The insulated glass unit is denoted IGU..

The normal 3-pane window :

	4 mm pane (Pilkington Float)
	43 mm air space
IGU	4 mm pane (Pilkington Float) 12 mm air gas 4 mm pane (Pilkington Float)

6.2 Heating and ventilation

The room had either an electric radiator of maximum 500 W or a radiator with maximum 1000 W. The smaller radiator had the dimensions 0.5 m x 0.05 m x 0.4 m (width x depth x height) and the larger radiator had the dimensions: 1.3 m x 0.024 m x 0.6 m. The radiator was placed either 0.2 m from the north (back) wall in the centre of the wall or 0.12 m from south wall under the window. The radiator was controlled by its own bimetallic thermostat and sometimes by a Proportional and Integrating controller (PI-controller) that controlled from different thermocouples in the room. The ventilation system had an air inlet terminal in the ceiling 0.30 m from the south wall and an air outlet at the top east corner of the north wall 0.09 m from the ceiling and 0.40 m from the east wall. The inlet terminal blew air vertically into the room parallel to the ceiling. The ventilation rate during the period was between 0 and 1.0 ach. No cooling system was installed.

6.3 Description of measurement system

The room was equipped with about 70 thermocouples of type T, a global solarimeter on the façade and an airspeed meter 100 mm from the centre of the glass pane perpendicular to the glass. Measurements were taken every minute and averaged to 10, 30 and 60 minutes mean values. The measurement system was four calibrated Acurex Netpak units.

The positions of most of the thermocouples are described in table 6.1.

Table 6.1 Thermocouples in the test room

VA	South wall	2.25 m	from floor	1 ->4	Out -> In
VB	South wall	1.45 m	from floor	1 ->4	Out -> In
VC	South wall	0.19 m	from floor	1 ->4	Out -> In
Floor	Floor	middle		1	
TA	Ceiling	middle		1->2	Out-> In
G_1-G_5	Window	1.44m	from floor	1->4	
WA	West wall	1.63 m	from floor	1	
WB	West wall	0.82 m	from floor	1	
EA	East wall	1.63 m	from floor	1	
EB	East wall	0.82 m	from floor	1	
BA	North wall	1.63 m	from floor	1	
BB	North wall	0.82 m	from floor	1	

The thermocouple rows in the exterior walls VA, VB and VC were used to estimate the conduction through the walls. Unfortunately was the conduction at VC not conclusive with a heat flow meter test. Therefore the results from VC are not included here. VC is only used in the visualisation of the air temperatures see chapter 9.

6.3.1 Thermocouples on interior surfaces

The positions and names of the thermocouples on the interior surfaces are shown in Figure 6.4 except for ceiling and floor which had one thermocouple each in the centre.

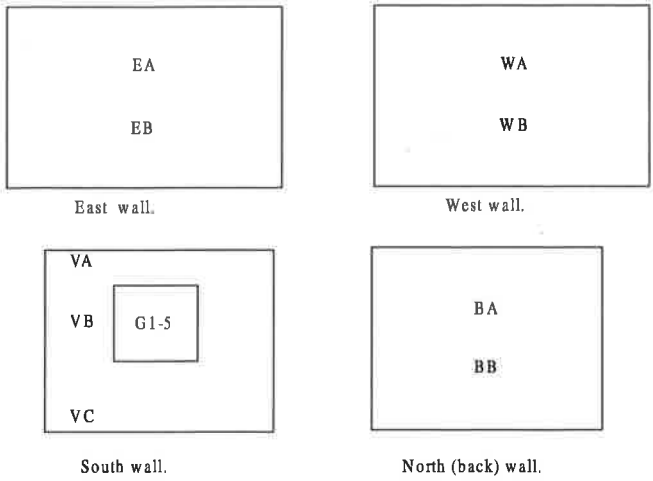

Figure 6.4 *The positions and denotions of the thermocouples on the walls.*

6.3.2 Thermocouples in air

There were 18 thermocouples in the air as shown in Figure 6.5. These thermocouples were made of 0.08 mm stripped wire and compensated. This means that there were in fact three thermal nodes where two of them were connected with a non-stripped wire giving an emf in the opposite direction of the stripped one. The idea of this setup was that the negative emf would compensate the absorbtion of solar radiation in the stripped wire. This is investigated in more detail in section 8.4.

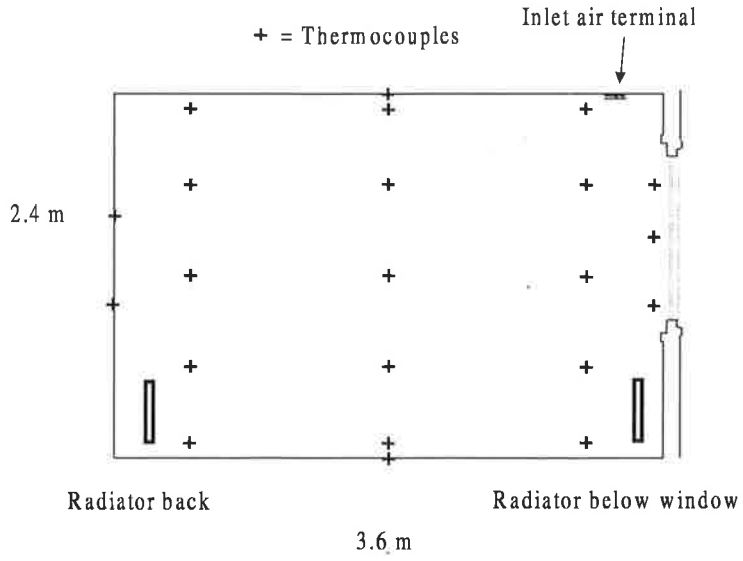

Figure 6.5 *Air, back wall, floor and ceiling thermocouples.*

6.3.3 Thermocouples on window panes

There were 11 thermocouples in the window. They were made of 0.08 mm silver coated wire glued to the window pane under a microscope cover glass of 0.1 mm. This was made to maximise the thermal contact between the thermocouple and the window pane. The cover glass also ensured that the surface was plane thus not effecting the heat transfer coefficient and that the emissivity was that of glass.

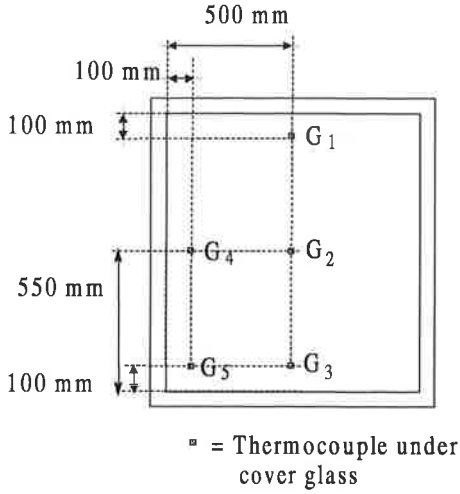

Figure 6.6 *Thermocouples on window seen from the inside.*

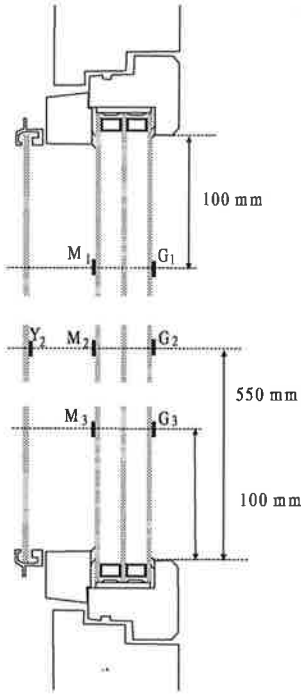

Figure 6.7 *Thermocouples in 4-pane window. The positions in the 3-pane window were similar.*

6.4 Tested heating and ventilation situations

Tests were performed for different positions of the radiator and different ventilation designs. The experiments are summarized in Table 6.1.

Table 6.1 The experiments that were performed.

Radiator position	Type	Ventilation	Inlet direction
back wall	500 W	0	-
back wall	1000 W	0	-
back wall	500 W	0.5 ach	north (back in room)
back wall	500 W	1 ach	north
back wall	500 W	1 ach	south (to window)
below window	500 W	0	-
below window	500 W	0.5 ach	north
below window	500 W	1 ach	north
below window	500 W	1 ach	south

The radiator was controlled by its own bimetallic thermostat and sometimes by a PI-controller with temperature input from different thermocouples in the room.

7 Thermal models

7.1 Thermal model for wall

The problem was to find q_{cond} in equation (3.1). In order to do this the heat transfer equation had to be solved. Suppose a composite material is made of N layers. The heat conduction equation in material nr. n is

$$\frac{\partial T(x,t)}{\partial t} = \frac{\lambda_n}{\rho_n c_n} \frac{\partial^2 T(x,t)}{\partial x^2} \qquad \text{(T/s)} \qquad (7.1)$$

Here λ_n, c_n and ρ_n are the conductivity, heat capacity and density of layer n. For the walls (7.1) was solved with the explicit finite difference method:

$$T_i^{n+1} = T_i^n + \frac{dt}{0.5 \cdot (dx_{i-1} c_{i-1} + dx_i c_i)} \Big[(T_{i-1}^n - T_i^n) \lambda_{i-1} / dx_{i-1} + (T_{i+1}^n - T_i^n) \lambda_{i+1} / dx_{i+1} \Big] \qquad (7.2)$$

This model was chosen to permit temperature dependent properties of the materials. The temperature dependency did not affect the result noticeable though. For the simulation of the wall the first (interior) and third thermocouple (between the two mineral wool layers) were used as boundary conditions. Typically 20 cells were used.

7.2 Model for radiation exchange in room

The longwave radiation from surface 1 to surface 2, for diffuse grey surfaces, is (Siegel and Howell):

$$Q_{1,2} = \sigma \varepsilon_1 T_1^4 \int_{A_1} \int_{A_2} \frac{\cos\theta_1 \cos\theta_2}{\pi r^2} \, dA_1 \, dA_2 \qquad \text{(W)} \qquad (7.3)$$

or with the view factor $F_{1,2}$:

$$Q_{1,2} = \sigma \varepsilon_1 T_1^4 A_1 F_{1,2} \qquad \text{(W)}$$

$$F_{1,2} = \frac{1}{A_1} \int_{A_1} \int_{A_2} \frac{\cos\theta_1 \cos\theta_2}{\pi r^2} dA_1 dA_2 \qquad (-) \tag{7.4}$$

From the definition of $F_{1,2}$ it follows that:

$$A_i F_{i,j} = A_j F_{j,i} \qquad (\text{m}^2) \tag{7.5}$$

The longwave radiation exchange in a room with diffuse grey surfaces can be described by (Siegel and Howell):

$$Q_i = A_i (G_i - J_i) \qquad \text{(W)} \tag{7.6}$$

Here Q_i is the net heat flow to surface i, A_i is the area, G_i is the total incoming radiation (per unit area) and J_i is the total radiation (per unit area) leaving the surface. The net heat flow Q_i is, if the surface is a wall, compensated by conduction into the wall and convection to the air. The radiation J_i is the sum of the reflected and emitted radiation:

$$J_i = \sigma \varepsilon_i T_i^4 + (1 - \varepsilon_i) G_i \qquad (\text{W/m}^2) \tag{7.7}$$

The total incoming radiation G_i is the sum of the J_i for all N surfaces:

$$A_i G_i = \sum_{j=1}^{N} A_j F_{j,i} J_j \qquad \text{(W)} \tag{7.8}$$

With (7.5) equation (7.8) becomes :

$$A_i G_i = A_i \sum_{j=1}^{N} F_{i,j} J_j \qquad \text{(W)} \tag{7.9}$$

If this is used in equation (7.7) we get:

$$J_i = \sigma \varepsilon_i T_i^4 + (1 - \varepsilon_i) \sum_{j=1}^{N} F_{i,j} J_j \qquad (\text{W/m}^2) \tag{7.10}$$

or

$$\sigma \varepsilon_i T_i^4 = \sum_{j=1}^{N} \left(\delta_{i,j} - (1-\varepsilon_i) F_{i,j} \right) J_j \qquad \text{(W)}$$

(7.11)

$$\delta_{i,k} = 1, \qquad i = j$$
$$\delta_{i,j} = 0, \qquad i \neq j$$

Assuming that no surface sees itself, $F_{i,i}$=0. If (7.11) is used for all N surfaces an equation system is produced:

$$\mathbf{T}_i = \sigma \varepsilon_i T_i^4 \qquad \mathbf{F}_{i,j} = \delta_{i,j} - (1-\varepsilon_i) F_{i,j} \qquad \mathbf{J}_i = J_i$$

(7.12)

$$\mathbf{T} = \mathbf{F}\,\mathbf{J}$$

with the solution:

$$\mathbf{J} = \mathbf{F}^{-1}\,\mathbf{T} \qquad \text{(W/m}^2\text{)} \qquad (7.13)$$

From (7.6) and (7.7) we get the net heat flow:

$$Q_i = A_i \frac{\varepsilon_i}{1-\varepsilon_i} \left(J_i - \sigma T_i^4 \right) \qquad \text{(W)} \qquad (7.14)$$

Finding the view factors $F_{i,j}$ can be done numerically or with analytical solutions for special problems. In this study the view factors are calculated with formulae from Gross et al (1981). Only two rectangular surfaces with parallel boundaries are dealt with here. The surfaces can be either parallel or perpendicular. Figure 7.1 shows the perpendicular case and Figure 7.2 the parallel case.

The view factor is calculated as a series of additions:

$$A_1 F_{1,2} = \sum_{l=1}^{2} \sum_{k=1}^{2} \sum_{j=1}^{2} \sum_{i=1}^{2} \left[(-1)^{(i+j+k+l)} V(x_i, y_j, \eta_k, \xi_l) \right] \qquad (7.15)$$

Here V is, for the perpendicular case:

$$V = \frac{1}{2\pi}\left[(y-\eta)(x^2+\xi^2)^{0.5}\arctan\left(\frac{y-\eta}{(x^2+\xi^2)^{0.5}}\right) - \frac{1}{4}\left(x^2+\xi^2-(y-\eta)^2\right)\ln\left(x^2+\xi^2+(y-\eta)^2\right)\right] \tag{7.16}$$

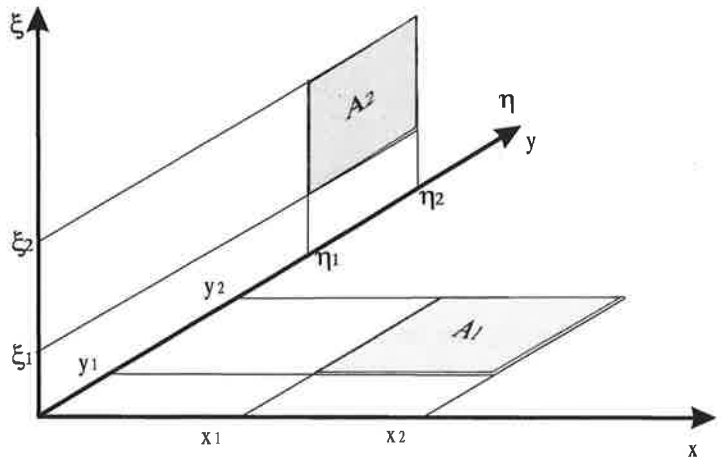

Figure 7.1 *Two surfaces in perpendicular planes.*

For the parallel case:

$$V=\frac{1}{2\pi}\left[(\xi-x)\left(z^2+(\eta-y)^2\right)^{0.5}\arctan\left(\frac{\xi-x}{\left(z^2+(\eta-y)^2\right)^{0.5}}\right)\right.$$

$$-(\eta-y)z\arctan\left(\frac{\eta-y}{z}\right)+(\eta-y)\left(z^2+(\xi-x)^2\right)^{0.5}\arctan\left(\frac{\eta-y}{\left(z^2+(\xi-x)^2\right)^{0.5}}\right)$$

$$+\frac{1}{2}(\xi-x)^2\ln\left(\frac{z^2+(\eta-y)^2+(\xi-x)^2}{(\xi-x)^2}\right)+\frac{1}{2}z^2\ln\left(z^2+(\eta-y)^2\right)$$

$$\left.-\frac{1}{2}\left(z^2+(\xi-x)^2\right)\ln\left(z^2+(\xi-x)^2+(\eta-y)^2\right)\right] \qquad (7.17)$$

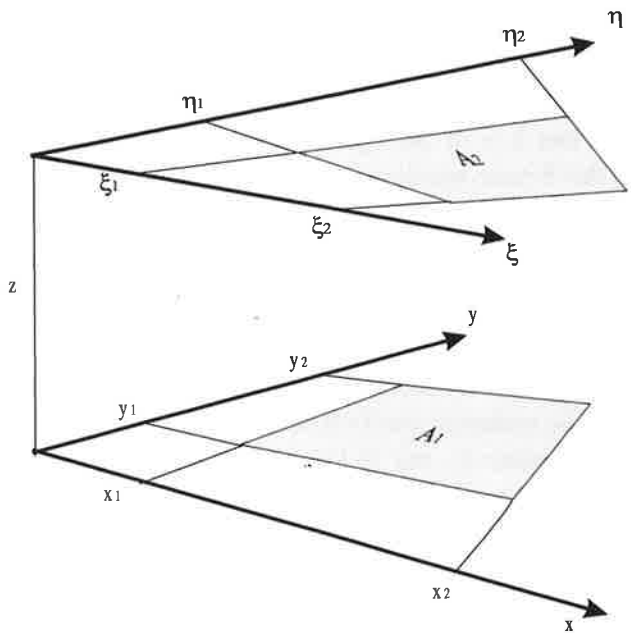

Figure 7.2 Two surfaces in parallel planes.

The matrix **F** in equation system (7.13) has only to be solved once, since it does not depend on the temperatures. The radiation flow Q_i can then be calculated for each sample period with (7.13) and (7.14).

The emissivities for which the calculations best matched the measurements were:

walls, ceiling, floor	$\varepsilon = 0.91$
radiator	$\varepsilon = 0.95$

From the manufacturer (Pilkington)

glass pane	$\varepsilon = 0.837$

7.3 Thermal model for window

The problem was to find q_{cond} in equation (3.2). To do this a lumped capacity model was used. For the inner pane this gives the following equation:

$$\frac{dT}{dt} C_{pane} = q_{2-1} + q_c + q_r + q_{abs} \qquad (\mathrm{W/m^2}) \qquad (7.18)$$

Here, C_{pane} is the heat capacity of the window pane per unit area, $q_{2\text{-}1}$ is the total heat transfer from pane 2 to pane 1. Pane 1 is the inner pane with thermocouples G_1-G_5. Pane 2 is in the 3-pane window the pane with thermocouples M_1-M_5, but in the 4-pane window it is the middle pane in the IGU. The heat flow $q_{2\text{-}1}$ was calculated as:

$$q_{2-1} = \left(\frac{d_{glass}}{\lambda_{glass}} + \frac{1}{h_c^{2-1} + h_r^{2-1}} \right)^{-1} (T_2 - T_1) \qquad (\mathrm{W/m^2}) \qquad (7.19)$$

Here is $h^{2\text{-}1}{}_c$ the convective/conductive heat transfer coefficient between pane 2 and 1 and $h^{2\text{-}1}{}_r$ is the radiation coefficient. In the 3-pane window there was only one unknown parameter q_c, but in the 4-pane window both q_c and the temperature of pane 2, T_2, were unknown. This led to an equation system which was solved numerically. These calculations were performed on each temperature sample.

7.3.1 Convective/conductive heat transfer

The model was one dimensional through the window. For the conductive/convective heat transfer the formulae from ElSherbiny et al (1982) were used.

$$
\begin{aligned}
&\mathrm{Ra} = \frac{g\beta \Delta T W^3}{\nu a} \\
&\mathrm{Nu}_1 = 0.0605\ \mathrm{Ra}^{1/3} \\
&\mathrm{Nu}_2 = 0.242\ (\mathrm{Ra} \cdot W / H)^{0.272} \\
&\mathrm{Nu}_3 = \left\{1 + \left[(0.104\ \mathrm{Ra}^{0.293} / \left(1 + (6310/\mathrm{Ra})^{1.36}\right)\right]^3\right\}^{1/3} \\
&\mathrm{Nu} = \max\left[\mathrm{Nu}_1, \mathrm{Nu}_2, \mathrm{Nu}_3\right]
\end{aligned}
\qquad (7.20)
$$

With:

W	width of air gap between the panes	(m)
H	height of panes	(m)
ΔT	temperature difference between panes	(K)

The convective/conductive heat transfer coefficient between pane 2 and 1 $h^{2\text{-}1}{}_c$ is then:

$$h_c^{2-1} = \frac{\lambda_{air} Nu}{W} \qquad (\mathrm{W/m^2K}) \qquad (7.21)$$

7.3.2 Longwave radiation heat transfer

The longwave radiation between the window panes is modelled as grey diffuse longwave exchange between two infinite parallel planes:

$$
\begin{aligned}
&h_r^{2-1} = \varepsilon_{eff}\, \sigma \left(T_1^2 + T_2^2\right)\left(T_1 + T_2\right) \qquad (\mathrm{W/m^2K}) \qquad T \text{ in Kelvin} \\
&\varepsilon_{\mathrm{eff}} = \frac{1}{1/\varepsilon_1 + 1/\varepsilon_2 - 1}
\end{aligned}
\qquad (7.22)
$$

Here the emissivity for the panes were 0.837 for the non coated pane and 0.12 for the coated one.

7.3.3 Shortwave radiation

For uncoated panes the shortwave radiation model was exactly the same as used by Källblad (1998). For coated panes the model used here was a bit different. The basic features were for each pane:

1. Calculations were based on refraction indices and extinction coefficients.

2. Fresnell's equations for optically thick layers were used.

3. In each pane parallel and perpendicular polarization were treated separately.

4. The diffuse properties were calculated by integrating over the half sphere.

5. Modelling coated panes are much more complicated than to model non coated panes. The reason is that the materials can no longer be considered as optically thick. Roos (1997) shows an excellent summary of the different approaches and suggests one himself. The best model is to use the basic physical properties of the coatings, layer by layer. This approach is difficult to perform since the exact compositions of the coatings are generally not known. The approach chosen here was to model panes with coatings as having a fictive refraction index and extinction coefficient. This fictive refraction index and extinction coefficient were adjusted to reproduce the mean reflectance and transmission at normal incidence. With these fictive parameters the Fresnell equations could be used to give angular dependent transmission and reflectance. The calculated reflectance was then adjusted by a factor to account for the fact that a coated pane has different reflectance on the coated and non coated side. Roos (1997) suggested instead of this to use a simple polynomial for the reflectance and transmission. In this study the advantage of different methods to model coated panes, have not been studied.

The features for the glazing package calculation were:

1. The direct and diffuse properties of each window pane were treated separately.

2. The parallel and perpendicular polarizations were *not* treated separately when calculating the behaviour of the whole package. The error when using this approximation is however small.

The measurement of the solar radiation was made with a global solarimeter. The diffuse and direct part were not measured separately. The shortwave model did however treat the direct and diffuse part differently. Therefore a simple linear model was used to model the diffuse and direct part as a function of the total radiation.

8 Verification of models

In this chapter we will investigate how the described models for wall and window can be verified. Two types of measurements were performed: a heat flow meter was used and a thermocouple ladder in the air. The first section deals with the theory needed to investigate how well the heat flow meter performs in interaction with window and wall.

8.1 Fourier analysis

Suppose a composite material is made of N layers. The heat conduction equation in material nr. n is

$$\frac{\partial T(x,t)}{\partial t} = \frac{\lambda_n}{\rho_n c_n}\frac{\partial^2 T(x,t)}{\partial x^2} \qquad \text{(T/s)} \qquad (8.1)$$

The Fourier transform of a function $f(..,t)$ is here denoted $\tilde{f}\,(..,\omega)$:

$$\tilde{f}\,(..,\omega) = \int_{-\infty}^{\infty} f(..,t)\cdot e^{-i\omega t}dt \quad \text{and} \quad f(..,t) = \frac{1}{2\pi}\int_{-\infty}^{\infty} \tilde{f}(..,\omega)\cdot e^{i\omega t}d\omega \qquad (8.2)$$

The Fourier transform in the time domain of (8.1) is:

$$i\omega\cdot\tilde{T}(x,\omega) = \frac{\lambda_n}{\rho_n c_n}\frac{\partial^2 \tilde{T}(x,\omega)}{\partial x^2} \qquad (8.3)$$

The general solution to (8.3) is:

$$\tilde{T}(x,\omega) = A(\omega)\sinh\left(x\sqrt{i\omega\rho_n c_n/\lambda_n}\right) + B(\omega)\cosh\left(x\sqrt{i\omega\rho_n c_n/\lambda_n}\right) \qquad (8.4)$$

where $A(\omega)$ and $B(\omega)$ is evaluated from the boundary conditions. The heat flow in the x direction is denoted q:

$$q = -\lambda_n\frac{\partial T(x,t)}{\partial x} \quad \Rightarrow \quad \tilde{q} = -\lambda_n\frac{\partial \tilde{T}(x,\omega)}{\partial x} \qquad (8.5)$$

If the two boundaries for a layer in the wall is $x=x_n$ and $x=x_{n+1}$ a matrix relationship can be formulated for $\tilde{T}$ and $\tilde{q}$:

$$\begin{pmatrix} \tilde{T}(x_{n+1},\omega) \\ \tilde{q}(x_{n+1},\omega) \end{pmatrix} =$$

$$\begin{pmatrix} \cosh\left(d_n\sqrt{i\omega\rho_n c_n/\lambda_n}\right) & -\dfrac{\sinh\left(d_i\sqrt{i\omega\rho_n c_n/\lambda_n}\right)}{\lambda_i\sqrt{i\omega\rho_n c_n/\lambda_n}} \\ -\lambda_n\sqrt{i\omega\rho_n c_n/\lambda_n}\cdot\sinh\left(d_n\sqrt{i\omega\rho_n c_n/\lambda_n}\right) & \cosh\left(d_n\sqrt{i\omega\rho_n c_n/\lambda_n}\right) \end{pmatrix} \begin{pmatrix} \tilde{T}(x_n,\omega) \\ \tilde{q}(x_n,\omega) \end{pmatrix} \tag{8.6}$$

or

$$\begin{pmatrix} \tilde{T}(x_{n+1},\omega) \\ \tilde{q}(x_{n+1},\omega) \end{pmatrix} = \mathbf{G}_n(\omega) \begin{pmatrix} \tilde{T}(x_n,\omega) \\ \tilde{q}(x_n,\omega) \end{pmatrix} \tag{8.7}$$

Here $\mathbf{G}_n(\omega)$ is the *transfer function* matrix from layer n to $n+1$. The transfer function matrix for layer 1 to layer n is simply the product of the different $\mathbf{G}_i$ matrices:

$$\begin{pmatrix} \tilde{T}(x_{n+1},\omega) \\ \tilde{q}(x_{n+1},\omega) \end{pmatrix} = \mathbf{G}_n \cdot \mathbf{G}_{n-1} \cdots \mathbf{G}_1 \cdot \begin{pmatrix} \tilde{T}(x_1,\omega) \\ \tilde{q}(x_1,\omega) \end{pmatrix} \tag{8.8}$$

$$\mathbf{G}_{n,1} = \mathbf{G}_n \cdot \mathbf{G}_{n-1} \cdots \mathbf{G}_1 = \begin{pmatrix} g_{n1}^{11}(\omega) & g_{n1}^{12}(\omega) \\ g_{n1}^{21}(\omega) & g_{n1}^{22}(\omega) \end{pmatrix} \tag{8.9}$$

The heat flow $\tilde{q}$ (x_{n+1},ω) becomes after some calculations:

$$\tilde{q}(x_{n+1},\omega) = \tilde{T}(x_1,\omega)\left(g_{n1}^{21} - \frac{g_{n1}^{22} g_{N1}^{11}}{g_{N1}^{12}}\right) + \tilde{T}(x_{N+1},\omega)\frac{g_{n1}^{22}}{g_{N1}^{12}} \tag{8.10}$$

or

$$\tilde{q}(x_{n+1},\omega) = \tilde{T}(x_1,\omega)\cdot G_n^1(\omega) + \tilde{T}(x_{N+1},\omega)\cdot G_n^N(\omega) \tag{8.11}$$

The absolute value and the phase angle of $G^1{}_n$ and $G^N{}_n$ have a simple physical connection. If the temperature $T(x_{N+1}, t)$ is a sinus with amplitude T_{N+1} the angle frequency ω and $T(x_1,t)=0$, the heat flow $q(x_{n+1}, t)$ will be:

$$q(x_{n+1},t) = T_{N+1}\left|G_n^N(\omega)\right| \cdot \sin\left[\omega \cdot t + angle\left(G_n^N(\omega)\right)\right] \qquad (8.12)$$

With a corresponding equation for $G^1{}_n$ with $T(x_{N+1}, t) = 0$ and $T(x_1, t)$ a sinus. The factor $|G^N{}_n(\omega)|$ is called the *gain* and angle($G^N{}_n(\omega)$) is the *phase*. The dependence of $q(x_{n+1}, t)$ on different frequencies can now easily be studied. Sometimes it is more convenient to deal with the period time t_p instead of the angle frequency:

$$t_p = 2\pi / \omega \qquad \text{(s)}$$

With $T_{N+1} = 1$ and $T(x_1, t)=0$ we get:

$$T(x_{N+1},t) = 1.0 \cdot \sin(2\pi \cdot t / t_p) \qquad \text{(K)} \qquad (8.13)$$

$$q(x_{n+1},t) = \left|G_n^N(t_p)\right| \cdot \sin\left[2\pi \cdot t / t_p + angle\left(G_n^N(t_p)\right)\right] \text{(W/m}^2\text{)} \qquad (8.14)$$

8.2 Windows

A heat flow meter was designed and built by Håkansson (1984). The heat flow meter was built from a circuit board with the thickness of 1.55 mm. The heat flow meter was tested by the Swedish National Test and Research Institute to have a voltage to heat flow constant of 19 +/- 1 W/m^2 /mV. This heat flow meter was applied to the window and the walls in the room.

8.2.1 Analysis of heat flow meter on inner 4-pane window

The frequency analysis of the window must be done with constant resistances in the airspace between the panes. This approximation is adequate for the convective/conductive heat transfer in the airspace since it is mainly conductive, thus not temperature dependent. The longwave radiation exchange depends on the absolute temperature but not on the temperature difference so the error of the approximation depends on the amplitude if the temperature variation. What is investigated here is how accurate the heat flow meter measures when placed on the inner pane where the temperature variation is moderate.

If the temperature inside or outside varies sinusoidally with the amplitudes $T^a{}_{in}$ and $T^a{}_{out}$ the transfer functions $G^{in}{}_n(t_p)$ and $G^{out}{}_n(t_p)$ describe how the heat flow varies at layer n.

$$q(x_{n+1},t_p) = \left|G_n^{in}(t_p)\right| \cdot T_{in}^a \sin\left(2\pi t / t_p + angle(G_n^{in}(t_p))\right) + \left|G_n^{out}(t_p)\right| \cdot T_{out}^a \sin\left(2\pi t / t_p + angle(G_n^{out}(t_p))\right) \quad (8.15)$$

Figure 8.1 shows the gain of the inner pane ($|G^{in}_{glass}|$), the flow into the heat flow meter ($|G^{in}_{hfm,in}|$) and the heat flow as measured by the heat flow meter ($|G^{in}_{hfm}|$) as dependent on the period in minutes. Figure 8.2 shows $|G^{out}_{glass}|$, $|G^{out}_{hfm,in}|$ and $|G^{out}_{hfm}|$. The quotient between $|G^{in}_{glass}/G^{in}_{hfm}|$ and $|G^{out}_{glass}/G^{out}_{hfm}|$ are shown in Figure 8.3. From these figures one can deduce that the heat flow meter measures the correct heat flow for any variation in temperature on the outer pane down to at least a period of 2 minutes. For a variation on the inner pane the heat flow meter measures within 10% error for periods over 10 minutes and within 5% error for periods over 4 hours. The heat flow meter can thus be used to verify the thermal window model (without solar radiation) with the accuracy of 5% if the temperature variation time period is more than 4 hours.

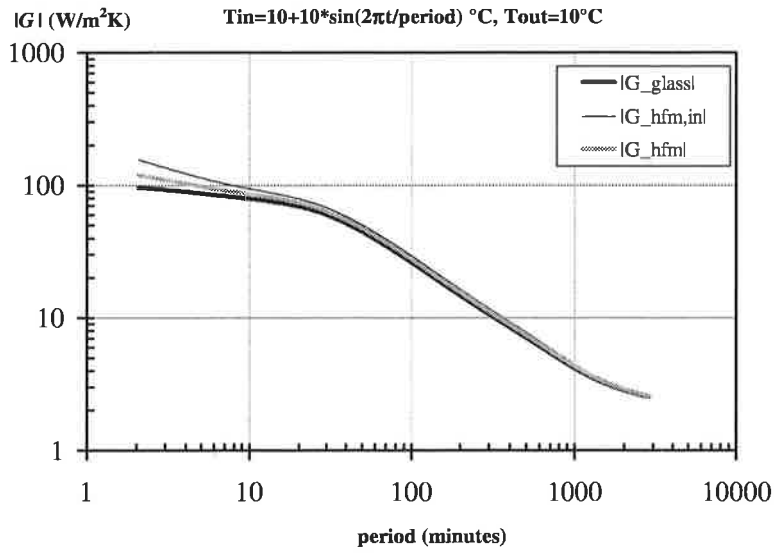

Figure 8.1 *The gain of the transfer functions $|G^{in}_{glass}|$, $|G^{in}_{hfm,in}|$ and $|G^{in}_{hfm}|$ for a sinusoidal temperature variation on the inside.*

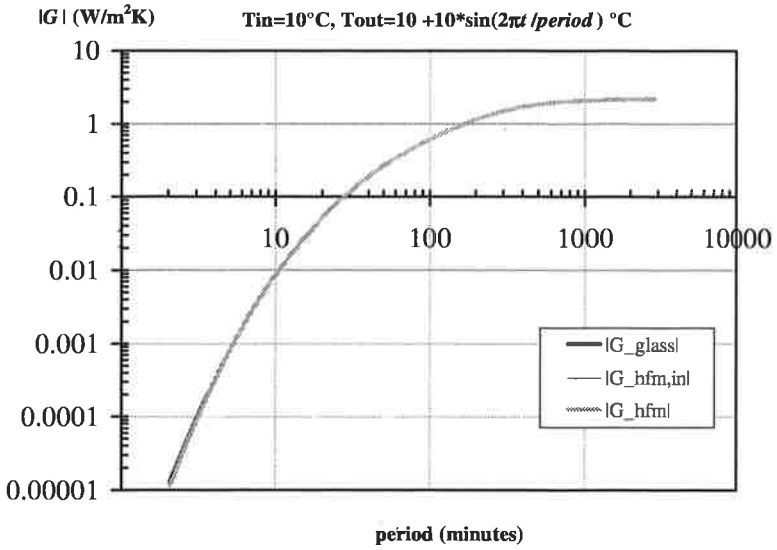

Figure 8.2 *The gain of the transfer functions* $|G^{out}_{glass}|$, $|G^{out}_{hfm,in}|$ *and* $|G^{out}_{hfm}|$ *for a sinusoidal temperature variation on the outside.*

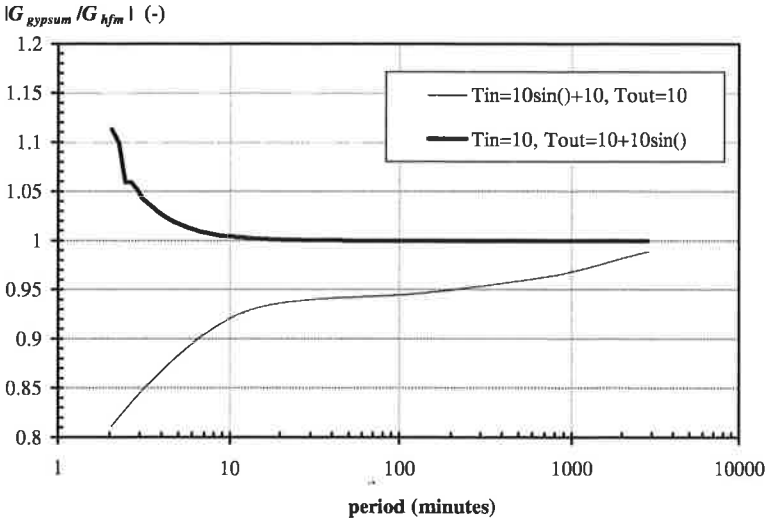

Figure 8.3 *The quotient* $|G^{in}_{glass} / G^{in}_{hfm}|$ *and* $|G^{out}_{glass} / G^{out}_{hfm}|$ *versus the period in minutes of the temperature.*

8.2.2 Comparison with heat flow meter measurements

Figure 8.4 shows a comparison between calculated and measured heat flow through the centre of the 4-pane window. The difference is in general less than 1 W/m^2 or 6 %. Figure 8.5 shows a comparison between calculated and measured heat flow through the centre of the 3-pane window. The difference is in general less than 2 W/m^2 or 7 %.

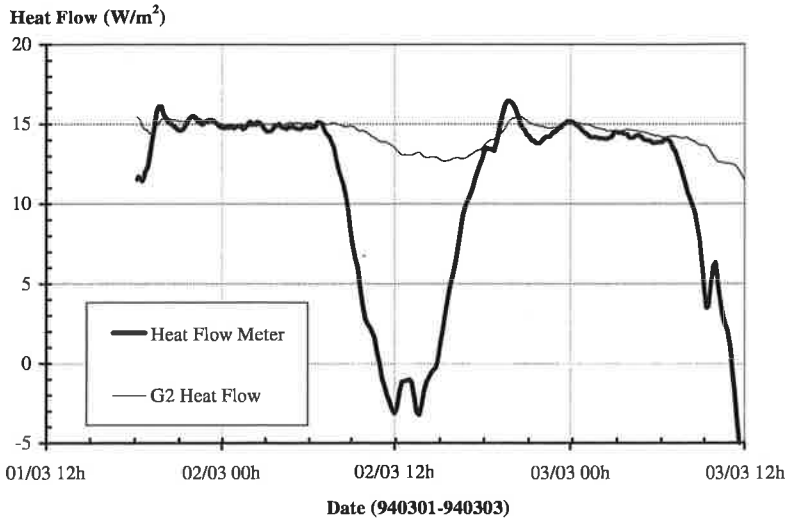

Figure 8.4 *Calculated and measured heat flow through the 4-pane window. The sun makes the daytime values unsuitable for comparison.*

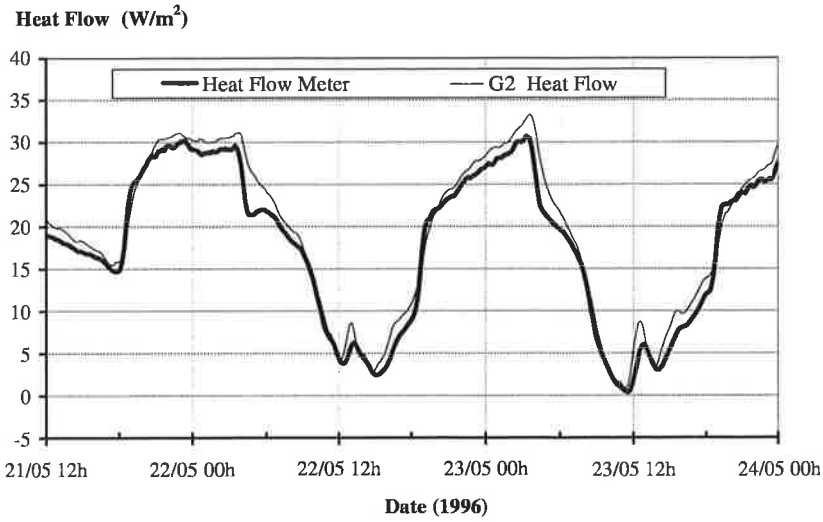

Figure 8.5 *Calculated and measured heat flow through the 3-pane window. Window completely shielded from sun.*

8.2.3 Mayer ladder

Measuring the convective heat transfer at a surface is difficult. In this report a roundabout method is used by first measuring and calculating the conductive heat transfer in the material, then the longwave radiation, then the solar absorption and finally finding the convective part as the difference between theses numbers. Delaforce (1993) used the temperature difference in the air close to the wall to estimate the convective heat transfer. The method is based on an instrument used by Mayer (1987) but Delaforce used different spacing of the thermocouples. Delaforce bases the calculations on the temperature profile:

$$T(x) = T_a + (T_{surf} - T_a) \cdot e^{-y/d_{bl}} \qquad \text{(K)} \qquad (8.16)$$

with

T_a	air temperature
T_{surf}	surface temperature
y	distance from surface
d_{bl}	thickness of thermal boundary layer

The convective heat flow at the surface is then

$$q_c = \lambda_{air}(T_a - T_{surf}) / d_{bl} \qquad (\mathrm{W/m^2}) \qquad (8.17)$$

The temperature profile usually proposed is for the turbulent case:

$$\begin{aligned} T^+ &= \mathrm{Pr}\cdot y^+ && y^+ < 5 && \text{Conductive sublayer} \\ T^+ &= A_1 \ln(y^+) + A_2 && 5 < y^+ < 40 && \text{Blending region} \\ T^+ &= A_3 \ln(y^+) + A_4 && 40 < y^+ && \text{Logarithmic (fully turbulent) region} \end{aligned} \qquad (8.18)$$

The equations for the velocity field are usually:

$$\begin{aligned} u^+ &= y^+ && y^+ < 5 && \text{Viscous sublayer} \\ u^+ &= B_1 \ln(y^+) + B_2 && 5 < y^+ < 40 && \text{Blending region} \\ u^+ &= B_3 \ln(y^+) + B_4 && 40 < y^+ && \text{Logarithmic (fully turbulent) region} \end{aligned} \qquad (8.19)$$

Dimensionless temperature : $T^+ = \rho c u_\tau \dfrac{T_{wall} - T(y)}{q_c}$ (–)

Dimensionless velocity: $u^+ = \dfrac{u}{u_\tau}$ (–)

Local Reynolds number: $y^+ = \dfrac{y u_\tau}{\nu}$ (–) (8.20)

Friction velocity: u_τ (m / s)

Prandtl number (=0.71 for air) Pr (-)

The coefficients in (8.18) and (8.19) can be determined by experiments or analysis. Yuan et al (1992) suggested the following formulae for both natural and forced turbulent convection air flow simulations in rooms. The equations are derived from forced convection but were validated with data from natural convection also:

$$
\begin{aligned}
T^+ &= \mathrm{Pr}\, y^+ && 0 < y^+ < 5 \\
T^+ &= 4.15 \ln(y^+) - 3.13 && 5 < y^+ < 18.6 \\
T^+ &= 3.60 \ln(y^+) - 1.52 && 18.6 < y^+ < 44.5 \\
T^+ &= 2.13 \ln(y^+) + 4.05 && 44.5 < y^+
\end{aligned}
\qquad (8.21)
$$

They suggested for the velocity profile:

$$
\begin{aligned}
u^+ &= y^+ && 0 < y^+ < 5 \\
u^+ &= 4.82 \ln(y^+) - 2.75 && 5 < y^+ < 18.6 \\
u^+ &= 3.47 \ln(y^+) + 0.98 && 18.6 < y^+ < 44.5 \\
u^+ &= 2.32 \ln(y^+) + 5.27 && 44.5 < y^+
\end{aligned}
\qquad (8.22)
$$

For natural convection Peng and Peterson (1995) suggested a variation on the formulae for laminar flow:

$$
\begin{aligned}
u &= u_1 \left(\frac{y}{\delta}\right)^{1/6} \left(1 - \frac{y}{\delta}\right)^2 \\
\delta &= \delta^* \, 3.138 \, \mathrm{Gr}_x^{-0.076} \\
\delta^* &= x \cdot \mathrm{Gr}_x^{-0.1} \\
u_1 &= 5.425 \frac{\nu}{x} \mathrm{Gr}^{0.424}
\end{aligned}
\qquad (8.23)
$$

Here Gr_x is the Grashof number :

$$
\mathrm{Gr}_x = \frac{g \beta (T_{air} - T_{wall}) x^3}{\nu^2} \qquad (8.24)
$$

This number times the Prandtl number is used to indicate whether a natural convection flow is turbulent or laminar. If $\mathrm{Gr}_x \, \mathrm{Pr} < 10^9$ the flow is mostly laminar. Over this value there is a transition zone until the flow is fully turbulent.

$$
\begin{aligned}
T &= T_{wall} + (T_{air} - T_{wall}) \left(\frac{y}{\delta_T}\right)^{\gamma} \\
\delta_T &= \delta^* \, 211.426 \, \mathrm{Gr}_x^{-0.38} && \text{inner layer} \\
\gamma &= 1.15 \\
\\
\delta_T &= \delta^* \, 7.810 \, \mathrm{Gr}_x^{-0.12} && \text{outer layer} \\
\gamma &= 1/7
\end{aligned}
\qquad (8.25)
$$

With these temperatures and velocity profiles the local heat transfer coefficient flow becomes:

$$h_c(x) = 0.0077 \cdot \lambda \, \mathrm{Gr}(x)^{0.46} / x \qquad (\mathrm{W/m^2}) \qquad (8.26)$$

where x is the distance from the leading edge.

A Mayer ladder was built at the Dep. of Building Science, see Figure 8.6 and Figure 8.7. The thermocouple wires had the diameter 0.08 mm. The ladder was placed on the window inner pane. Measurements were performed both with and without solar radiation.

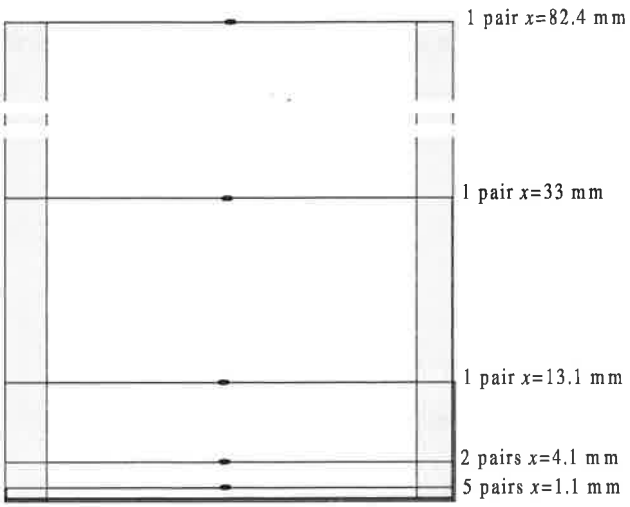

Figure 8.6 *Mayer ladder built at Dep. of Building Science by Håkansson.*

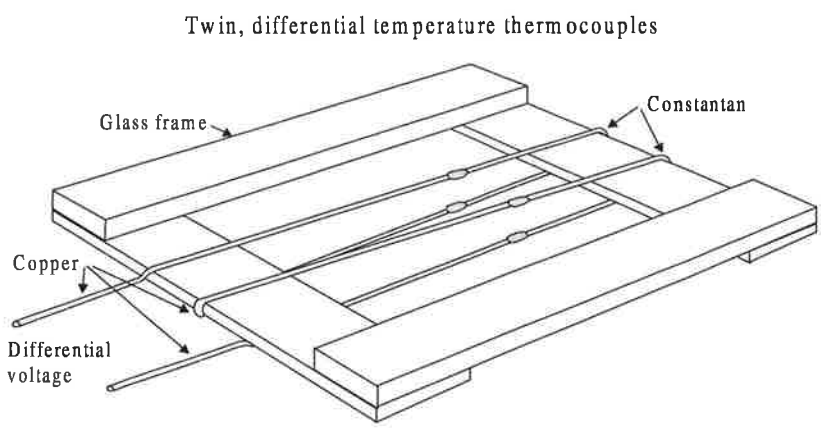

Figure 8.7 *The principle of how the first 5 thermocouple pairs are mounted. Only two pairs are shown in the figure.*

Figure 8.8 shows the temperature difference between surface and air according to the Mayer ladder. Strong solar radiation reverses the temperature difference during the day. The radiator was beneath the window and one can clearly see when it went on and off during the night. It should be emphasised that even though thermocouple measurements can not give the absolute temperature with a better accuracy than at best +/- 0.1 °C, a temperature difference measurement is very accurate. The reason for this is that the inaccuracy when measuring a reference temperature disappears. To increase the accuracy even more, 5 thermocouple pairs were used for the first node, 2 for the second and one for the rest. Even if the thermocouples absorb sun, this will not affect the net temperature difference between the nodes.

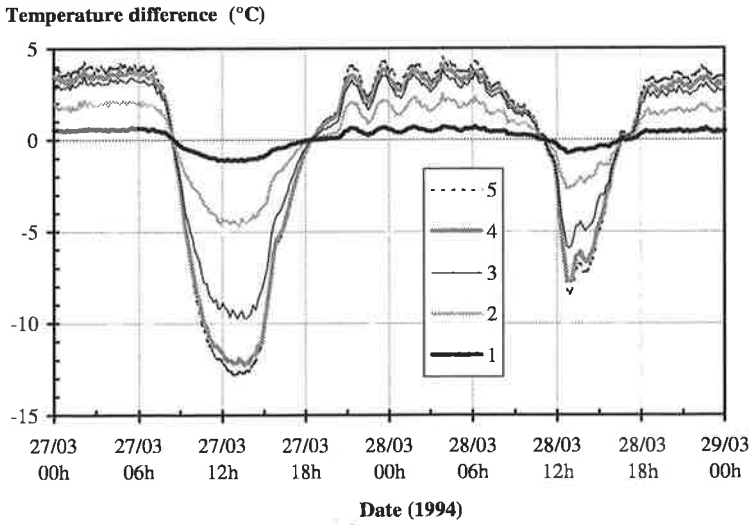

Figure 8.8 *Temperature difference between surface and air according to the Mayer ladder. Strong solar radiation reverses the temperature difference during the day. The radiator was beneath the window.*

To test equations (8.16)-(8.25) the different temperature profiles together with the measured values were plotted against the distance, see Figure 8.9 (radiator below window) and Figure 8.10 (radiator at back wall).

The case with radiator at the back wall is likely to result in laminar natural convection. The window is positioned in the middle of the wall 0.92 m from the floor. The effective length in the middle of the window might be more than 0.5 meter due to the wall. The frame of the window will of course affect the air flow. These two facts should increase the chances of getting a more turbulent flow. In Figure 8.9 all equations give reasonable accuracy when there is no sun. Equation (8.16) and (8.21) give very similar results. For the case with solar radiation (8.21) gives the best result and (8.25) has the largest discrepancy.

When the radiator is below the window the air flow is not only affected by the temperature of the window but also of the heated plume that raises above the radiator. The situation is not just natural convection. Figure 8.10 clearly shows that equation (8.25) which is valid for almost laminar natural convection does not describe what happens. Equation (8.16) and (8.21) give very similar results for this case also. Overall (8.21) gives the best results.

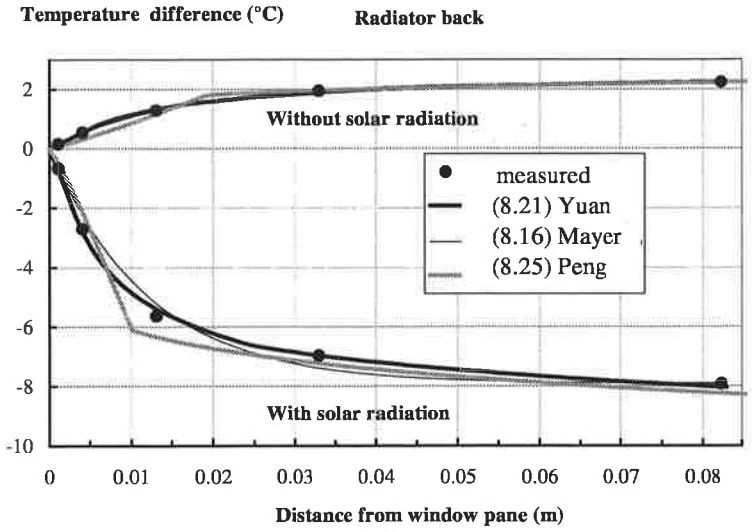

Figure 8.9 *Temperature difference between surface and air from equations (8.16), (8.21), (8.25) together with the measured values. Radiator beneath the window.*

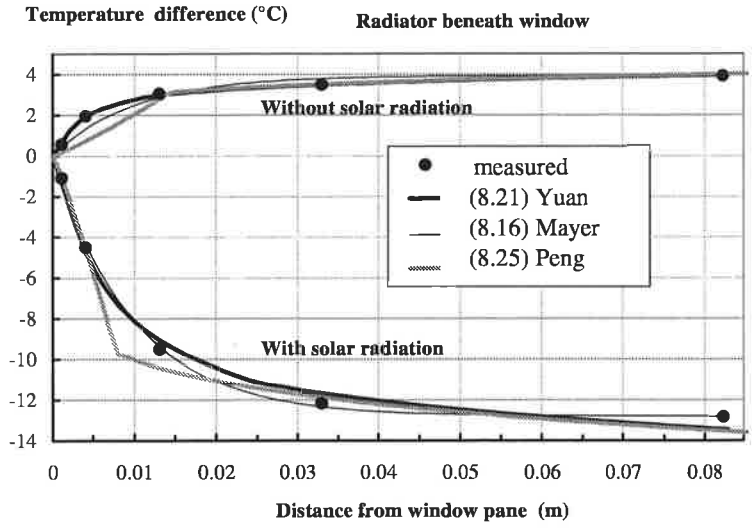

Figure 8.10 *Temperature difference between surface and air from equations (8.16), (8.21), (8.25) together with the measured values. Radiator at the back wall.*

Figure 8.11 shows the calculated air velocity from equations (8.22) and (8.23) together with two measured values. The case with solar radiation is not included here, since the anemometer is likely to be affected by the sun. The results from equation (8.22) are based on a numerical fit of heat flow q and the friction velocity u_τ. The anemometer did not have enough accuracy to be used to estimate u_τ so there is no verification of this value. Figure 8.11 indicates that u_τ is much too high or that the air velocity function is not valid so far away from the window pane.

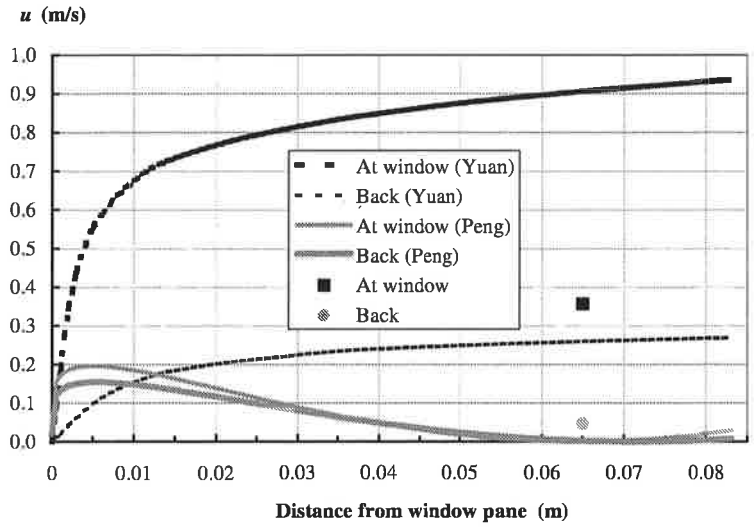

Figure 8.11 *The calculated velocity profiles from equations (8.22) and (8.23) together with measured values. Radiator beneath window and at the back wall, no sun.*

Table 8.1 shows the heat flow by conduction in the air between the pairs of thermocouples. The estimated heat flows based on equations (8.16)-(8.26) are also tabulated. In the air closest to the wall all heat transfer is performed by conduction. This is sometimes called the conductive sub layer. One would therefore expect that the estimated heat flows in Table 8.1 would increase with the distance from the window pane if the first one is beneath this layer. This is true except when the sun heats the pane. The difference in heat flow as measured by the first and second thermocouple pair (1.1 mm and 4.1 mm from the pane respectively) is however quite small even then. It seems reasonable to estimate the convective heat flow to the window as the conductive heat flow over

the first thermocouple pair. Only equation (8.21) has a linear behaviour close to the wall and consequently the equation whose results are closest to pure conduction close to the window is (8.21).

Table 8.1 *Heat flow from pure conduction and from estimations based on equations (8.16)-(8.26).*

	Radiator at window		Radiator at the back wall	
	no sun	sun	no sun	sun
y (m)	$q_{cond} = \lambda_{air} (T_a - T_{surf}) / y$ (W/m^2)			
0.0011	12.89	-24.47	3.49	-15.14
0.0041	11.97	-27.32	3.34	-16.48
0.0131	5.85	-18.09	2.46	-10.76
0.0330	2.63	-9.23	1.47	-5.27
0.0824	1.19	-3.88	0.68	-2.40

Exponential (8.16)				
d_{bl} (m)	0.0010	0.0010	0.0155	0.0122
q_c (W/m^2)	9.88	-32.07	3.60	-16.22

Yuan (fully turbulent) (8.21)				
u_τ (-)	0.0509	0.0271	0.0170	0.0271
$5y^+ =$ (m)	0.0015	0.0028	0.0044	0.0028
q_c (W/m^2)	15.10	-29.74	3.35	-17.75

Peng (mainly laminar) (8.26)				
$PrGr_{0.5}$ (-)	$5.25\ 10^7$	$1.71\ 10^8$	$2.98\ 10^7$	$1.06\ 10^8$
δ_T outer (m)	0.0152	0.0086	0.0200	0.0109
δ_T outer (m)	0.0813	0.0627	0.0921	0.0697
q_c (W/m^2)	6.33	-35.45	2.77	-17.56

Figure 8.12 shows the heat flow through the inner window pane as measured by the first thermocouple (Mayer 1) and calculated from the temperatures at the centre of the window (G_2). The radiator is positioned in the back of the room. Figure 8.13 shows the measured and estimated heat flow for a period with the radiator beneath the window.

In general the estimated and measured convective heat flow match quite well: the difference below +/- 1W/m^2 or relative difference +/-15%. This is achieved even when the window is exposed to strong sunlight. The largest discrepancy occurred during some of the nights when the radiator was back in the room. The difference then was ~1.5 W/m^2 under estimation or 10% under estimation for the G_2 measurements. The reason for this is not clear but the consequence is that the accuracy can be poor for low convective heat transfer (q_c< 4 W/m^2)

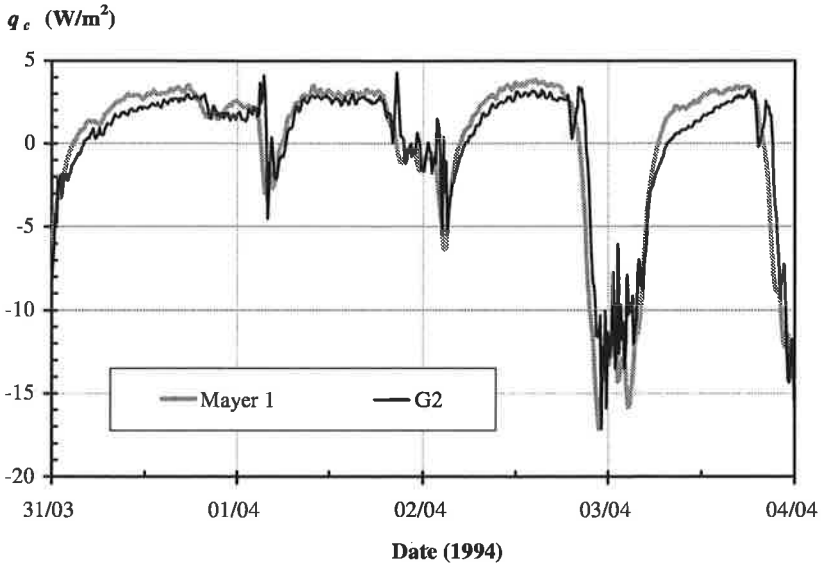

Figure 8.12 *The heat flow through the inner window pane as measured by the Mayer ladder and calculated from the temperatures at the centre of the window (G_2). The radiator is positioned in the back of the room.*

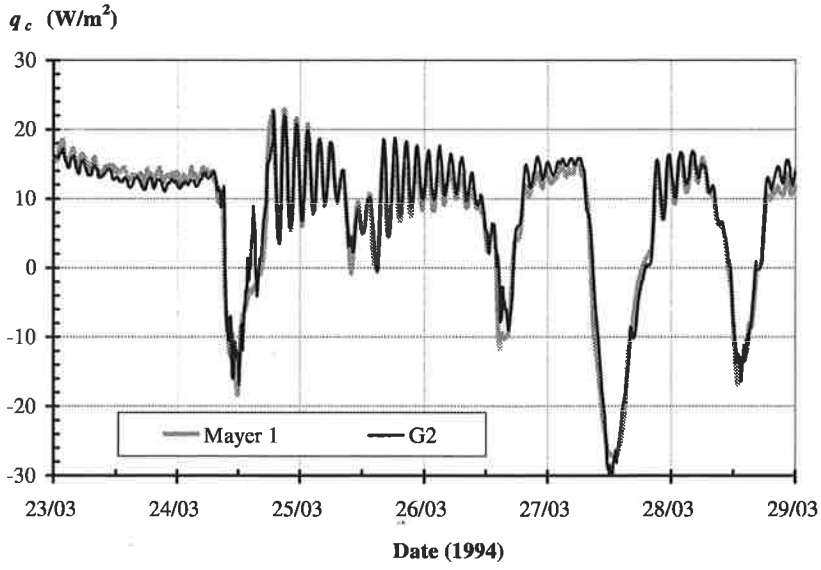

Figure 8.13 *The heat flow through the inner window pane as measured by the Mayer ladder and calculated from the temperatures at the centre of the window (G_2). The radiator is positioned below the window.*

Figure 8.14 shows the convective heat transfer coefficient h_c as measured by the Mayer ladder and calculated with the window model at G_2.

$$h_c = \frac{q_c}{T_{ref} - T_{G_2}} \qquad (\mathrm{W/m^2K}) \qquad (8.27)$$

In Figure 8.14 and Figure 8.15 the reference temperature is the average temperature 0.1 m from the window pane. In Figure 8.14 the ventilation was 1.0 ach from the window with the radiator below. Equations from Churchill and Chu and Min et al are shown for comparison. The difference between the Mayer h_c and G_2 h_c are small for large negative values of ΔT. Above –4 the difference increases. The reason for this is that the accuracy of the measurements becomes more noticeable for small absolute values for ΔT and, more important, the accuracy in the shortwave window model decreases with increasing inlet angle. For the air temperatures warmer than the window pane (ΔT>0) there seems to be a slight systematic overestimation of G_2 h_c compared to the Mayer h_c. The reason for this is not known.

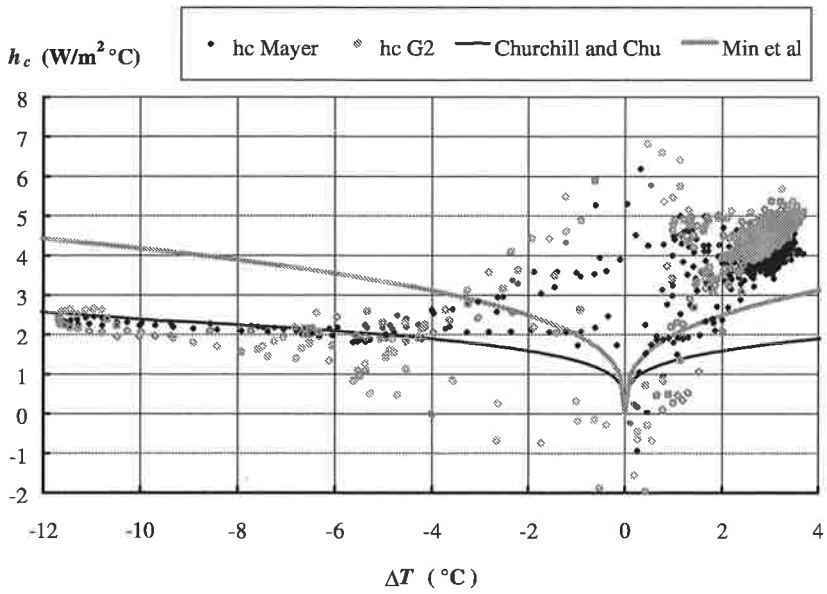

Figure 8.14 *Convective heat transfer coefficient h_c as measured by the Mayer ladder and calculated with the window model at G_2. Inlet 1.0 ach from the window. Radiator below window. Equations from Churchill and Chu and Min et al are shown for comparison.*

Figure 8.15 shows the same comparison as above but for a period with the ventilation directed towards the window. The match between G_2 h_c and Mayer h_c are similar to the case above, good for large negative ΔT values and decreasing above –4 °C. The difference here is that the match for positive ΔT is quite good also.

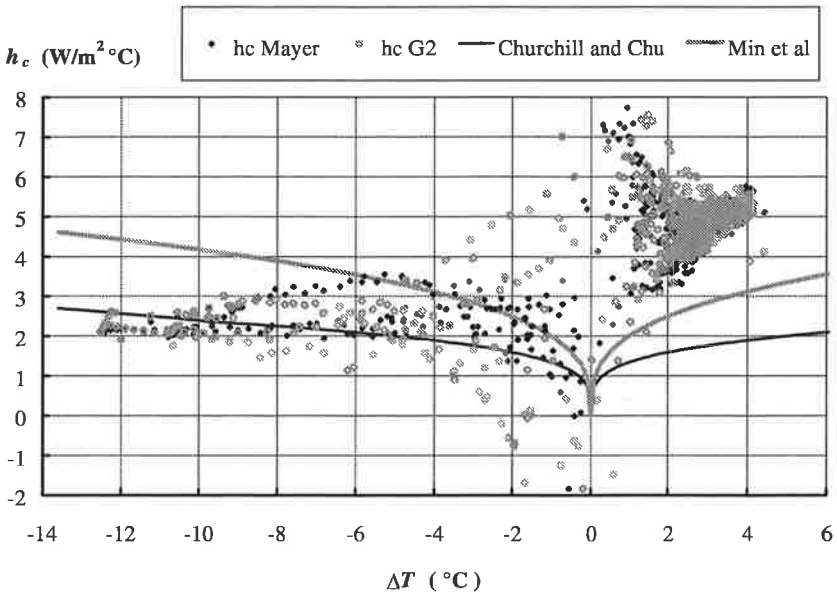

Figure 8.15 *Convective heat transfer coefficient h_c as measured by the Mayer ladder and calculated with the window model at G_2. Inlet 1.0 ach towards the window. Radiator below window. Equations from Churchill and Chu and Min et al are shown for comparison*

8.2.4 Accuracy of the one dimensional model of the window

The thermal model for the 3- and 4-pane window used in this study was one dimensional. The results from measurements never gave a Nusselt number over 1.15 for the 4-pane window and never over 1.005 for the 3-pane window. Thus, the heat transfer was all the time dominated by conduction especially for the 3-pane window. The effect of longwave radiation was of course still 3 dimensional between the glass panes. Wright and Sullivan (1995) and Shapiro et al (1987) used complete 2-and 3-dimensional models to calculate the local heat

transfer in a window. The model by Shapiro et al was transient with 3-dimensional for the panes but 1-dimensional for the vertical heat transfer between the panes. In spite of this simplification they found good agreement between measurements with sun and calculations. Wright and Sullivan used a full 2-dimensional model for both the solid materials and the gas (air and argon), but did not model solar radiation. They used both a specular and diffuse radiation model but concluded that the specular model was unnecessary. From their results it is not clear how much a 1-dimensional approximation of the vertical heat transfer between the window panes would affect the results. They found that, in general, the local heat transfer varied very little within 10%-90% of the glass height.

The results from Shapiro indicated that a calculation with a 1-dimensional model for the vertical heat transfer between the panes and a 2-dimensional model for the solid material would give a realistic result. The calculation of a 3-pane insulated glass unit is the worst case, with a Nusselt number of 1.15 is the conduction increased 15% in the gap between the panes. On the other hand did the 3-pane unit have panes with low-e coatings thus reducing the importance of the longwave multidimensional effects.

The hypothesis that the local heat transfer coefficient could me measured by using the thermocouples on both sides of the IGU was therefore tested with a 2D calculation of the 4-pane window. The calculation was done with Heat2 (Blomberg 1996). An example of how the heat transfer coefficient can vary over the window pane is shown by Curcija (1992) who calculated the heat transfer in window and frame with a full 2-dimensional model. The model included radiation and laminar natural convection on inside, outside and between panes. Figure 8.16 shows the geometry Curcija used to calculate the heat transfer coefficient. The boundary conditions were:

Window pane	Boundary in air
T_w=7.2 °C	T_a=21.1 °C
u =0 m/s	u = 0 m/s
v = 0m/s	

Here u is the air velocity in the x direction and v the air velocity in the y direction. Figure 8.17 shows the convective heat transfer coefficient at a vertical line over the window.

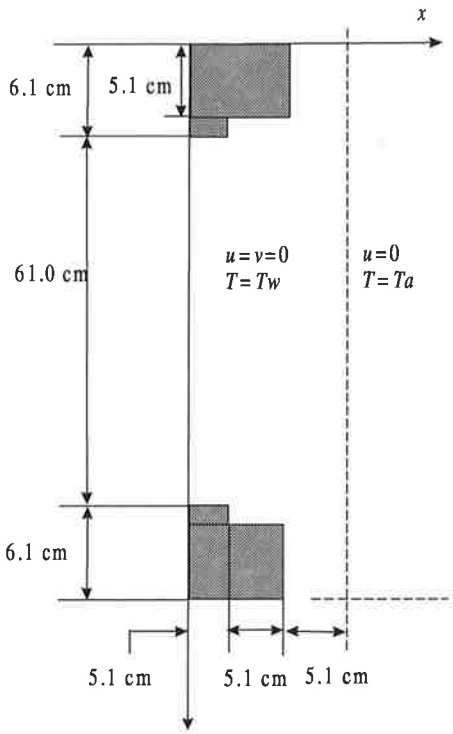

Figure 8.16 *Model used by Curcija to calculate the convective heat transfer coefficient on the inside surface of a window. T_w=7.2 °C and T_a=21.1 °C.*

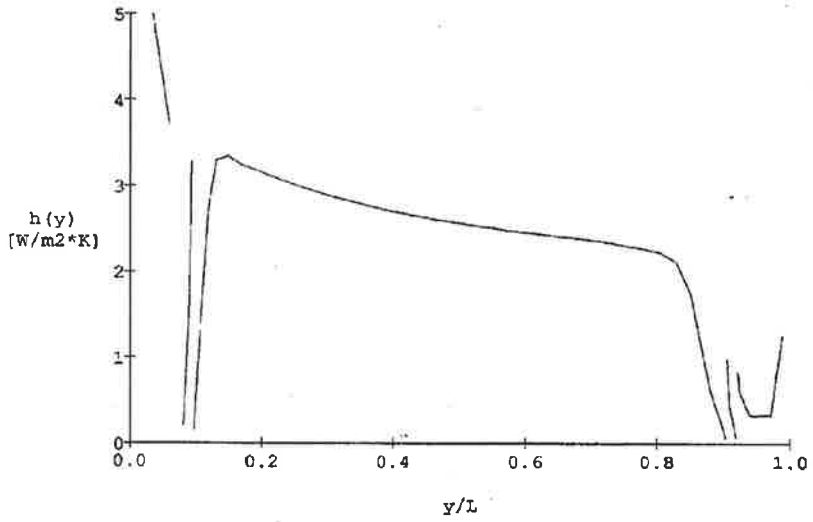

Figure 8.17 *The calculated heat transfer coefficient at a vertical line over window including frames. L=0.61m is here the total length of the simulation including frame, y is taken from top to bottom. (Curcija, 1992)*

In the investigation here the total heat transfer coefficient was set to fixed values over the height of the window pane. The values were chosen similar to those of Curcija. Figure 8.18 shows the fixed values for h_{tot} as well as the h_{tot} values based on a one dimensional calculation from pane 3 to pane 1, with the inner pane as number 1. The h_{tot} calculated this way resembles very much the method used in this study to measure the local heat transfer at a window pane. Figure 8.18 shows that the "measured" and fixed heat transfer coefficient matches quite well even 10 cm from the window corner. Figure 8.19 shows the same calculation except that the fixed h_{tot} has rather arbitrarily been set to vary contrary to the previous example. Even here the match between h_{tot} fixed and h_{tot} "measured" is good 10 cm from the corner.

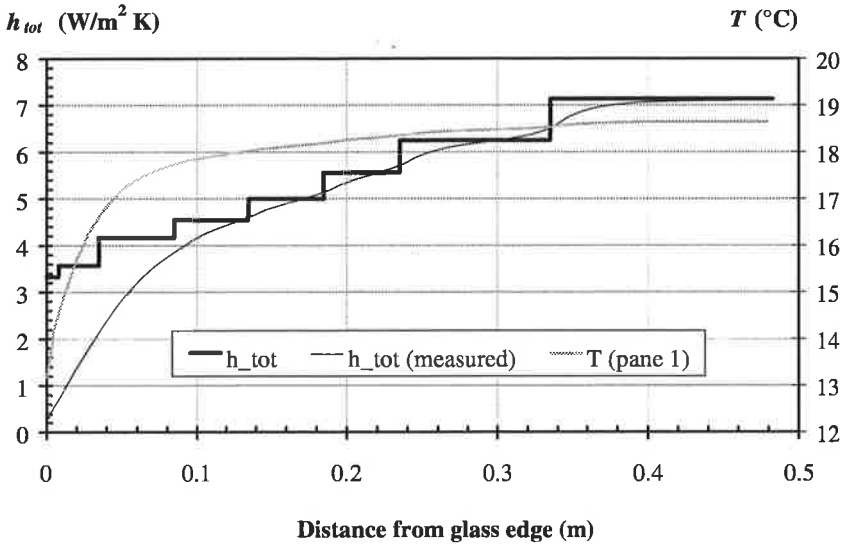

Figure 8.18 *The simulated measured and actual heat transfer coefficient used as boundary condition for window heat transfer calculation.*

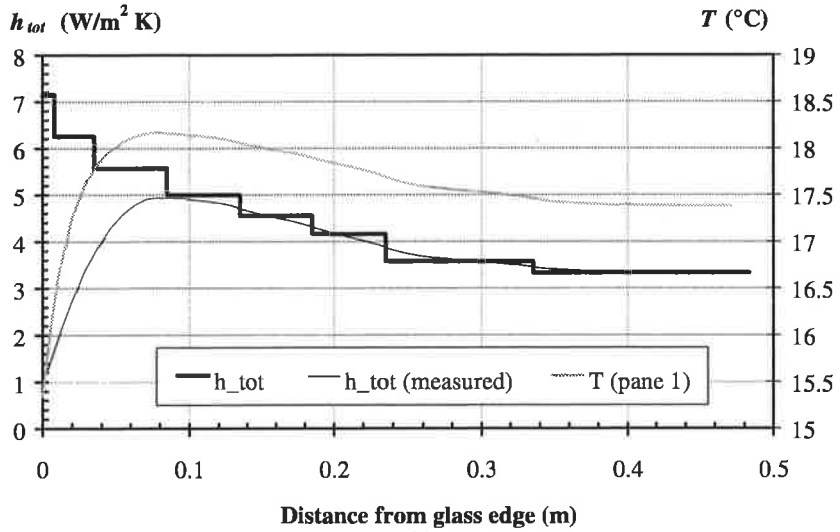

Figure 8.19 *The simulated measured and actual heat transfer coefficient used as boundary condition for window heat transfer calculation.*

The conclusion from this numerical experiment was that the thermocouples 10 cm from the glass edge (G_1, G_3 and G_4) could be used to estimate the local heat transfer coefficient. The thermocouple in the down left corner G_5 was however ruled out as being too affected by the 2 and 3 dimensional effects. The numerical experiment was not repeated for the 3 pane window. In this case the thermocouples were on each side of a 2-pane insulated glass unit instead of a 3-pane unit. If the local heat transfer coefficients were acceptable for the 4-pane window, the transfer coefficients on the 3-pane window should be even better.

8.3 Wall

8.3.1 Finite difference or frequency analysis model

We will here show a comparison between a frequency and finite difference approach for solving equation (8.1). Both methods have their advantages and disadvantages. Given is: temperatures at the discrete times $T_{in}(t_n)$ and $T_{out}(t_n)$ for n = 1 to N and the physical description of the wall.

Frequency model

With the above model it is possible to calculate the heat flow through a wall with given temperatures on both sides of the wall, Anderlind (1996). The discrete Fourier transform for temperatures given at the discrete times $T_{in}(t_n)$ and $T_{out}(t_n)$ is calculated as:

$$\tilde{T}_{in}(\omega_k) = \int_{-\infty}^{\infty} e^{i\omega_k t} T_{in}(t)\,dt \approx \Delta_t \sum_{n=1}^{N} e^{i\omega_k \Delta_t n/N} T_{in}(t_n)$$

$$\omega_k = k\frac{2\pi}{N\Delta_t}, \qquad -N/2-1 < k < N/2+1 \tag{8.28}$$

$$\Delta_t = t_{n+1} - t_n \qquad \text{(constant)}$$

The approximation in (8.28) suffers from two limitations: the input signal is only N steps long and the sample is done with the timestep Δ_t. The *Nyquist* frequency $1/(2N\,\Delta_t)$ defines the maximal frequency that can be correctly sampled if the input signal is infinitely long.

The temperatures can now be used in for example (8.5) to give $\tilde{q}\,(x, \omega)$. The inverse discrete Fourier transform can now be used to produce $q(x,t_n)$. Heat flow calculated from this method is hereafter called $q_{frequency}$.

Finite difference model

Another possibility to solve (8.1) numerically is to use a finite difference model:

$$\frac{T(x_i,t_{n+1}) - T(x_i,t_n)}{\delta t} \approx \frac{\lambda}{\rho c}\left\{\theta \cdot D_{2x}T(x_i,t_{n+1}) + (1-\theta)\cdot D_{2x}T(x_i,t_n)\right\} \tag{8.29}$$

$$D_{2x}\,T(x_i,t_n) = \frac{T(x_{i+1},t_n) - 2T(x_i,t_n) + T(x_{i-1},t_n)}{\delta x^2}$$

If $\theta = 0$ equation (8.29) is an explicit difference method. If $\theta > 0$ it is an implicit method. If $\theta = 0.5$ equation (8.29) is the Crank-Nicolson method. The advantage of implicit methods is that a larger timestep δt can be used than for explicit methods. The disadvantage is that a system of equations has to be solved. In this study both methods have been used.

	Frequency approach	**Finite difference approach**
+	Based on analytical solution Faster.	Possible to model parameter depending on e.g. temperature. No penalties for finite input signals.
-	Long calculations Physical properties dependent on the temperature can not be modelled Frequencies more than half of the Nyquist frequency will be distorted due to the finite length of the input signal	Slower Accuracy depends on time discretisation and length discretisation

8.3.2 Analysis of heat flow meter on wall

Measurements have been performed with a heat flow meter placed on window and wall. Lindfors and Christoffersson (1995) showed that the thermal properties of the heat flow meter, when measuring on 0.78 m insulation, is not negligible. They used a frequency or transfer function analysis of the heat conduction. The physical parameters for the wall investigated here are listed below. Only the heat flow meter, gypsum board and the first mineral wool slice were used. The second slice was not needed when the thermocouple between the two mineral wool slices was used as boundary condition.

λ_{gypsum}	= 0.22	W/mK
$\lambda_{minwool}$	= 0.036	W/mK
λ_{hfm}	= 0.224	W/mK
$c_{minwool}$	= 19 740	J/m^{3}K
c_{hfm}	= 2.12	MJ/m^{3}K
$d_{minwool}$	= 0.09	m
d_{hfm}	= 0.00155	m
d_{gypsum}	= 0.013	m

The heat transfer measured by the heat flow meter is approximately the temperature difference over the heat flow meter divided by the resistance over the meter. This will not be exactly the same heat flow that goes into the internal surface of the heat flow meter. The measured heat flow is here called q_{hfm} and the heat flow that goes into the surface of the heat flow meter is called $q_{hfm,in}$. The temperature on the internal side is denoted $T_{hfm,in}$. The transfer functions with only internal temperature variation are here defined:

$$\tilde{q}_{hfm,in}(t_p) = \tilde{T}_{hfm,in}(t_p) \cdot G_{hfm,in}(t_p)$$

$$\tilde{q}_{hfm}(t_p) = \tilde{T}_{hfm,in}(t_p) \cdot G_{hfm}(t_p) \qquad (8.30)$$

$$\tilde{q}_{gypsum}(t_p) = \tilde{T}_{hfm,in}(t_p) \cdot G_{gypsum}(t_p)$$

Here q is defined as positive from inside to outside. The dependency on the period time t_p can now be investigated. Figure 8.20 shows the gain of the transfer functions: G_{gypsum}, $G_{hfm,in}$ and G_{hfm} versus the period in minutes of the temperature. Figure 10.2 shows the phase angle of the same functions.

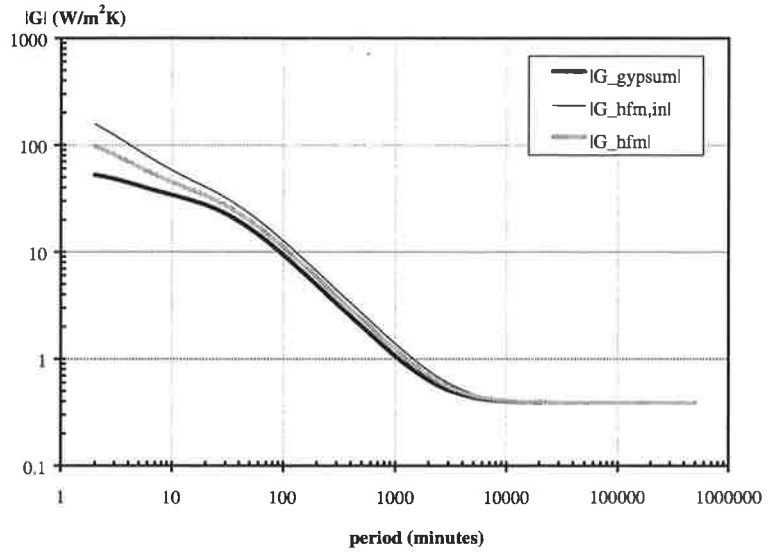

Figure 8.20 *The gain on the transfer functions: G_{gypsum}, $G_{hfm,in}$ and G_{hfm} versus the period in minutes (t_p).*

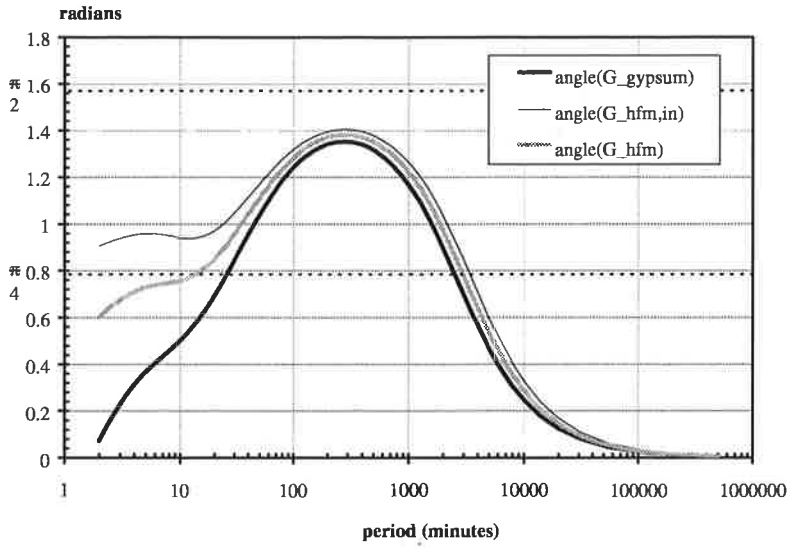

Figure 8.21 *The angle on the transfer functions: G_{gypsum}, $G_{hfm,in}$ and G_{hfm} versus the period in minutes of the temperature.*

Figure 8.22 shows the quotient between the gains $|G_{gypsum} / G_{hfm}|$ versus the period. It is clear that the amplitude of the heat flow on the gypsum surface is less than 85% of the measured heat flow if $t_p < 100$ min. If the period is less than 1100 min or 18h the flow into the gypsum board is still only 90% of the measured one. Figure 8.23 shows the phase difference between G_{hfm} and G_{gypsum}. For 24h period the phase difference is 0.067 rad which means a time lag of 15 min between the peak for the heat flow meter and the peak for the gypsum surface.

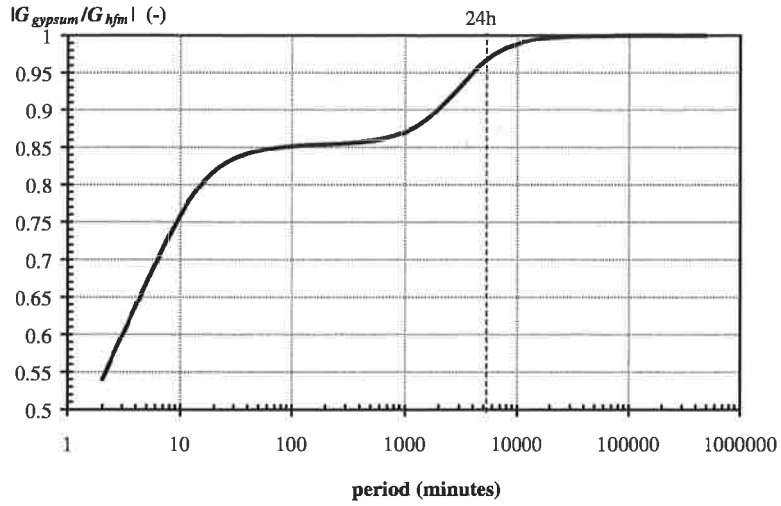

Figure 8.22 *The quotient $|G_{gypsum} / G_{hfm}|$ versus the period in minutes of the temperature.*

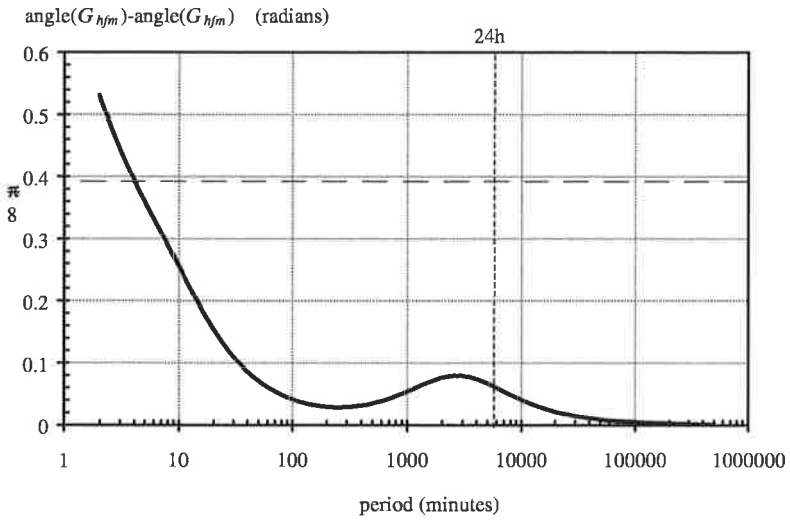

Figure 8.23 *The difference in radians between the phase of: G_{gypsum} and G_{hfm} versus the period in minutes.*

From these calculations it is quite clear that the capacity of the heat flow meter is very important when the temperature on the inside varies with a period less than 18h.

8.3.3 Comparison with measured and simulated heat flow

Calculations performed with both the frequency and finite difference model have been compared with measurements from the heat flow meter. During 1998-01-12-16 and 1996-05-29-31 the sample frequency was 10 minutes and during 1994-04-28-1994-05-08 the sample frequency was 30 minutes. Figure 8.24 shows the temperatures at position vb-4 and vb-2 1996-05-29-1996-05-31. The thermocouple vb-4 is on the middle of the wall on the gypsum board and vb-2 between the two mineral wool layers. The electric heater was either maximal 500W 29/5 (18:10-30/5 4:00 and 30/5 19:00 - 31/5 3:40) or completely off.

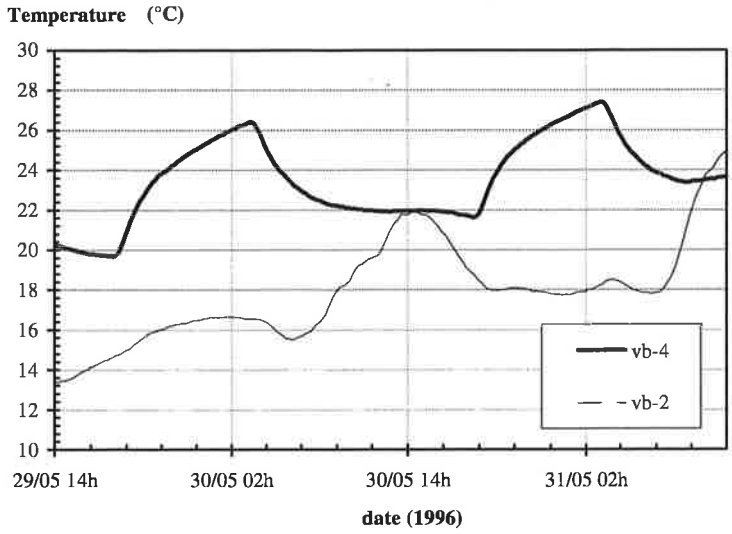

Figure 8.24 *Temperature on the inside (vb-4) and between the two mineral wool layers.*

Figure 8.25 shows the measured, $q_{measured}$, the calculated heat flow through the heat flow meter $q_{hfm,frequence}$ and through the gypsum surface $q_{gypsum,frequence}$. Calculations are made with frequency analysis. The distortion in beginning and end is due to the fact that the frequency analysis is based on a finite time series. From Figure 8.25 one can see that the calculated and measured heat flow is very similar except when the temperature increases slowly after the first sharp increase when the electric heater has been turned on. The mean 30 min difference was +/- 0.3 W/m^2 and the difference during the slow rise in temperature was with, addition to the variation above, 0.5 W/m^2 systematic under estimation. When the heater is turned off the calculation fits well again. Exactly what

part of the model that creates this discrepancy in heat flow is not clear. It could be that the heat flow is not one-dimensional for these large temperature steps on the inside or maybe a moisture transport in the mineral wool. It is obvious from the figure that the heat flow through the gypsum board surface has a lower amplitude than the heat flow through the heat flow meter. This fits well with the calculations in section 8.3.2.

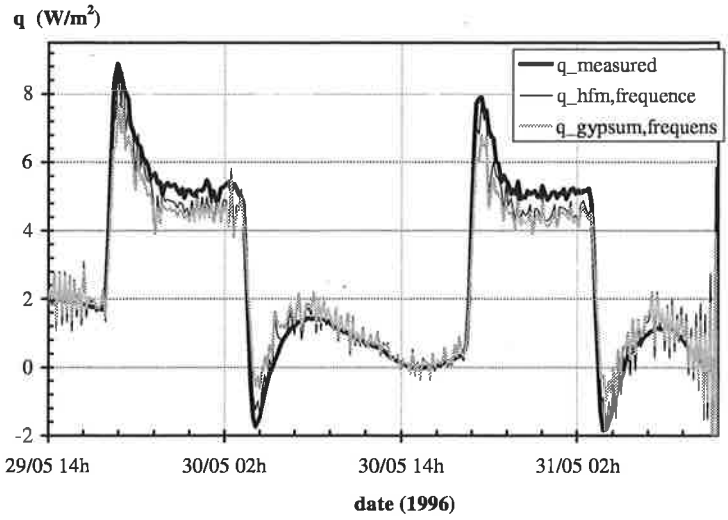

Figure 8.25 *The measured heat flow , $q_{measured}$, the calculated heat flow through the heat flow meter $q_{hfm,frequence}$ and through the gypsum surface $q_{gypsum,frequence}$. Calculations with frequency analysis.*

Figure 8.26 shows the temperature on the inside (vb-4) during 1998 –01-12 to 1998-01-16. The heater had a maximal effect of 1000 W and had set temperatures of 25 °C, 34°C, 0°C (off) and 34°C respectively.

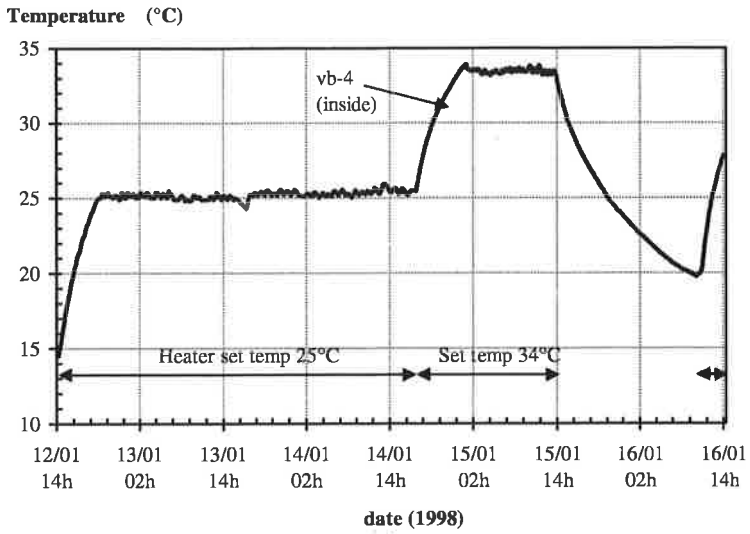

Figure 8.26 Temperature on the inside (vb-4).

Figure 8.27 shows the calculated and measured heat flow through the heat flow meter for 12/1 to 13/1. The heat flow is calculated with both the frequency model ($q_{frequency}$) and the finite difference model (q_{FD}). The distortion in the beginning is due to the finite time series. It is clear that except in the beginning the finite difference and frequency models are adequate and give a heat flow very close to the measured one. Note that the temperature on the wall surface increases from 15 to 25 °C during this period. The discrepancy in heat flow from Figure 8.27 can not be seen here in spite of this increase in temperature. The mean 30 min error was +/- 0.5 W/m^2. The reason that the heat flow goes up and down frequently is due to the fact that the heater is controlled by its own bimetallic control and the fact that the heater is overdimensioned (1000 W) for this small room.

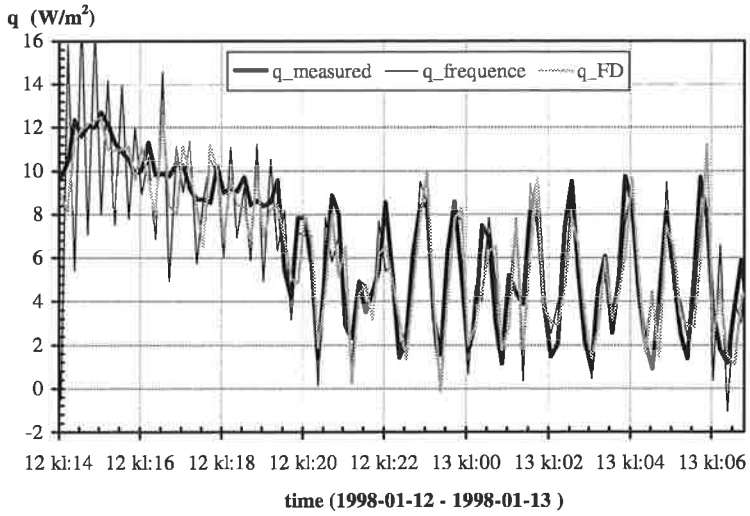

Figure 8.27 *The measured, $q_{measured}$, and calculated heat flow through the heat flow meter from frequency analysis $q_{frequence}$ and finite difference q_{FD}.*

Figure 8.28 shows the same as above for the period 1998-01-14 –16. Here the discrepancy in heat flow can be seen when the temperature increases from 25 to 34 °C. At all other times the fit is quite good.

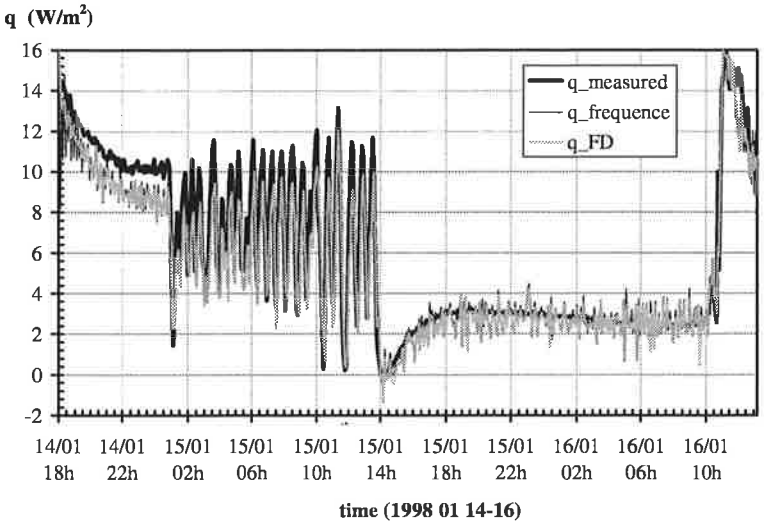

Figure 8.28 *The measured, $q_{measured}$, and calculated heat flow through the heat flow meter from frequency analysis $q_{frequence}$ and finite difference q_{FD}.*

Figure 8.29 is a blow up of Figure 8.28. One can see that the calculated heat flow has a slightly smaller amplitude than the measured one.

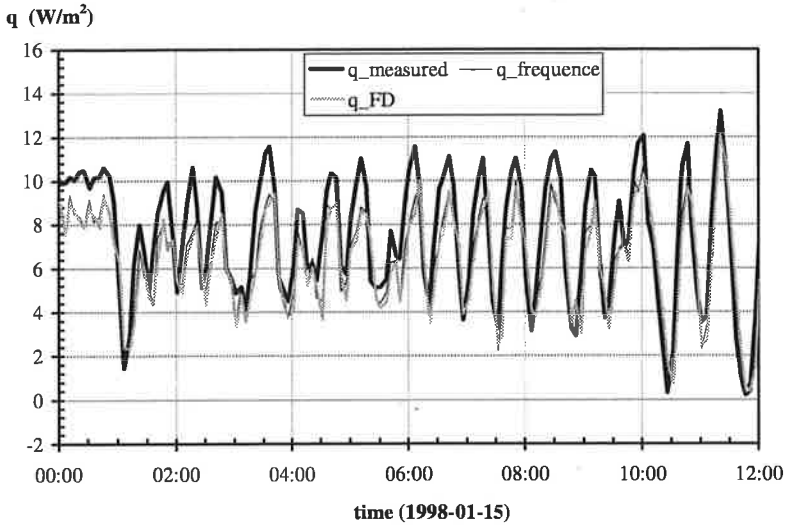

Figure 8.29 *The measured, $q_{measured}$, and calculated heat flow through the heat flow meter from frequency analysis $q_{frequence}$ and finite difference q_{FD}.*

Figure 8.30 shows the measured and calculated heat flow 1994-04-28 – 1994-05-08. The sampling frequency was 30 minutes. The fit between measured and simulated heat flow is quite satisfying with a mean error less than +/- 0.3 W/m^2

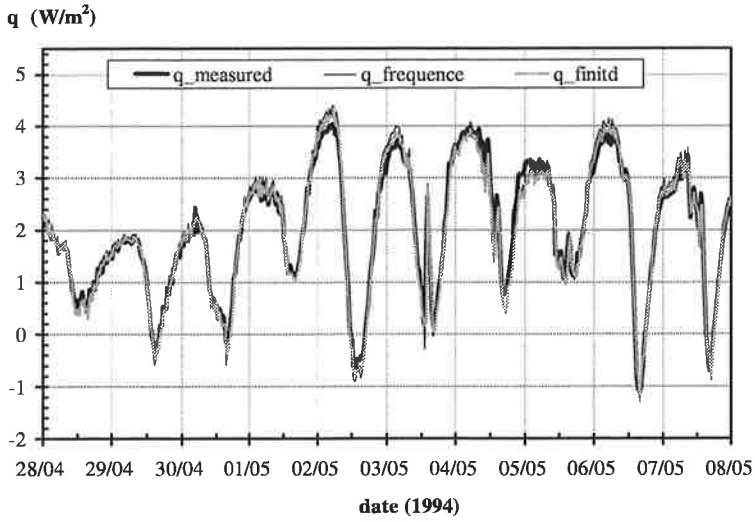

Figure 8.30 *The measured, $q_{measured}$, and calculated heat flow through the heat flow meter from frequency analysis $q_{frequence}$ and finite difference q_{FD}.*

8.4 Importance of thin thermocouples

8.4.1 Theory

The main problem of measuring temperatures in a room with a window is the fact that the thermocouples will absorb solar and longwave radiation. When a surface temperature is to be measured it is enough to make the contact between the surface and the thermocouple good and the surface of the thermocouple similar to the surface. When measuring air temperature one can use different diameters of thermocouple wire or try to shield the thermocouple with a metal cylinder etc. This may lead to a change in the airflow close to the thermocouple.

To investigate the proportion between radiation and convection exchange for a thermocouple wire a brief calculation follows:

To find the convective heat transfer coefficient a simple calculation with the Nusselt number from McAdams (1954) gives (for $Re_D<1000$):

$$\mathrm{Re}_D = \frac{uD}{\nu} \qquad (-)$$

$$\mathrm{Nu}_D = 0.32 + 0.43\ \mathrm{Re}_D{}^{0.52} \qquad (-) \tag{8.31}$$

$$h_c = \frac{\lambda\,\mathrm{Nu_D}}{\mathrm{D}} \qquad (\mathrm{W/m^2{\circ}C})$$

$$H_c = 2\pi D h_c = 2\pi\lambda\left(0.32 + 0.43\ \mathrm{Re}_D{}^{0.52}\right) \qquad (\mathrm{W/m{\circ}C})$$

Here D is the diameter of the thermocouple, u the air velocity, ν the kinematic viscosity and λ the thermal conductivity. The convective heat transfer coefficient per unit area is h_c and the convective heat transfer coefficient per meter thermocouple is H_c. For the longwave radiation exchange the following is true:

$$h_r = \sigma\varepsilon_{eff}\left(T_t + T_r\right)\left(T_t^2 + T_r^2\right) \qquad (\mathrm{W/m^2K})$$

$$H_r = 2\pi D\sigma\varepsilon_{eff}\left(T_t + T_r\right)\left(T_t^2 + T_r^2\right) \qquad (\mathrm{W/mK}) \tag{8.32}$$

Here σ is Stefan-Boltzmann's constant, ε_{eff} is the effective emissivity, T_t and T_r are the thermocouple and surrounding radiation temperatures. The radiation heat transfer coefficient per unit area is h_r and the radiation heat transfer coefficient per meter thermocouple is H_r. The radiant part will decrease faster than the convective part when the diameter is reduced. The static energy balance per unit length thermocouple is:

$$(T_t - T_a)H_c + (T_t - T_s)H_s = q_{abs} \qquad (\mathrm{W/m}) \tag{8.33}$$

Here q_{abs} is the shortwave (solar) radiation absorbed by the thermocouple and T_a is the air temperature. The temperature T_t becomes:

$$T_t = T_a\frac{H_c}{H_c + H_r} + T_r\frac{H_r}{H_c + H_r} + \frac{q_{abs}}{H_c + H_r} \qquad (\mathrm{°C}) \tag{8.34}$$

Figure 8.31 shows the quotient $H_r/(H_r + H_c)$ as a function of the diameter.

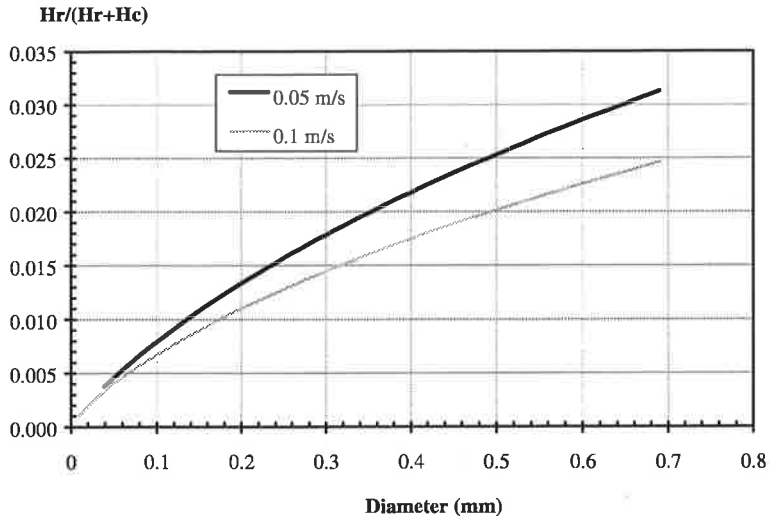

Figure 8.31 *The quotient $H_r/(H_r+H_c)$ as a function of the diameter D. All the temperatures at 20°C (ε_{eff}=0.2).*

The heat transfer coefficient for radiation exchange is only 3% of the total heat transfer if q_{abs} is zero. In practice the radiation temperature is negligible. According to this simple calculation it is about three times better to use a thermocouple with the diameter 0.08 mm than one with the diameter 0.5 mm with respect to the longwave radiation. A simple model for the solar absorption of solar radiation of the thermocouple is:

$$q_{abs} = D\alpha q_{sol} \qquad (\mathrm{W/m}) \tag{8.35}$$

Here α is the absorption coefficient for the metal. The energy balance for the thermocouple is then:

$$(T_t - T_a)H_c + (T_t - T_s)H_s = D\alpha q_{sol} \qquad (\mathrm{W/m}) \tag{8.36}$$

The difference between the air temperature and the thermocouple temperature is here called ΔT:

$$\Delta T = \frac{D\alpha q_{sol} + (T_r - T_l)H_r}{H_r + H_c} \qquad (°\mathrm{C}) \tag{8.37}$$

Figure 8.32 shows ΔT as a function of the diameter when q_{sol} is 400 W/m^2 and α is 0.4 (copper). Figure 8.33 shows ΔT as a function of the solar radiation q_{sol}.

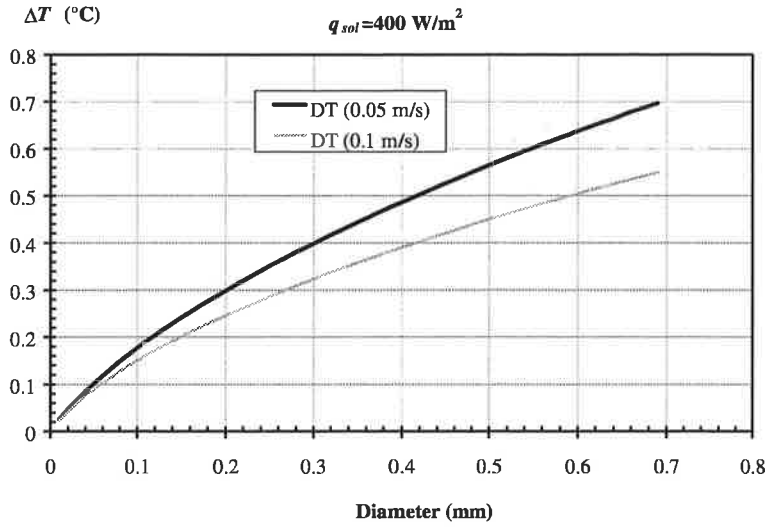

Figure 8.32 *The temperature difference ΔT between air and thermocouple as a function of the diameter, α=0.4.*

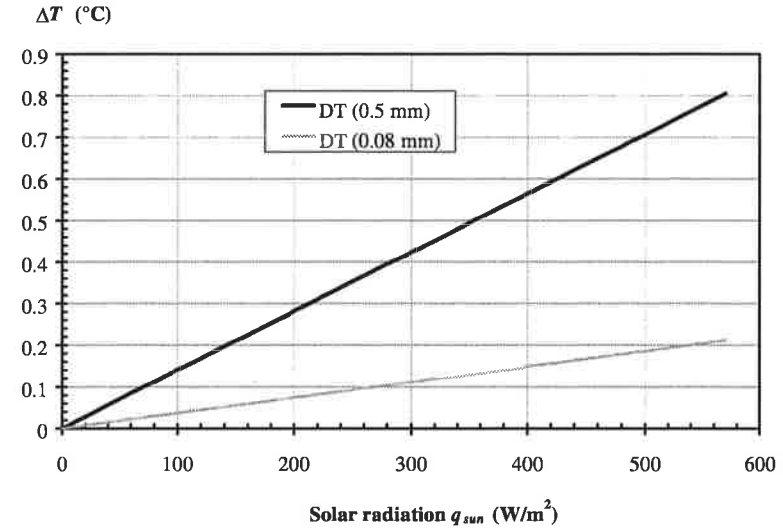

Figure 8.33 *The temperature difference ΔT as a function of the solar radiation, u=0.1 m/s, α=0.4.*

8.4.2 Measurements

At the Dep. of Building Science some simple tests have been performed to test the importance of the thermocouple design (Wall 1992). The thermocouples that were tested were:

1. "Ordinarily twisted". The thermocouple was stripped about 10 mm, twisted together and soldered. Diameter 0.5 mm.
2. "Chimney". A thermocouple of the ordinarily twisted type is placed in a 20 mm diameter metal tube. The tube faces upward.
3. "Aluminium foil". An ordinarily twisted thermocouple with aluminium foil clamped on as a radiation shield.
4. Thermocouple stripped 50 mm and twisted and soldered.
5. Thermocouple stripped 100 mm.
6. Thermocouple stripped 150 mm.
7. Thin 0.08 mm diameter with 100 mm stripped.

Figure 8.34 shows the temperature measured July 8, 1991 in a glazed room. Number 4, 5 and 6 gave a similar result and therefore only 5 is plotted here. The global radiation was 800 W/m^2 on a vertical surface at noon.

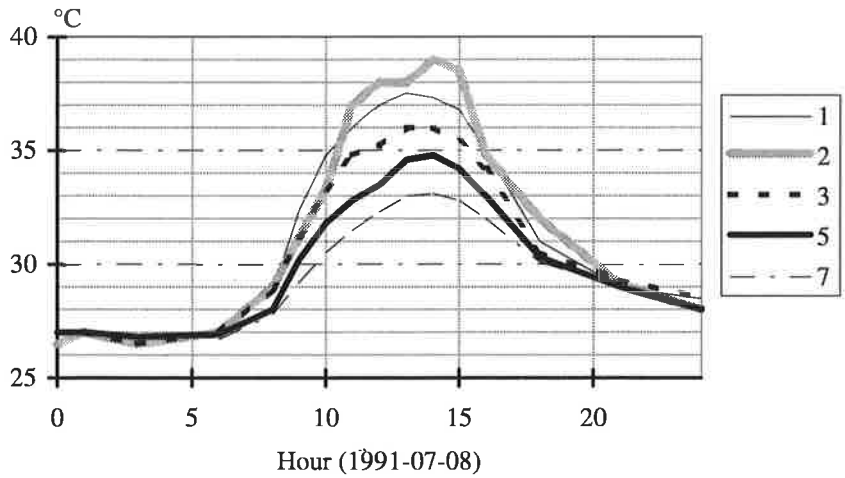

Figure 8.34 *Temperature as measured by the thermocouples. For the thin wires the copper one was silver plated.*

The general conclusion was that a thermocouple of small mass and small surface area gave the best results.

Another experiment was performed during October 1997. The thermocouples tested are shown in table Table 8.2. The tube used for protecting the thermocouple was an 0.5 mm thick rolled aluminium tube with diameter 50 mm and length 100 mm. The tube was positioned vertically. To reduce the effect of sunlight for a thin thermocouple a construction of three thermocouples soldered in series was constructed. This is here denoted as the *compensated* case. The basic idea was that two nodes would give a positive emf and one a negative. The negative node would be a non-stripped 0.08 mm wire. This makes the non-stripped node absorb more sunlight and thus compensate down the higher temperature of the other two nodes. Figure 8.34 shows the temperature difference as measured by the different thermocouples.

Table 8.2 *The different tested thermocouples. All thermocouples are of type T.*

Wire diameter (mm)	Special properties	Air velocity (m/s)
0.08		0.1
0.08	silver coated	0.1
0.08	compensated by 2 nodes	0.1
0.5	stripped 10 cm	0.1
0.5	protected by tube	0.1
0.5	protected by tube	0.4
0.5	protected by tube	0.7

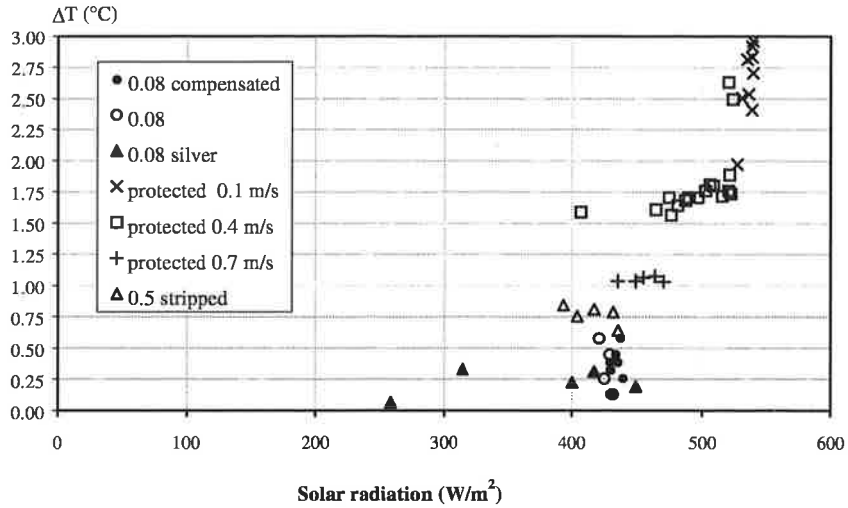

Figure 8.35 *Temperature difference as measured by the different thermocouples. The reference temperature was a 0.08 mm thermocouple shielded from the sun by a thin metal bar.*

The order of decreasing accuracy is the same as in Figure 8.34. It is clear that the idea of protecting the thermocouple by a tube is a bad idea even with high air velocity. The compensated thin thermocouple is not necessarily better than the normal one and probably worse than the silver coated one. The conclusion is that in theory the thin thermocouple should give less error than 0.2 °C at 450 W/m^2 sun but in practise this value is closer to 0.5 °C. The compensated thermocouple used in this study to measure the air temperatures will probably overestimate the temperature with the same value 0.5 °C at direct sunlight. The thermocouples glued to the window pane beneath a 0.1 mm cover glass were not explicitly tested. The results from the Mayer ladder comparison in 8.2.3 did show however that the window model using thermocouples on the window gave the same convective heat transfer as the Mayer ladder when exposed to strong sunlight.

8.5 Accuracy of the heat transfer coefficient calculation

The accuracy of the heat transfer coefficient calculation depends on the accuracy of the model and the measured parameters. The heat transfer coefficient is measured as :

$$h_c = \frac{q_c}{T_{ref} - T_{surface}} = \frac{q_c}{\Delta T} \qquad (W/m^2K) \qquad (8.38)$$

If the errors are uncorrelated the sensitivity to error in the input parameters is:

$$\delta h_c = \frac{1}{\Delta T}\sqrt{\left(\frac{q_c}{\Delta T}\delta\Delta T\right)^2 + \delta q_c^{\,2}} \qquad (W/m^2K) \qquad (8.39)$$

or with $q_c = q_{cond} - q_r$

$$\delta h_c = \frac{1}{\Delta T}\sqrt{\left(\frac{q_c}{\Delta T}\delta\Delta T\right)^2 + \delta q_r^{\,2} + \delta q_{cond}^{\,2}} \qquad (W/m^2K) \qquad (8.40)$$

The relative error is then

$$\frac{\delta h_c}{h_c} = \frac{1}{q_c}\sqrt{\left(\frac{q_c}{\Delta T}\delta\Delta T\right)^2 + \delta q_r^{\,2} + \delta q_{cond}^{\,2}} \qquad (-) \qquad (8.41)$$

The accuracy of the temperature measurement is here estimated to +/- 0.2 °C. The accuracy of measurements with type T thermocouples is usually said to be +/- 0.1 °C for calibrated thermocouples and +/- 0.5 °C for non calibrated. In the study here the thermocouples were not individually calibrated. The Netpac instruments were however calibrated to less than +/- 0.05 °C at room temperature and +/- 0.1 at 0°C. The variation over the 20 thermocouples at the same aluminium block was <0.1°C. The accuracy of the absolute temperature measurements is estimated to +/- 0.5 °C. The critical temperatures in this study are not however the absolute temperatures but the difference between temperatures. The accuracy of the temperature measurement is therefore estimated to +/- 0.2 °C.

The accuracy of the conductive heat flow calculations for the wall q_{cond} is, from 8.3.3, about +/- 0.3 W/m^2. The accuracy increases somewhat for lower absolute values of q_{cond}. The accuracy for the convective heat transfer q_c at the window is, from section 8.2.3, +/- 1 W/m^2.

The error for the longwave radiation part is not easy to estimate. Apart from the direct measurement error there is also the question if the temperature is representative for the whole area. For the floor for example, there were noticeable errors compared to the Mayer ladder measurement when the floor thermocouple was exposed to strong sunlight. The larger part of the floor did not have the high temperature of the part exposed to direct sun. This had to be taken into account in the calculations. Based on solar angles and window size the sunlit area was calculated and there the floor temperature was used. For the rest of the floor the lower wall values were used instead. The errors introduced by the individual temperature errors are on the other hand much reduced due to the nature of the longwave radiation exchange which smoothes out the dependency on individual surfaces. The error chosen here was simply:

$$\delta q_r = h_r \delta \Delta T \approx 5 \cdot 0.1 = 0.5 \qquad (\mathrm{W/m^2}) \qquad (8.42)$$

Based on the error estimation above, the absolute δh_c and relative error $\delta h_c/h_c$, when estimating the heat flow coefficient at the walls and at the window could be calculated. These results are summarized in Table 8.3 and Table 8.4 for different choices of q_c and ΔT.

Table 8.3 *Errors in the convective heat transfer coefficient estimation for the window.*

Window						
ΔT= (°C)	0.5	1	2	0.5	1	2
q_c	δh_c	δh_c	δh_c	$\delta h_c/h_c$	$\delta h_c/h_c$	$\delta h_c/h_c$
(W/m^2)	(W/m^2K)	(W/m^2K)	(W/m^2K)	(-)	(-)	(-)
1	2.1	1.0	0.5	1.06	1.01	1.00
2	2.5	1.1	0.5	0.64	0.53	0.5
3	3.1	1.2	0.5	0.52	0.39	0.35
4	3.8	1.3	0.5	0.47	0.32	0.27
5	4.5	1.4	0.6	0.45	0.28	0.22
6	5.2	1.6	0.6	0.43	0.26	0.19
7	5.9	1.7	0.6	0.42	0.25	0.17
8	6.7	1.9	0.6	0.42	0.24	0.16
9	7.5	2.1	0.7	0.42	0.23	0.15
10	8.2	2.2	0.7	0.41	0.22	0.14

Table 8.4 *Errors in the convective heat transfer coefficient estimation for the wall.*

Wall				
$\Delta T=(°C)$	0.5	1	0.5	1
q_c	δh_c	δh_c	$\delta h_c/h_c$	$\delta h_c/h_c$
(W/m^2)	(W/m^2K)	(W/m^2K)	(-)	(-)
1	1.4	0.6	0.71	0.62
2	2.0	0.7	0.50	0.35
3	2.7	0.8	0.44	0.28
4	3.4	1.0	0.43	0.25
5	4.2	1.2	0.42	0.23

From these calculations it is clear that estimating the heat transfer coefficient by the method chosen in this study is not very accurate. For the window the convective heat flow must be at least 4 W/m^2 and the temperature difference 2 °C for the relative error to be less than 30%. This accuracy is achieved for ΔT=1 °C and q_c =5 W/m^2. The situation for the wall is slightly better. The accuracy 30% is achieved for q_c = 4 W/m2 and ΔT=1°C. Unfortunately the heat flow through the wall is much lower than through the window due to the low U-value of the wall.

The accuracy of the measurement when solar radiation is accounted for is obviously even worse. Instead of estimating this accuracy in detail does section 8.2.3 handle this in a more general way. The result is that measurements of the convective heat transfer coefficient on the window pane are reasonable if $\Delta T <$ -4°C or ΔT>1°C.

The drawback of doing experiments under these realistic conditions is clearly a lack of accuracy. Nevertheless the results can give an idea of how the heat transfer coefficient changes with different experimental setups. The accuracy is however not enough for proposing exact equations for the convective heat transfer coefficient.

9 Results

9.1 Heat transfer coefficients with radiator at the back wall

The results from the calculations and measurements of the local convective heat transfer coefficient $h_c(T)$ are presented here:

$$h_c = \frac{q_c}{T_{ref} - T_{surface}} = \frac{q_c}{\Delta T} \qquad (\mathrm{W/m^2K}) \qquad (9.1)$$

Here q_c is positive for the convective heat flow to the surface. The reference temperature in all the calculations is the average temperature of the middle vertical row of thermocouples. This reference temperature T_{ref} could also have been chosen as the average of all air temperatures, but this would only have a minor effect on the results. In all diagrams a positive temperature difference ΔT means that the reference temperature is warmer than the window pane or wall temperature. For the wall h_c is calculated at positions VA (2.25 m from floor, 0.60 m from east wall) and VB (1.46 m from floor, 0.60 m from east wall). For the window h_c is calculated at positions G_1 to G_4 as shown in Figure 9.1. Two formulae are used as references in the figures Churchill and Chu (5.9) and Min et al (5.13). They represent extreme values found in the literature. Min et al is based on full scale experiments and Churchill and Chu is close to the analytic solution for laminar flow. These two formulae describe the mean heat transfer coefficients, not the local ones, but they nevertheless give an idea of the general behaviour. See Figure 5.1.

The local convective heat transfer coefficients on the window are referred to as: $G_1\ h_c$, $G_2\ h_c$, $G_3\ h_c$ and $G_4\ h_c$. These are all shown separately. For the 3-pane window the Nusselt number never were above 1.01 so the heat transfer in the air between the panes was almost pure conduction. The coefficients $G_1\ h_c$ –$G_4\ h_c$ should therefore be good estimates for the local heat transfer. For the 4-pane window the Nusselt number was always below 1.15, usually 1.05. This means up to 15% more heat transfer than by pure conduction. In this case are the coefficients not as good for estimating the local heat transfer. They are neverthe-

less also shown separately, since they give a more complete picture of how the heat transfer varies over the window.

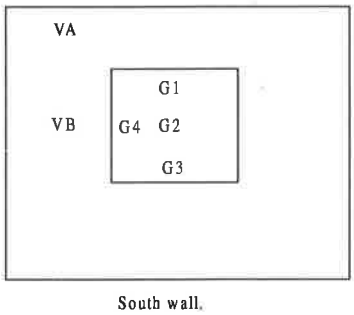

Figure 9.1 *Positions on the south wall where the heat transfer coefficient was measured.*

The air temperatures will be shown below. Figure 9.2 shows the thermocouples where the air and wall temperatures are measured. A note on the following air temperature figures are that although the air is measured by 18 thermocouples , the back wall is measured by only 2, the ceiling 1 and the floor 1. For the south wall VA, VC, and G_1-G_3 are used. The thermocouples VA and VC are not in the centre of the room but are considered representative for the wall temperatures. The temperatures in the corners and between the walls and air thermocouples are interpolated and drawn with the program Matlab. The temperatures in the corners in these figures should therefore not be viewed as exact.

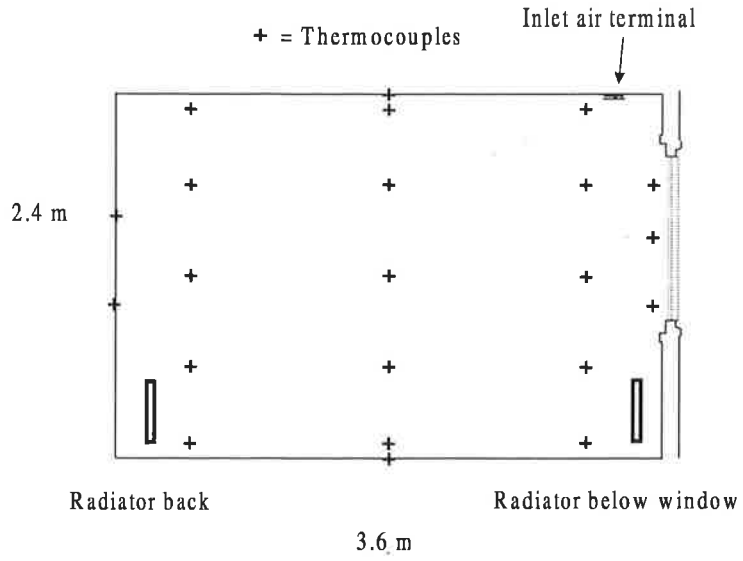

Figure 9.2 *Air, ceiling, back wall and floor thermocouples.*

The results from calculations and measurements are shown without any filtering of the values. The exception is that for most values with $|\Delta T| < 0.4$ and very large negative and positive values for h_c are not shown. From section 8.2.3 we found that for the window values for $-4\ °C < \Delta T < 2$ were rather uncertain especially for low values of h_c. The relative error in h_c could easily be 40%. For the wall h_c values for $\Delta T <= 1$ have an estimated error of around 35%. The reason for not filtering out these values is that the general trends can still be considered and that the increasing error is identifiable in most of the figures. The absolute values should in the intervals mentioned not be trusted too much, however.

9.1.1 No ventilation

The first case is with the radiator 0.2 m from the north (back) wall with no ventilation. Bimetallic radiator control with maximal 10 min average effect 180 W. The window was the 3-pane window. Figure 9.3 shows h_c for the window.

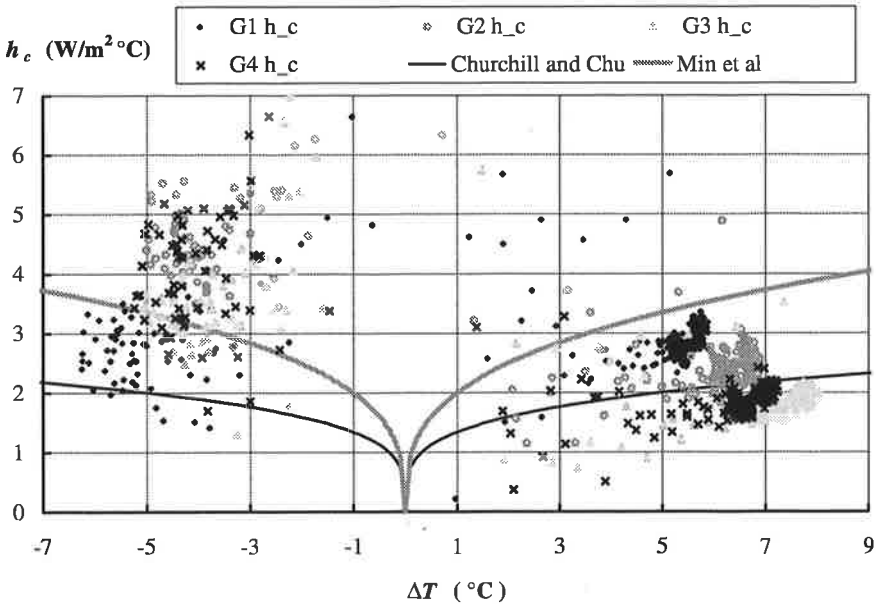

Figure 9.3 *Convective heat transfer coefficient at 3-pane window with radiator at the back wall and no ventilation, 20min average, 3-pane window. (980128 11.00-980130 00.00)*

The order of the coefficients for positive ΔT are as expected since the natural convection is downwards the pane: G_1 h_c >G_2 h_c >G_3 h_c. The coefficient G_4 h_c is lower than G_2 h_c which might also be expected being close to the left edge of the window pane. The average values are slightly above Churchill and Chu. For negative ΔT the situation is not clear due to low accuracy. In Figure 9.3 G_1 gives the lowest h_c which it should do, since the direction of the air flow is upwards here. The other values are not very close together but give in general an h_c which is about 2.5 times the one from Churchill and Chu.

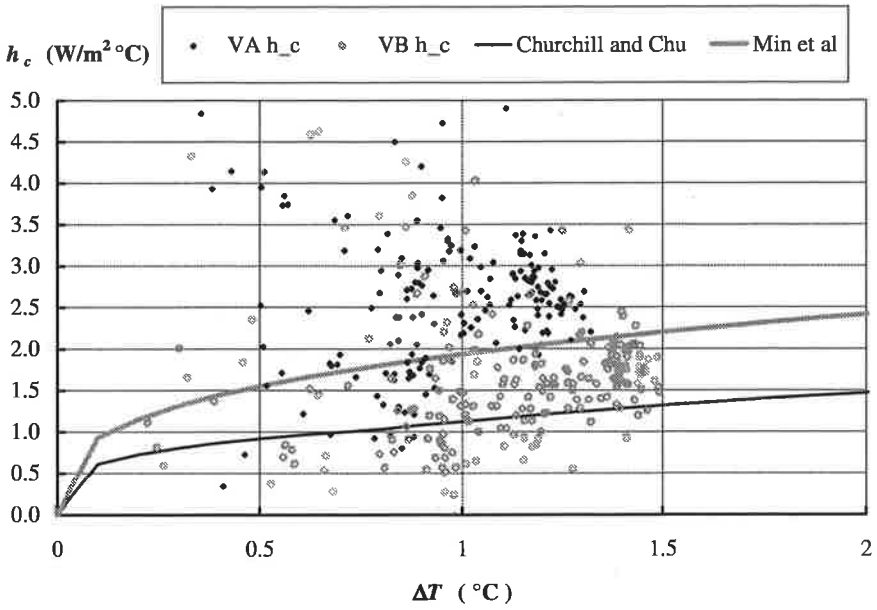

Figure 9.4 Convective heat transfer coefficient at wall with radiator at the back wall and no ventilation, 20 min average. (980128 11.00-980130 00.00)

Figure 9.4 shows h_c for the wall. VA gives the highest value, whereas VB gives a value between Churchill and Chu and Min et al. As was stated before, the error in the heat transfer coefficient measurements increases with decreasing ΔT. In addition to this the fact that the reference temperature is not chosen at a position close to the wall but in the middle of the room will also become more important with decreasing ΔT. If the air temperature close to the wall is different, the calculated h_c will of course not match Churchill and Chu or Min et al.

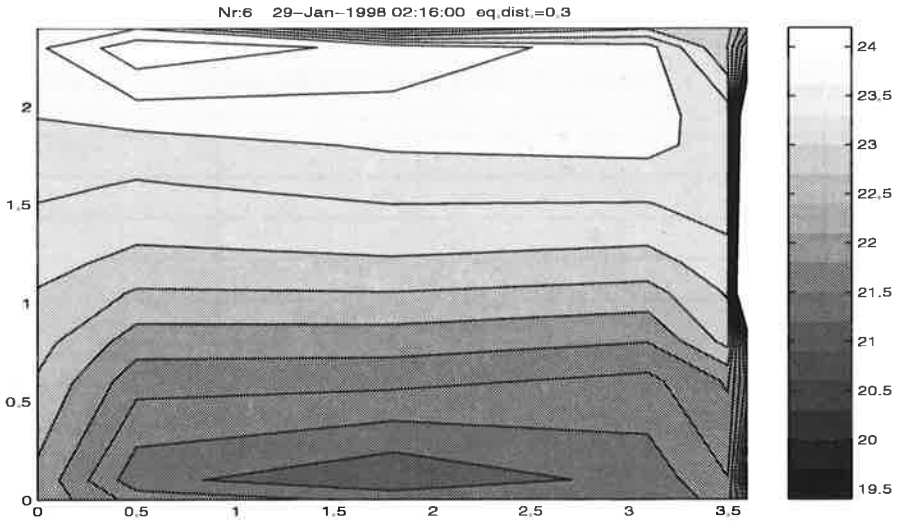

Figure 9.5 Air temperatures in the room 980129 2:16, radiator effect 180 W.

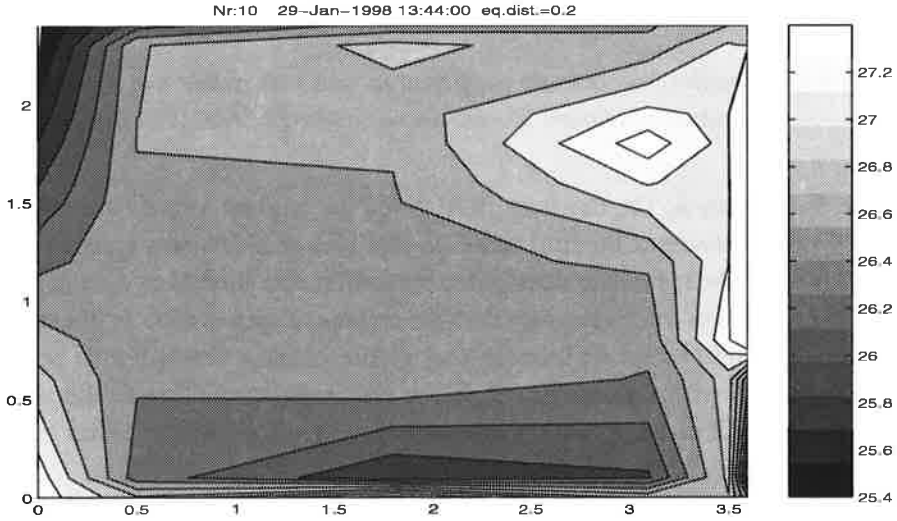

Figure 9.6 Air temperatures in the room 980129 13:44, radiator effect 0 W.

Figure 9.5 shows the air temperatures at night with the radiator effect 180 W. Figure 9.6 shows the temperatures with sun and no radiator effect. In Figure 9.5 the plume from the radiator can not be seen. This is because the plume is between the wall and the first row of thermocouples. This row is located 0.5 m from the back wall. The warm air is first measured under the ceiling where it is

spread out. The vertical temperature difference is ~3 °C with radiator and ~1.5 °C with sun.

The next figure shows measurements from a situation with the 1000 W radiator controlled by its own bimetallic controller. The effect was a rapid fluctuation between 0 and 1000 W. The radiator was also turned completely off at times making the average temperature in the room to drop 15 °C. Only 10 min average temperatures are used for the calculations which are then averaged to 30 min values. The rapid change of the radiator can therefore not be seen here. The window was a 4-pane window. It is clear from Figure 9.7 and Figure 9.8 that the heat transfer coefficients are much affected by the high radiator effect though. In Figure 9.7 the measurements are collected in two clusters. The higher values with high ΔT are from measurements with the radiator turned on and the lower ones with the radiator turned off. Both the higher and lower ones have the same order of h_c: G_1 h_c >G_2 h_c >G_3 h_c. The lower ones are slightly beneath Churchill and Chu and the higher ones are (with large differences) closer to Min et al.

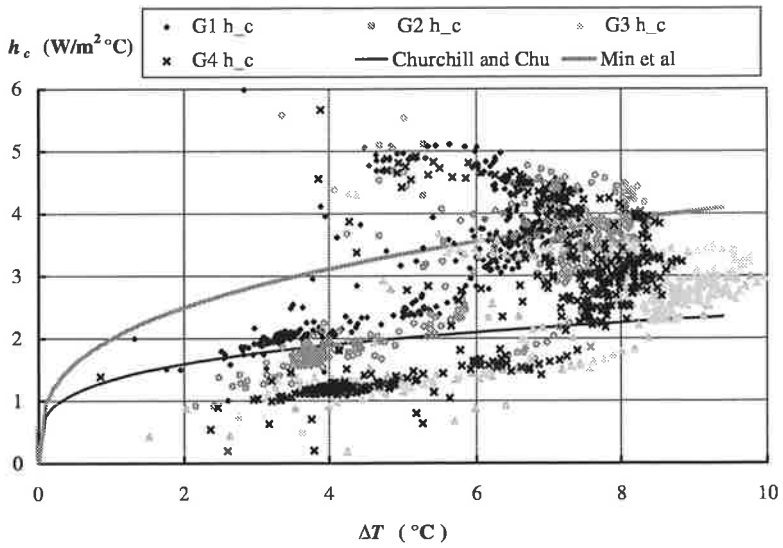

Figure 9.7 *Convective heat transfer coefficient at 3-pane window with radiator at the back wall and no ventilation. (980114 17.00-980125 00.00 , 30 min average)*

From the coefficients at the wall, Figure 9.8, it is clear that T_{ref} is not representative for the air temperature close to the wall. At position VB the results

are about 1.5 -2 times Min et al but at position VA the coefficient is much higher. From Figure 9.9 the vertical temperature difference is ~5 °C. The radiator clearly heats the back wall to over 40°C.

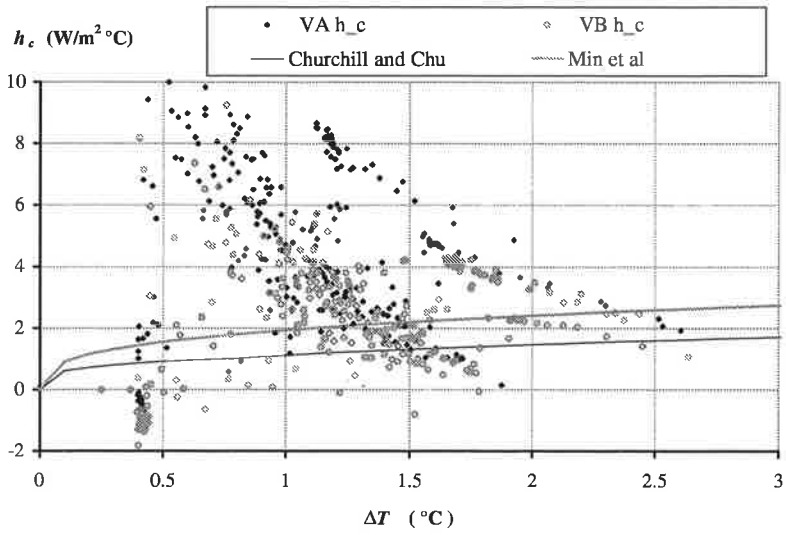

Figure 9.8 *Convective heat transfer coefficient at wall with radiator at the back wall and no ventilation. (980114 17.00-980125 00.00 , 30 min average)*

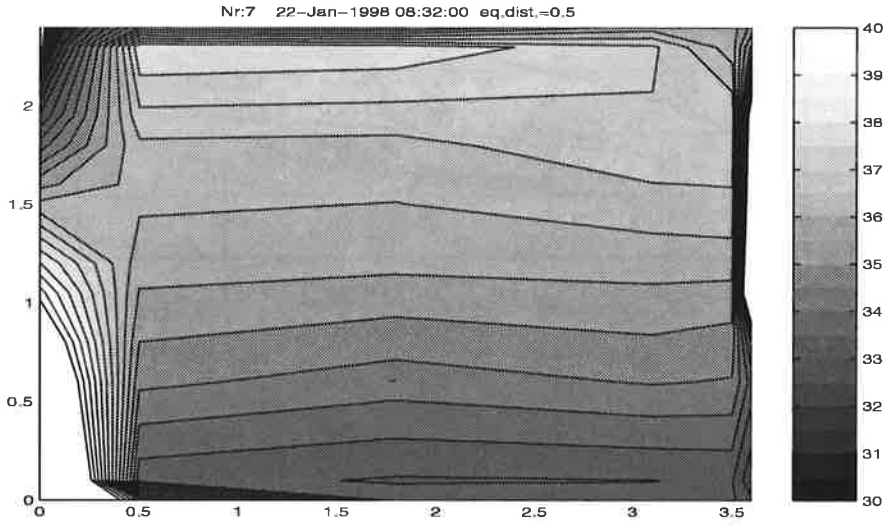

Figure 9.9 *Air temperatures in the room 980122 8:32, radiator effect 600 W.*

Figure 9.10 shows the third period tested with radiator at the back wall and no ventilation. This time with a 4-pane window and the smaller PI controlled radiator with 10 min average effect below 120 W. The coefficients here are higher than the ones in Figure 9.3. Instead of G_1 h_c giving the highest values, the order here is: G_2 h_c >G_1 h_c >G_3 h_c. There is a risk that G_1 h_c ,G_3 h_c and G_4 h_c are slightly underestimated in the 4-pane window, see section 8.2.4. But even so G_2 $h_{c\ is}$ noticeably higher than in Figure 9.3. The ΔT's are lower since the window is better insulated. On average the results are between Min et al and Churchill and Chu.

Figure 9.11 shows the wall h_c. These results are similar to those in Figure 9.4 with VB h_c between Min et al and Churchill and Chu and VA h_c on and above.

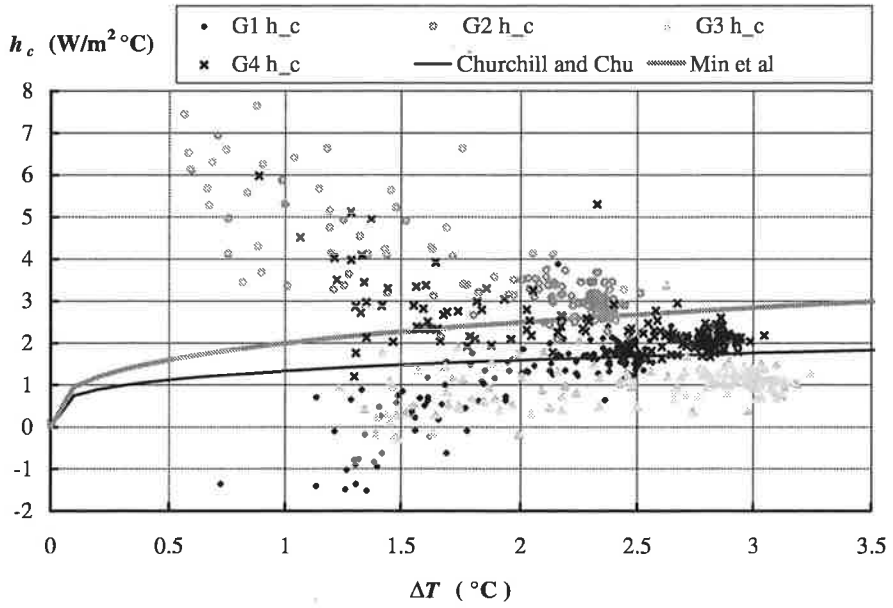

Figure 9.10 *Convective heat transfer coefficient at the window with radiator at the back wall and no ventilation, 4-pane window. (940227 18.00-940302 18.00 , 30 min average)*

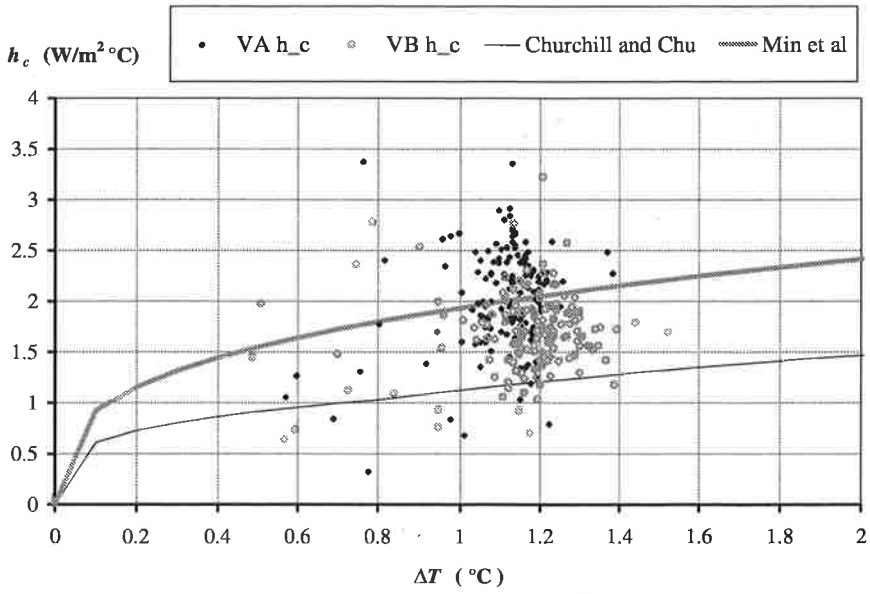

Figure 9.11 *Convective heat transfer coefficient at the wall with radiator at the back wall and no ventilation, 940227 18.00-940302 18.00 , 30 min average.*

9.1.2 Ventilation from window 0.5 air changes per hour

The radiator was at the back wall with bimetallic control, ventilation was 0.5 ach from the window and the window type 3-pane for this experiment. The inlet temperature was about 6°C below the room temperature. The maximal 10 min average radiator effect was 100 W. The sun was completely shielded by a metal plate outside the window. Figure 9.12 shows h_c for the window. All values are below Churchill and Chu which differs in sharp contrast to the previous examples without ventilation. The direction of the ventilation is opposite to the direction of the convective cell and this together with the undertempered inlet air is the reason for the low values. The same is true for the wall, Figure 9.13. Both VA h_c and VB h_c have been reduced compared to the non ventilated case. However, the temperature difference ΔT is so small for the wall that the measurements error makes it impossible to do more than estimate the trends The negative values are probably not correct but the difference between VA and VB is probably realistic.

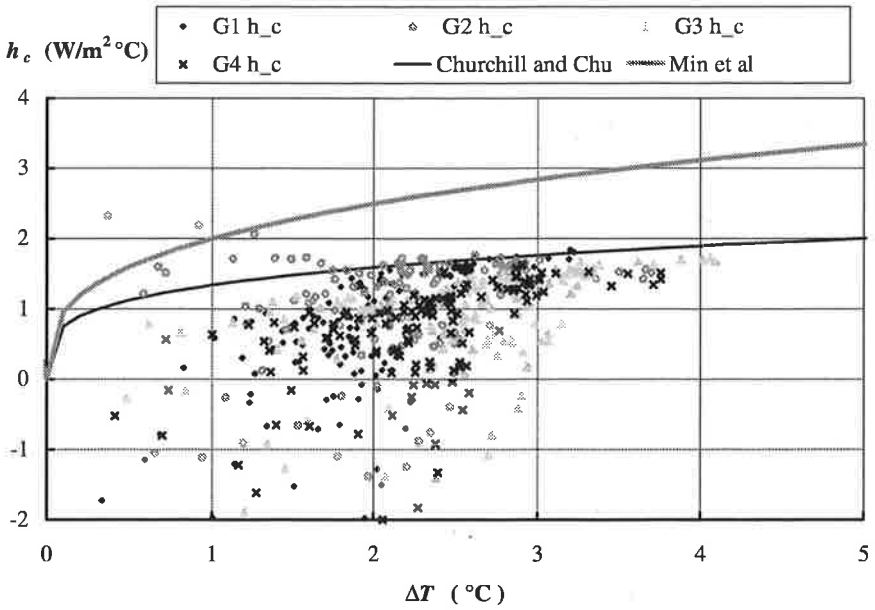

Figure 9.12 *Convective heat transfer coefficient at 3-pane window with radiator at the back wall and 0.5 ach. 960531 18.00-960604 5.00 , 30 min average, no sun.*

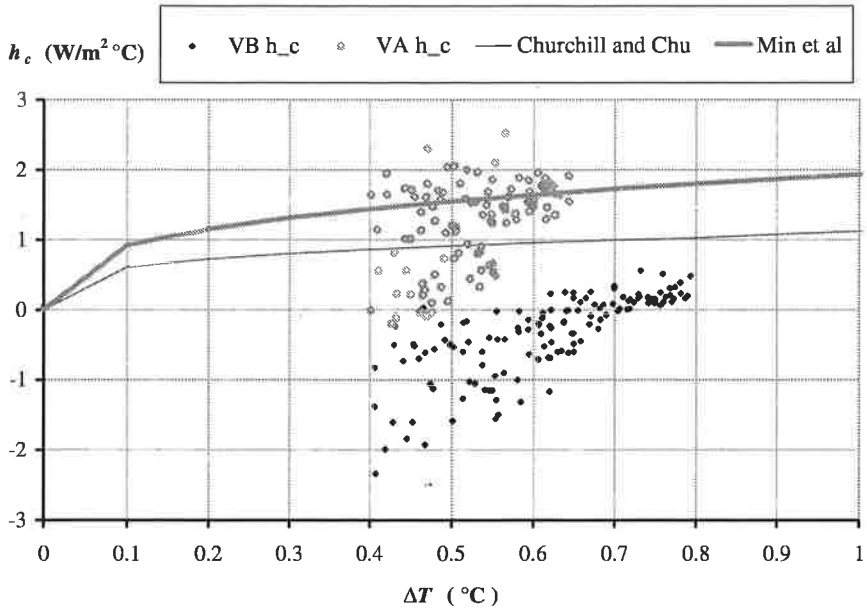

Figure 9.13 *Convective heat transfer coefficient at wall with radiator at the back wall and 0.5 ach. (960531 18.00-960604 5.00 , 30 min average, no sun)*

The air temperatures in Figure 9.14 differ from Figure 9.5 in that the horizontal temperature gradient is higher above 1.5 m. Close to the ceiling the warm air is pushed back. The air is more mixed in the middle giving a more even temperature in the vertical direction.

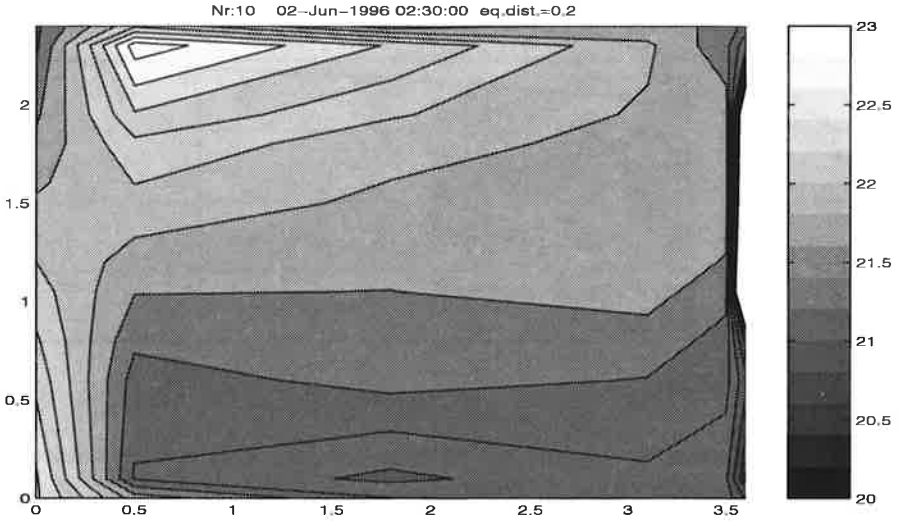

Figure 9.14 Air temperatures in the room 960602 2:30, radiator effect 100 W, inlet temperature 16 °C, outlet temperature 22.4 °C.

9.1.3 Ventilation from window, 1.0 air changes per hour

The radiator was at the back wall with PI-control, ventilation was 1 ach from the window and the window type 4-pane. The inlet temperature was about 2°C below the room temperature. The maximal 10 min average radiator effect was 120 W. Figure 9.15 shows h_c for the window. The results are similar to those with 0.5 ach. All values with positive ΔT are below Churchill and Chu. The values for negative ΔT are around Churchill and Chu with G_1 h_c the highest.

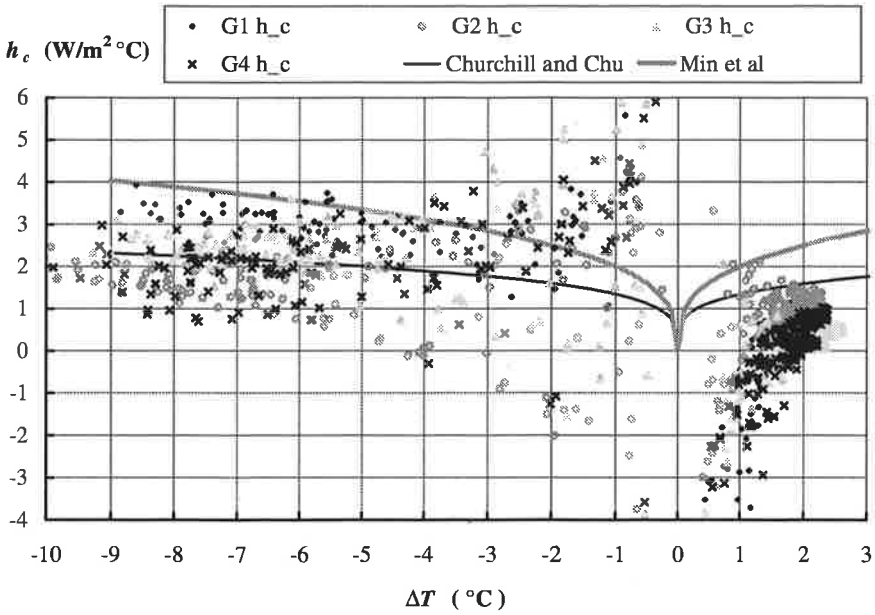

Figure 9.15 *Convective heat transfer coefficient at the 4-pane window with radiator at the back wall and 1.0 ach. 940331 18.00-940409 16.00 , 30 min average.*

Figure 9.16 is similar to Figure 9.13 except that the values from VA have also been reduced to the same level as VB. Almost all the values are negative but the measurement error makes it impossible to deduce more than the general behaviour of h_c.

The air temperatures in Figure 9.17 resemble those in Figure 9.14. The vertical temperature gradient is bigger though. Even if the ventilation rate was higher in Figure 9.17 the temperature difference between inlet air and room air was less than in Figure 9.14.

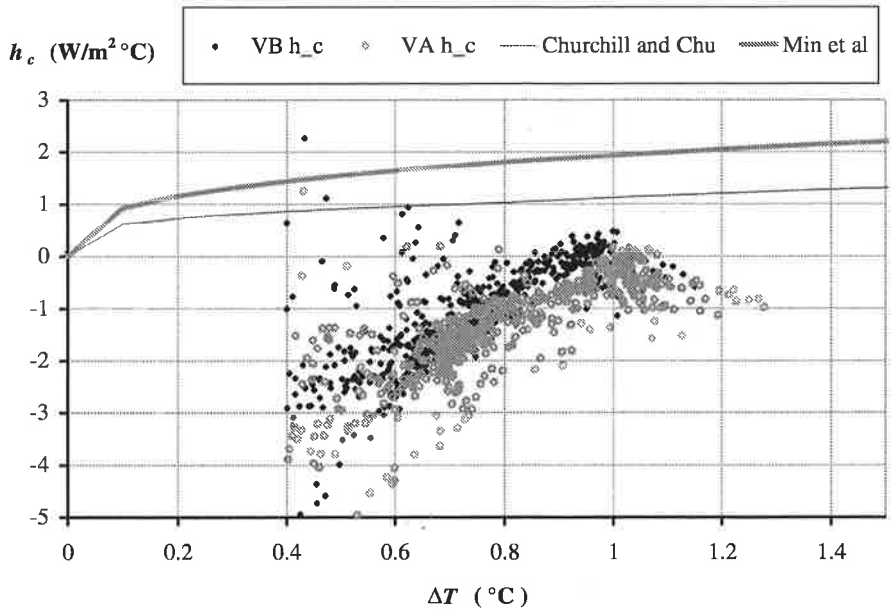

Figure 9.16 *Convective heat transfer coefficient at wall with radiator at the back wall and 1.0 ach. (940331 18.00-940409 16.00 , 20 min average)*

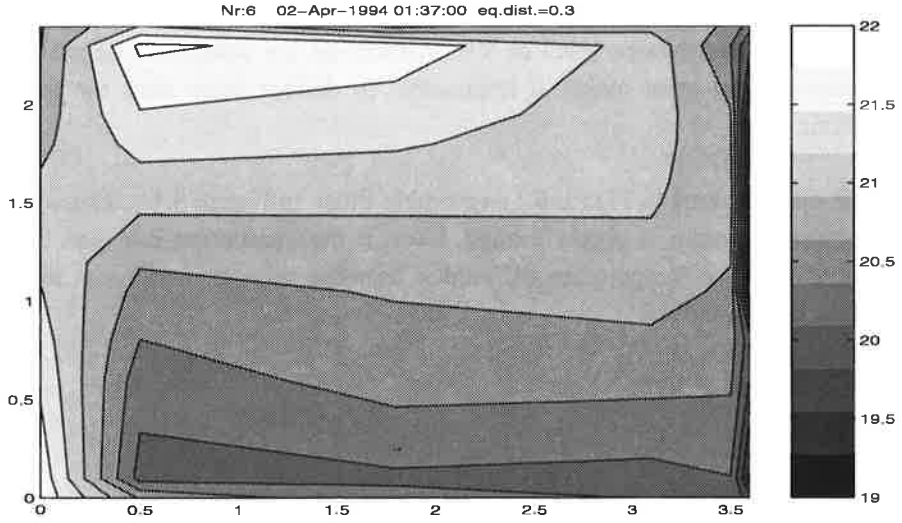

Figure 9.17 *Air temperatures in the room 940402 1:37, radiator effect 120 W, inlet temperature 20.0 °C, outlet temperature 21.8 °C.*

9.1.4 Ventilation towards window 1.0 air changes per hour

The radiator was at the back wall with bimetallic control, the ventilation was 1 ach from the window and the window type 4-pane. The inlet temperature was about 5°C below the room temperature. The maximal 10 min average radiator effect was 220 W. Figure 9.18 shows the h_c for the window. The values are slightly above those in Figure 9.10, 4-pane window with no ventilation, except for G_1 h_c which gives much higher values. On average the values are 1.5 times Min et al.

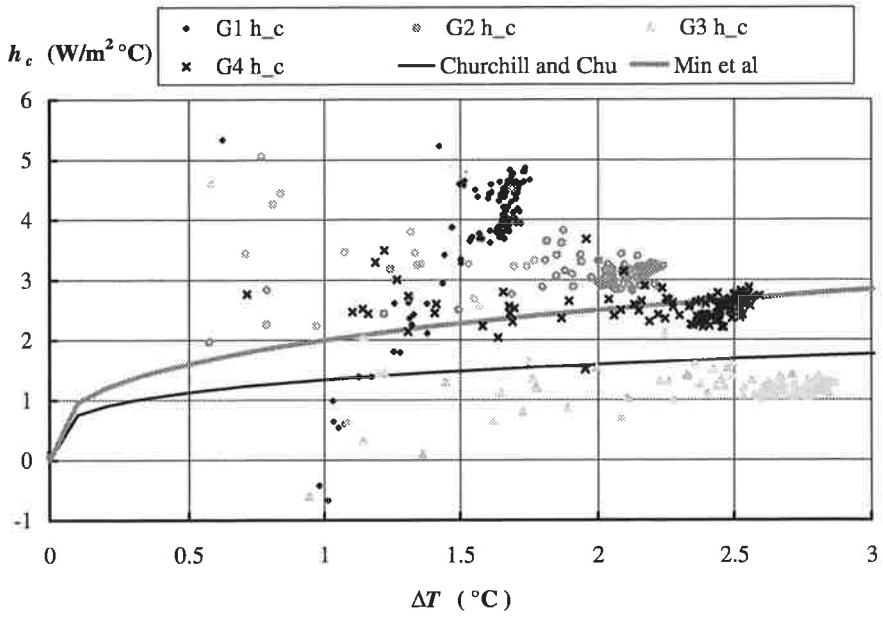

Figure 9.18 *Convective heat transfer coefficient at 4-pane window with radiator at the back wall and 1.0 ach towards window. (940316 18.00-940318 12.00 , 20 min average)*

The h_c values for the wall shown in Figure 9.19 are higher than those for ventilation rate 0.5 ach (Figure 9.16) but lower than the ones with no ventilation (Figure 9.11). All are below Churchill and Chu.

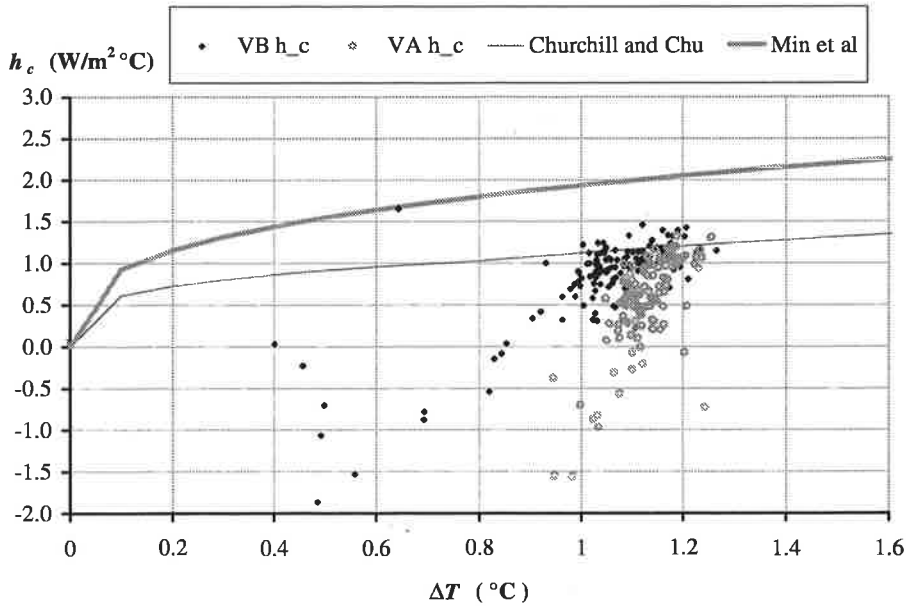

Figure 9.19 *Convective heat transfer coefficient at the wall, radiator at the back wall and 1.0 ach towards window. (940316 18.00-940318 12.00 , 20 min average)*

From the air temperatures in Figure 9.20 it is not easy to deduce the direction of the ventilation air flow. The air temperatures resemble the ones from the non ventilated case quite closely, Figure 9.5.

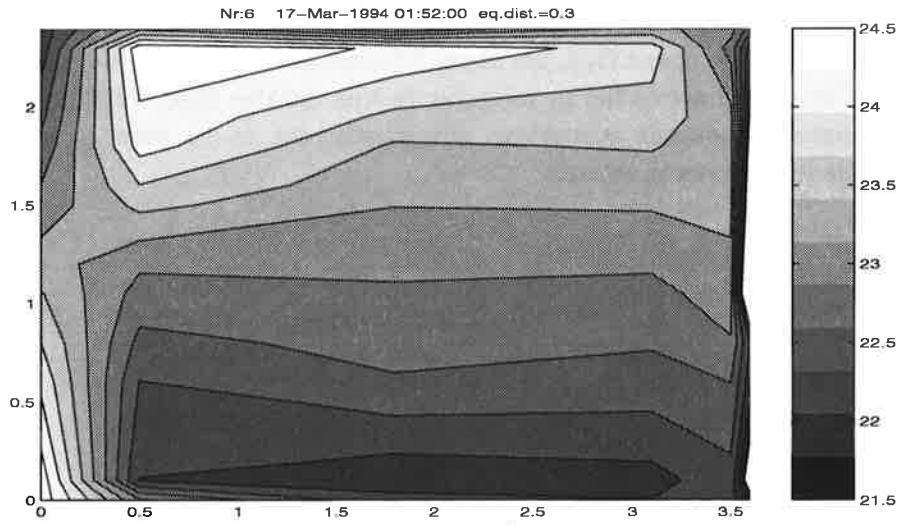

Figure 9.20 *Air temperatures in the room 940317 1:52, radiator effect 220 W, inlet temperature 19.5 °C, outlet temperature 24.5 °C.*

9.2 Heat transfer coefficients with radiator below window

The same ventilation types that were tested with the radiator 0.2 m from the north (back) wall were tested with the radiator 0.12 m from the south wall under the window.

9.2.1 No ventilation

The radiator was below the window with PI control, the ventilation was off and the window was of the 3-pane type. The maximal 10 min average radiator effect was 80 W. With the radiator below the window the heat transfer coefficients on the window surface is strongly dependent on whether the radiator is turned on or off. In the following the results from radiator turned on with more than 5 W per 10 min average are shown separately from the results with radiator effect < 5 W.

Figure 9.21 shows the h_c for the window with the radiator effect >5 W. The radiator obviously increases h_c at all measured positions G_1-G_4. Strongest af-

fected is G_2 h_c. The order from highest to lowest is: G_2 h_c> G_1 h_c> G_3 h_c> G_4 h_c. The values for G_1 h_c and G_2 h_c are about 2.5 times the ones from Churchill and Chu. Figure 9.22 shows the air temperature with radiator effect 75 W. The air flow pattern , upwards at window, downwards back in the room is easy to imagine for these temperatures.

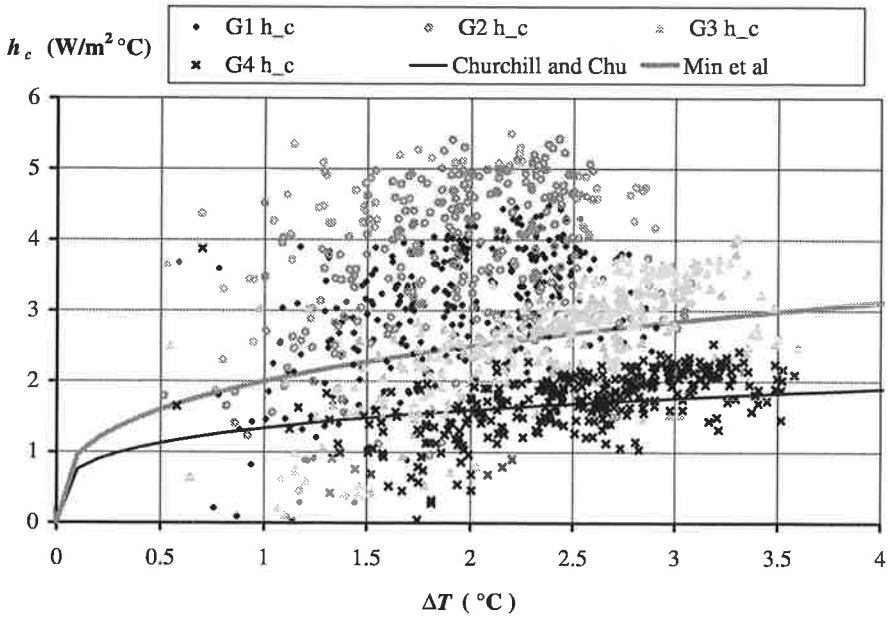

Figure 9.21 *Convective heat transfer coefficient at 3-pane window with radiator below window, no ventilation radiator effect >5 W. 960626 02.00-960709 22.00 , 30 min average.*

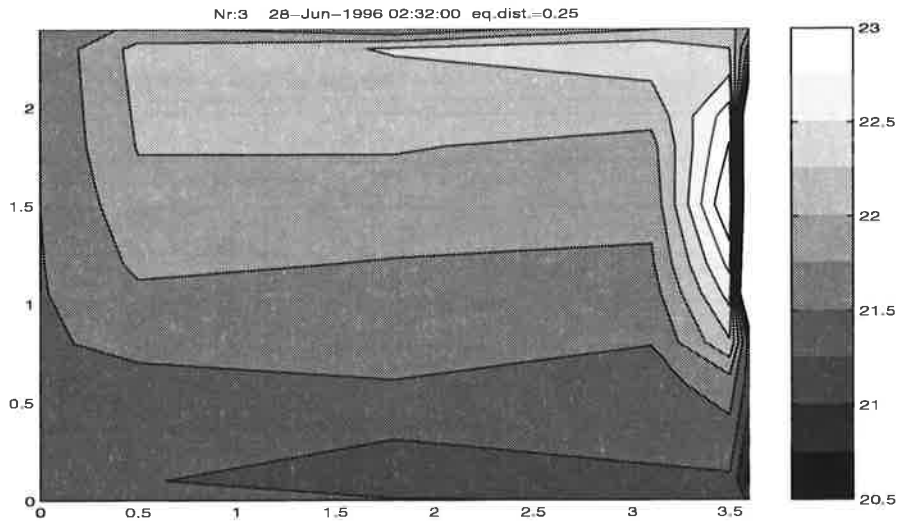

Figure 9.22 Air temperatures in the room 960628 2:47, radiator effect 75 W.

Figure 9.23 shows the heat transfer coefficients with the radiator effect below 5 W. The values are lower than e. g. in Figure 9.3 with ventilation turned off. In the case with radiator turned off the warm area that drives the convection loop is not the radiator but the back wall. The back wall obviously has a much lower over temperature to the air compared with the radiator. This situation resembles the lower values in Figure 9.7 which was the case with the 1000 W radiator turned off. The results for $-4\ °C < \Delta T < 1°C$ are too uncertain to be conclusive.

Figure 9.24 shows the air temperatures with radiator off.

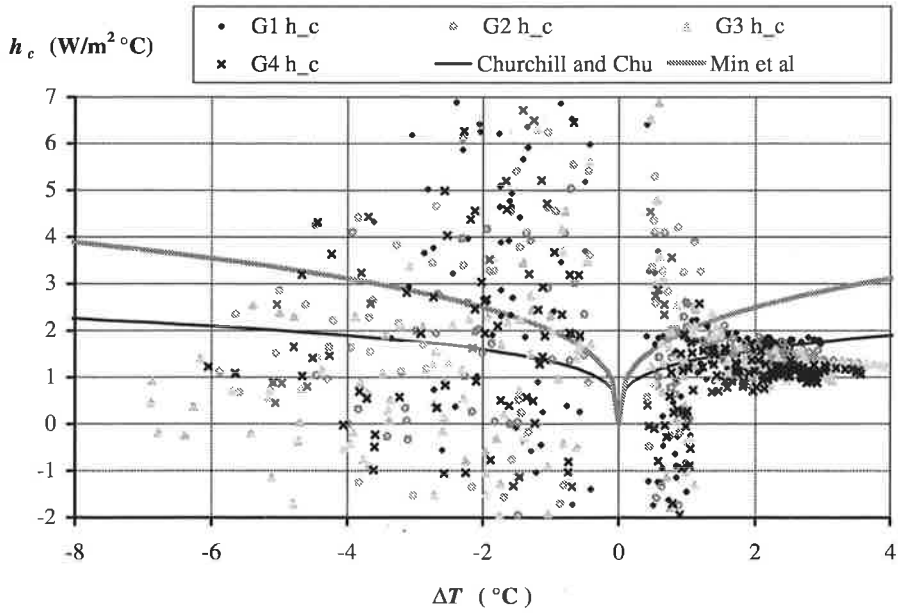

Figure 9.23 *Convective heat transfer coefficient at 3-pane window with radiator below window, no ventilation, radiator effect <5 W, 960626 02.00-960709 22.00 , 30 min average.*

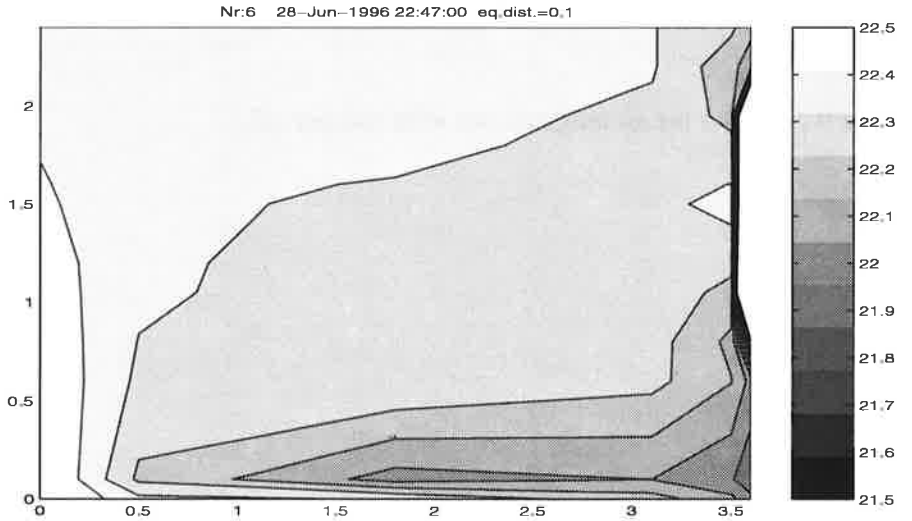

Figure 9.24 *Air temperatures in the room 960628 22:32, radiator effect 0 W, inlet temperature 19.9 °C, outlet temperature 22.2 °C.*

Figure 9.25 shows the h_c for the wall. The values for VB are below Churchill and Chu but the values for VA are much above Min et al. The warm plume from the radiator is probably the reason for these high values.

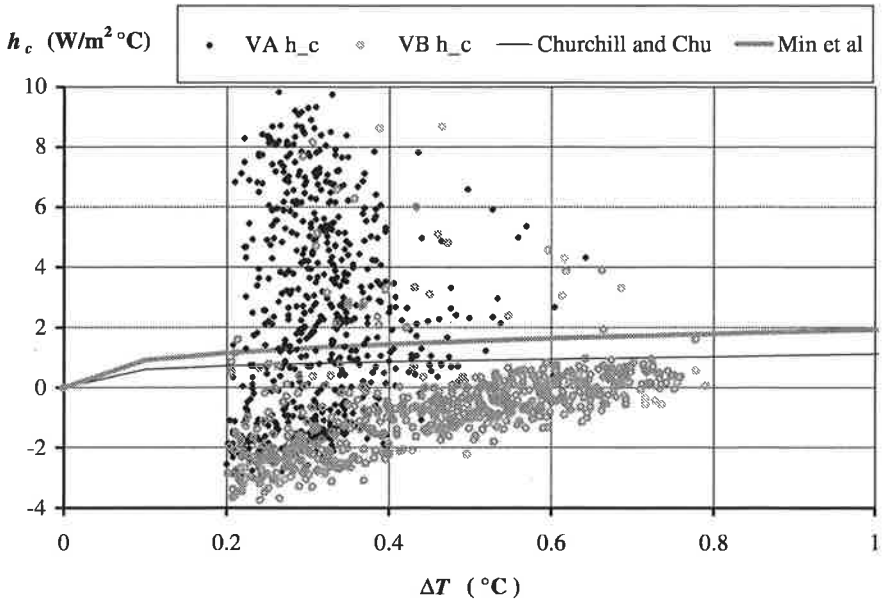

Figure 9.25 *Convective heat transfer coefficient at wall with radiator below window, no ventilation, 960626 02.00-960709 22.00 , 30 min average.*

9.2.2 Ventilation from window 0.5 air changes per hour

The radiator was below the window with PI-control, the ventilation was 0.5 ach and the window was of the 3-pane type. The inlet air temperature was ~ 4°C below room temperature. The maximal 10 min average radiator effect was 75 W.

Figure 9.26 shows h_c when the radiator effect was > 5W. The values here are all, except for G_4 h_c, higher than the case with no ventilation, Figure 9.21. The values for G_4 h_c are 1.5 times more. The ventilation has the same direction as the natural convection from the radiator and this obviously has a strong effect.

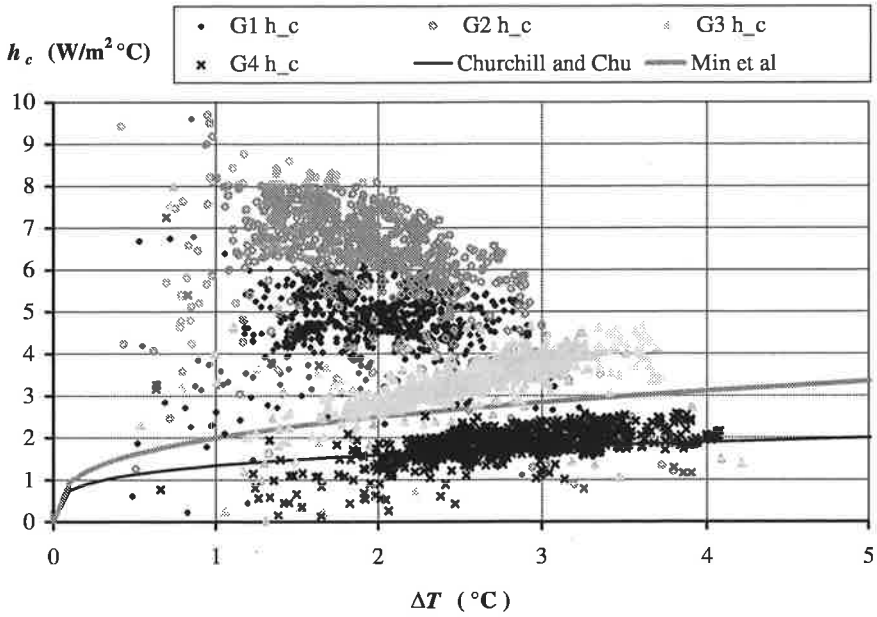

Figure 9.26 *Convective heat transfer coefficient at 3-pane window with radiator below window, 0.5 ach, radiator effect >5 W, 961015 -961104 , 30 min average.*

The air temperatures in Figure 9.27 also indicate that the ventilation increases the natural convection pattern, compare with Figure 9.22.

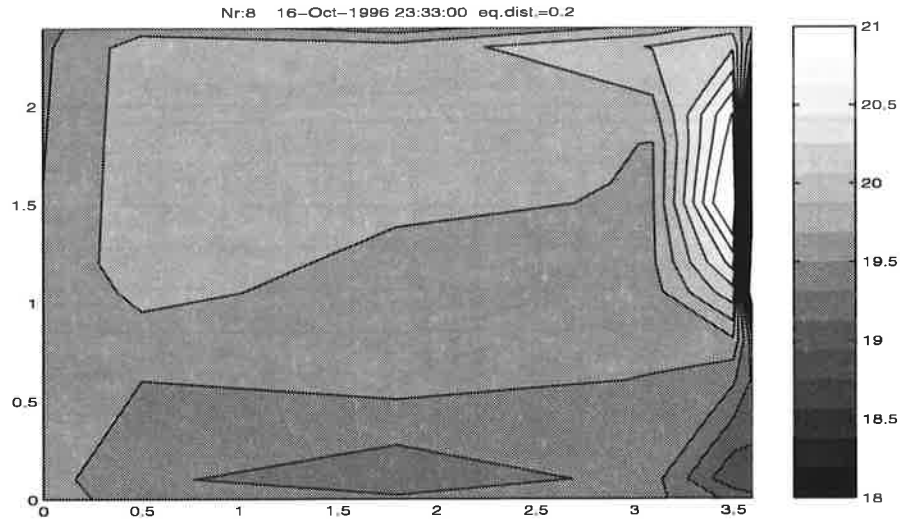

Figure 9.27 *Air temperatures in the room 961016 23:33, radiator effect 70 W, inlet temperature 16.1 °C, outlet temperature 19.6 °C.*

The heat transfer coefficients for the window with radiator effect <5 W, Figure 9.28, are quite similar to those without ventilation, Figure 9.23. The values for negative ΔT are perhaps higher. This is natural since in this case, as when the radiator is on, the inlet air increases the natural convection pattern in the room.

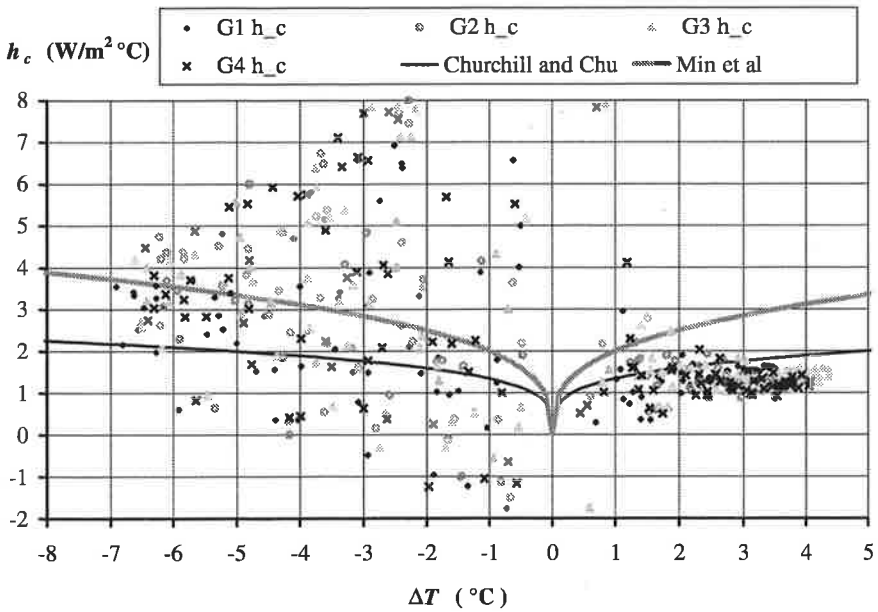

Figure 9.28 *Convective heat transfer coefficient at window with radiator below window, 0.5 ach^{-1}, radiator effect <5 W, 961015 -961104, 30 min average.*

The air temperatures in Figure 9.29 clearly show that the convection loop, with radiator turned off but with no sun, is deformed by the ventilation. The difference between Figure 9.24 and Figure 9.29 is easy to see.

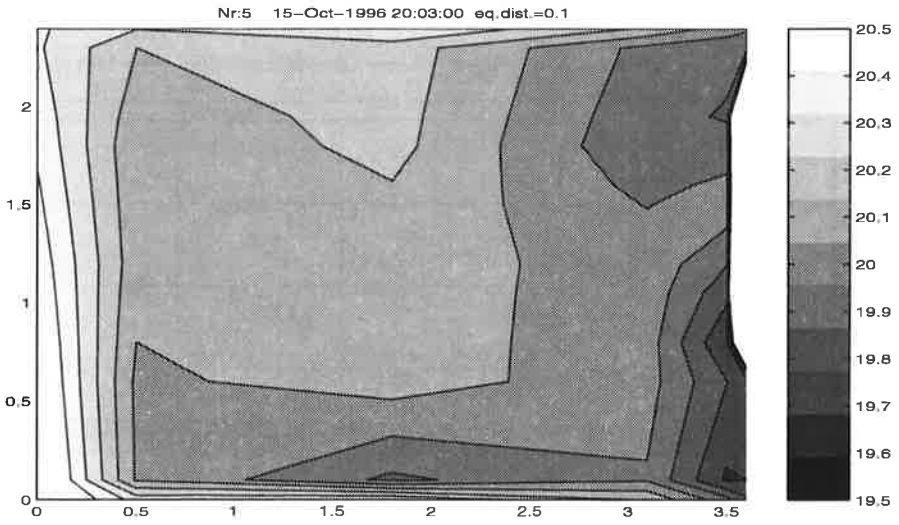

Figure 9.29 *Air temperatures in the room 961015 20:03, radiator effect 0 W, inlet temperature 15.5 °C, outlet temperature 20.1 °C.*

The h_c values for the wall with case with ventilation, Figure 9.30, are similar to the h_c values for the case with no ventilation, Figure 9.25, just as the h_c values for the window. VA h_c seems a bit higher with ventilation.

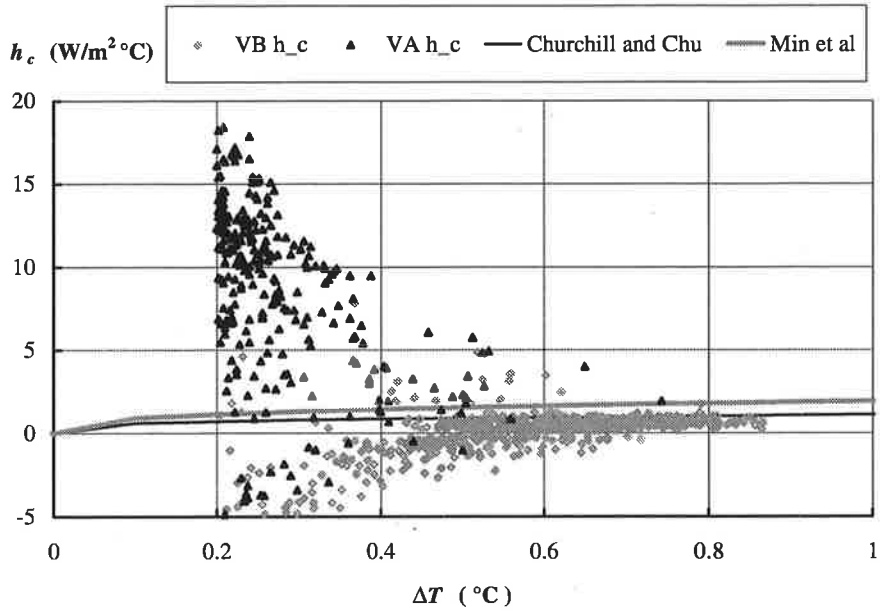

Figure 9.30 *Convective heat transfer coefficient at the wall with radiator below window, 0.5 ach, 961015 -961104, 30 min average.*

9.2.3 Ventilation from window, 1.0 air changes per hour

The radiator was below the window with PI-control, the ventilation was 1.0 ach from the window and the window was of the 3-pane type. The inlet air temperature was ~ 2°C below the room temperature. The maximal 10 min average radiator effect was 140 W.

The results for h_c for the window are about the same as with ventilation 0.5 ach. G_4 still gives the lowest values and G_2 the highest ones. The air temperatures in Figure 9.32 are very similar to the case with half this ventilation shown in Figure 9.27.

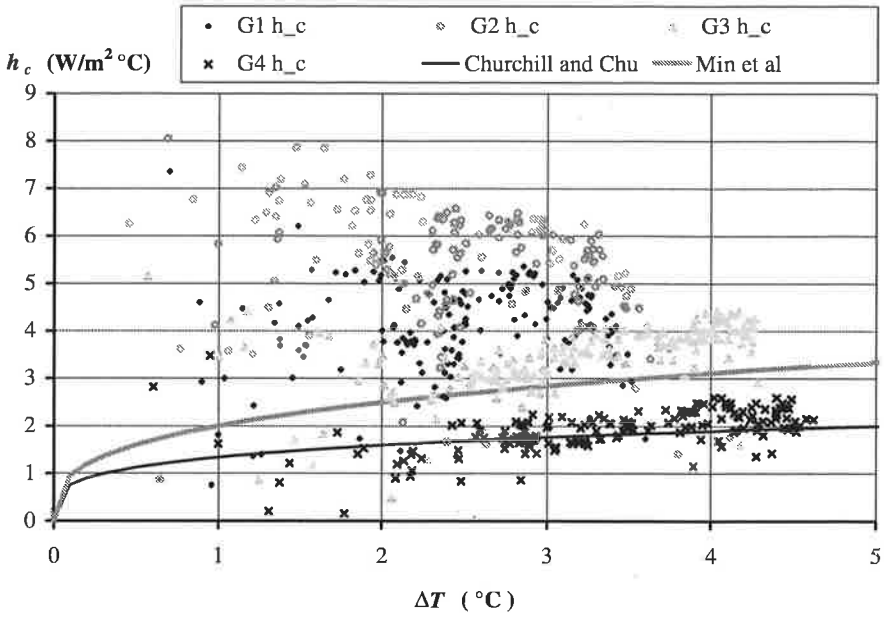

Figure 9.31 *Convective heat transfer coefficient at 3-pane window with radiator below window, radiator effect > 5W, 1.0 ach, 960911 -960917, 30 min average.*

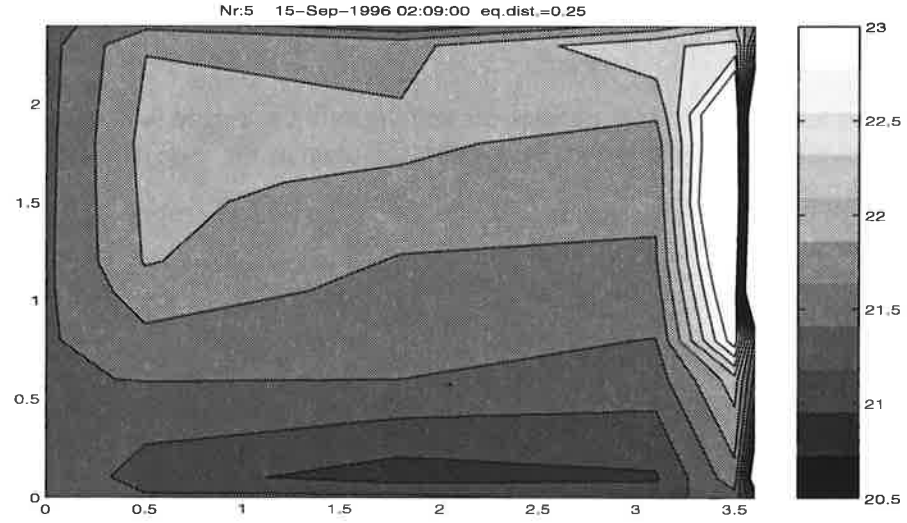

Figure 9.32 *Air temperatures in the room 960915 2:09, radiator effect 130 W, inlet temperature 19.4 °C, outlet temperature 21.6 °C.*

The heat transfer coefficients for the window with the radiator < 5 W are also similar to those with half the ventilation and those without ventilation.

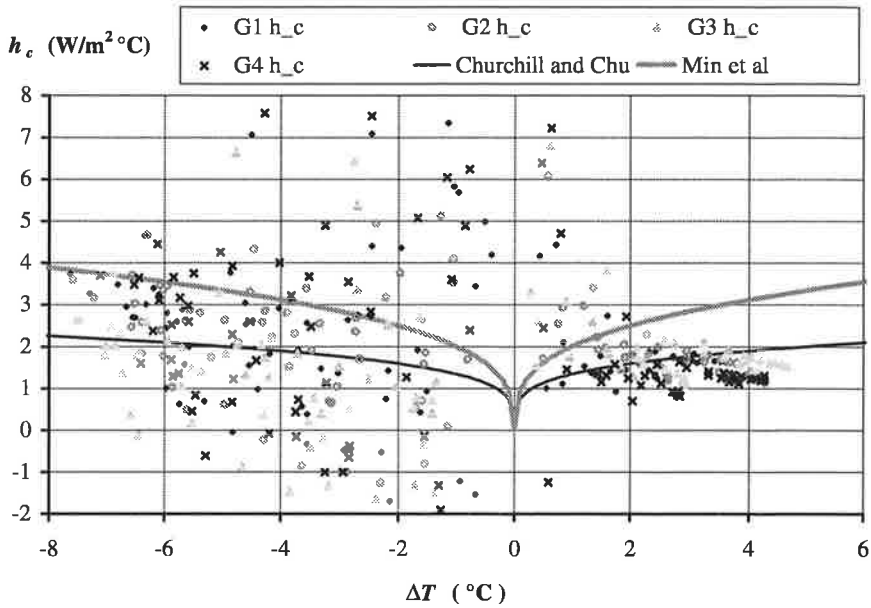

Figure 9.33 *Convective heat transfer coefficient at 3-pane window with radiator below window, 1.0 ach, radiator effect < 5W, 960911 -960917, 30 min average.*

The air temperatures with radiator off and no sunlight, Figure 9.34, show that the convection loop is even more deformed than in the case with 0.5 ach, Figure 9.29.

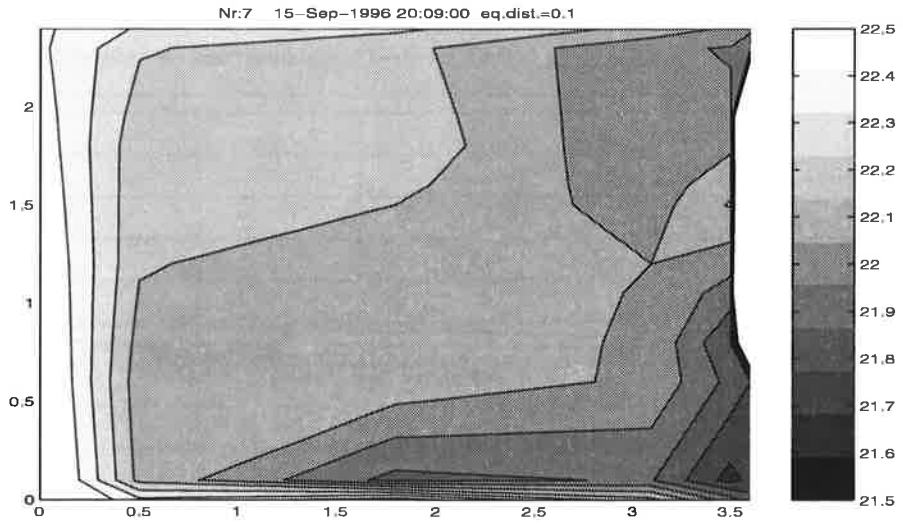

Figure 9.34 *Air temperatures in the room 960915 20.09, radiator effect 0 W, inlet temperature 19.3 °C, outlet temperature 22.0 °C.*

The h_c for VB has been reduced to value of the situation with 0.5 ach, Figure 9.35. VA h_c is about the same as with 0.5 ach. The reason might be that the inlet temperature is only 2 °C below the room temperature here, whereas in the 0.5 ach case the inlet air temperature was 4°C below the room temperature.

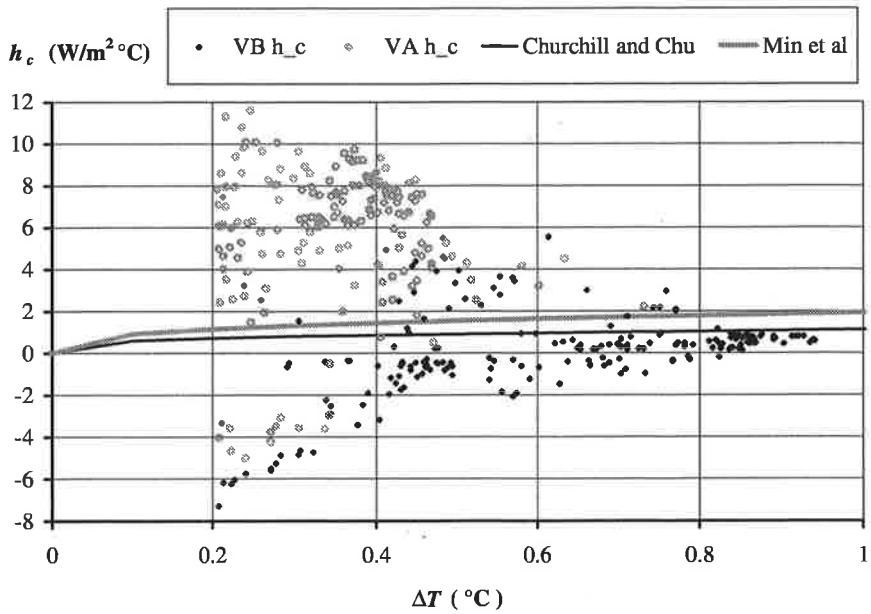

Figure 9.35 *Convective heat transfer coefficient at wall with radiator below window, 1.0 ach, 960911 -960917, 30 min average.*

9.2.4 Ventilation towards window 1.0 air changes per hour

The radiator was below the window with PI-control, the ventilation was 1.0 ach towards the window and the window was of the 4-pane type. The inlet air temperature was ~ 5°C below the room temperature. The maximal 10 min average radiator effect was 240 W.

In this case the difference between radiator on or off was quite small. The dominant effect here was the ventilation. From Figure 9.36 it is clear that $G_1 h_c$ and $G_2 h_c$ for positive ΔT are very much affected by the ventilation. It is quite pointless to look for a temperature dependent variation of h_c here. More surprising is that the air temperatures in Figure 9.37 are so similar to the case without ventilation, see Figure 9.22.

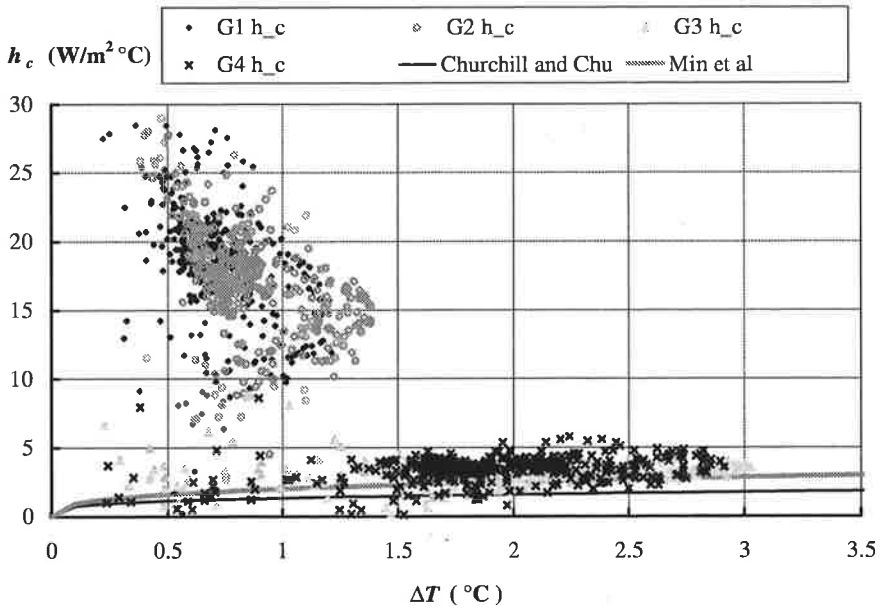

Figure 9.36 *Convective heat transfer coefficient at 4-pane window with radiator below window, 1.0 ach, 940321 -940325, 10 min average. Only values with positive temperature difference.*

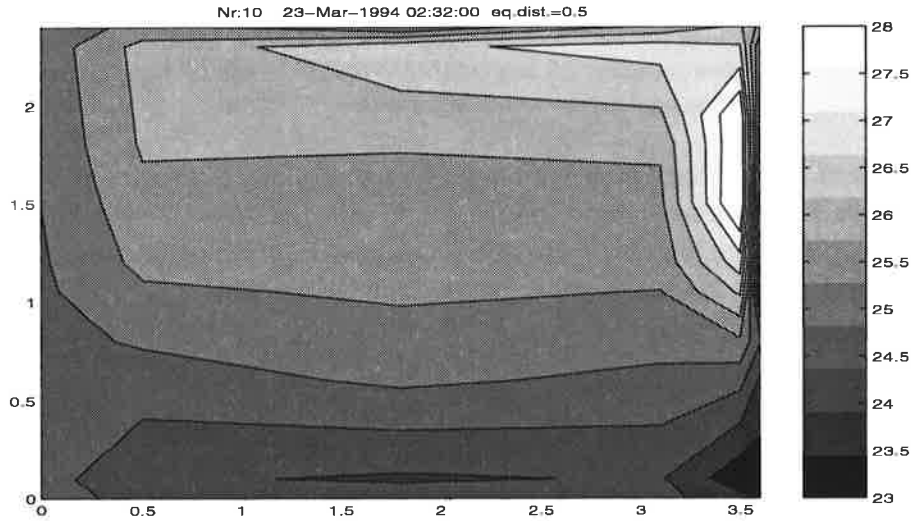

Figure 9.37 *Air temperatures in the room 940323 2:32, radiator effect 240 W, inlet temperature 19.9 °C, outlet temperature 26.0 °C.*

For large negative values of ΔT, i. e. with sun, does the h_c values for the window resemble Min et al. For small negative ΔT the results are as usually not conclusive.

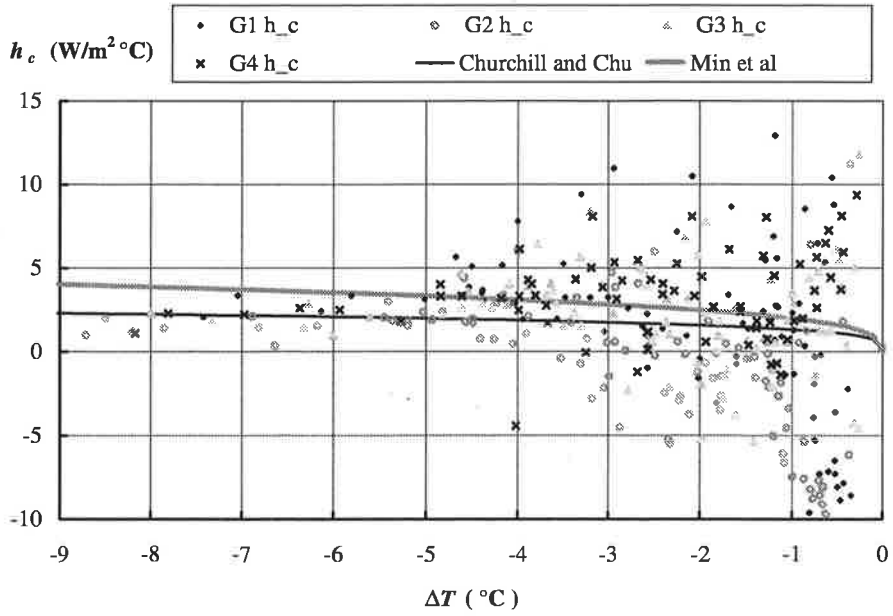

Figure 9.38 *Convective heat transfer coefficient at 4-pane window with radiator below window, 1.0 ach, 940321 -940325, 10 min average. Only values with negative temperature difference.*

The wall h_c with ventilation 1 ach towards the window, The values in Figure 9.39 are much the same as the in Figure 9.35 with 1 ach *from* the window. For VA the values are high and seem almost independent of the temperature difference and for VB the values are similar to Churchill and Chu.

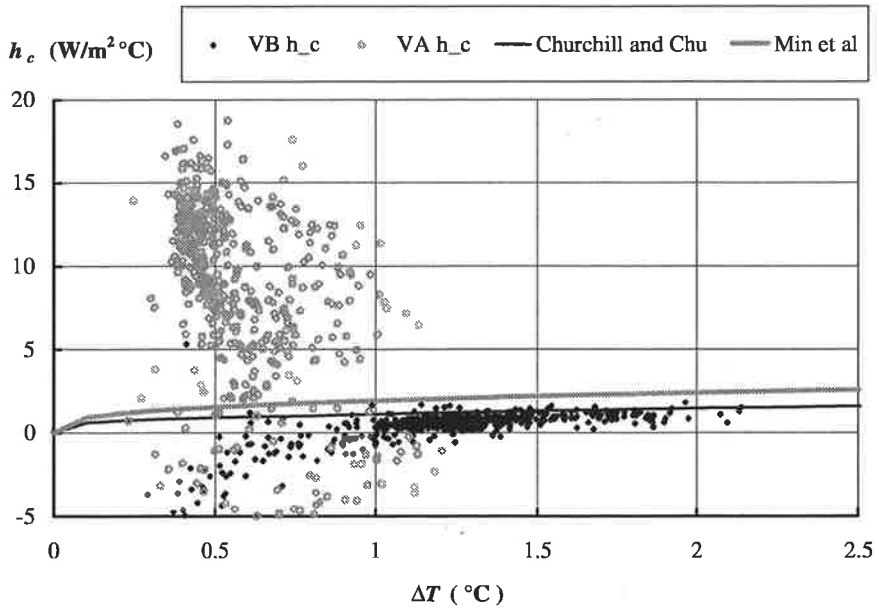

Figure 9.39 *Convective heat transfer coefficient at the wall with radiator below window, 1.0 ach, 940321 -940325, 10 min average.*

9.3 Summary of results from convective heat transfer measurements

The results presented in the previous section show that the importance of the ventilation design and position of radiator. The results a tentatively summarized in Table 9.1. The results are presented as a quotient of measured results to the function of Churchill and Chu.

$$f = \frac{\text{measured } h_c}{\text{Churchill and Chu } h_c} \quad (-) \qquad (9.2)$$

This gives at least a rough idea of how the convective heat transfer coefficients vary with temperature. For the window, the match between measurements and formula was much better when the reference temperature was chosen as the air temperature close to the window. For energy and comfort calculations this temperature is however not known.

Table 9.1 *The quotient, f, from (9.2) for the different tested situations, ↓ = ventilation from window, ↑ = ventilation towards window. Numbers in parenthesis mean that no temperature dependence could be established and that the absolute number should be used for h_c (W/m^2K).*

Radiator position	**Vent.**	**Nr. of panes**	**Window $\Delta T > 0$**	**Window $\Delta T < 0$**	**Wall high**	**Wall middle**
	ach (↓↑)		*f rad on/radoff*	*f*	*f*	*f*
back	off	3	1	2	2	1.3
back (big)	off	3	1.5/0.9	-	(5)	(3)
back	off	4	1.4	-	1.7	1.4
back	0.5 ↓	3	0.8	-	1.7	0.2
back	1.0 ↓	4	0.5	1	(-1)	(-1)
back	1.0 ↑	4	2	-	0.9	0.9
window	off	3	2.5 / 0.7	-	(4)	0.5
window	0.5 ↓	3	3 /0.7	2	(10)	0.6
window	1.0 ↓	3	2.5/0.7	1.4	(8)	0.8
window	1.0 ↑	4	(15)	1	(10)	0.9

9.4 Generalized values

It is not easy to recommend values to use based on this study. Only one room geometry and 4 ventilation situations were tested. Due to the low temperature difference between surface to air the accuracy of the measurement, in most cases, were no better than 30%. On the other hand were many tests under different realistic situations performed. One should also bear in mind that the tested room was empty of obstacles. The convection loops were only disturbed by the ventilation. In a room with furniture the convection loops will also be disturbed.

Having said this, if the values *should* be generalized , we suggest that the results from the situations with 0.5 or 1.0 ach from the window should be used if nothing else is known. This means for the radiator at the back wall: f=0.7 for the window and f=1 for the wall. For radiator below window: f=2.5 for the

window with the radiator power on and f=0.7 with radiator off and f=0.7 for the wall. For buildings with room height much above 2.5 m the results cannot directly be used.

When calculating comfort it usually better to underestimate the heat transfer coefficient. When calculating energy the opposite is true.

9.5 Heat balance for the inner pane

The heat flow balance for the inner pane in the 3- and 4-pane window is shown in Figure 9.40 and Figure 9.41 together with the pane temperatures. The heat flow balance is defined here as positive for energy received by the pane. The outer pane is number 1. The temperature at pane nr 3 in the 4-pane window is not measured. This pane was in the middle of the insulated glass unit. This temperature was however dynamically estimated based on solar absorption and the temperature history of the other panes.

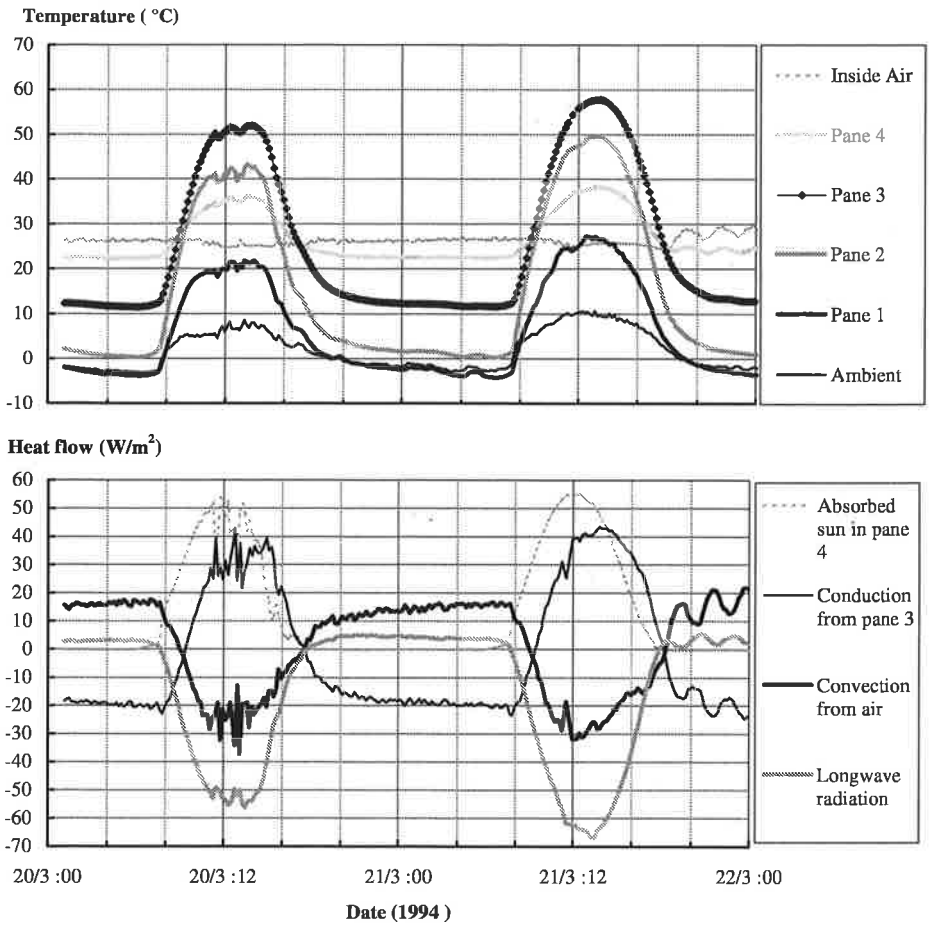

Figure 9.40 Temperatures and heat flows in the four pane window 940322-21

The temperatures of the window panes during the two days shown in Figure 9.40 vary between 0 °C and 58 °C. The set temperature for radiator was 25°C for this period. The global solar radiation on the façade was 880 W/m^2 at noon. The figure clearly shows the difficulty of determining the convective heat transfer when the window is exposed to sunlight. The convective heat transfer is the difference between large numbers (noon the 21/3):

0	=	-30	+	55	+	40	-	65	(W/m^2)
		Convection from air		Absorbed sun in pane		Conduction from pane 3		Longwave radiation to room	

Figure 9.41 shows the a day with 660 W/m^2 on the facade with the 3-pane window.

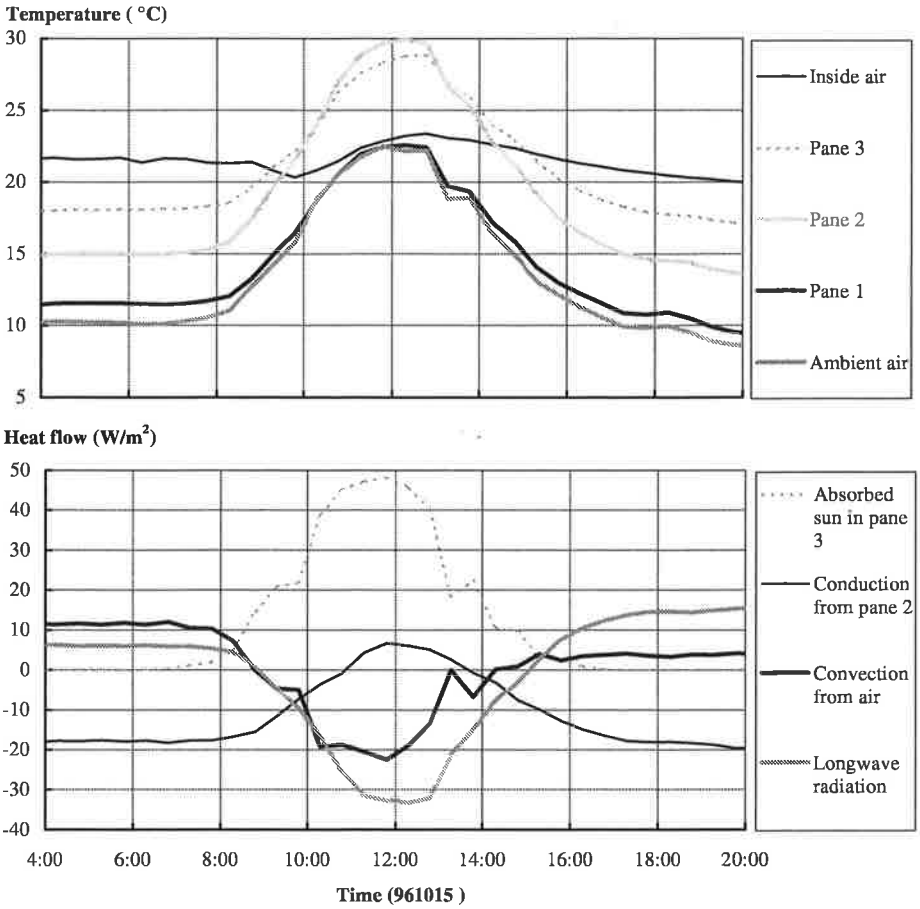

Figure 9.41 Temperatures and heat flows in the three pane window 961015.

The temperature difference in the window is less dramatic than in the previous case 10°C -30°C. The heat balance for the inner pane at noon is here:

0	=	-19	+	46	+	6	-	33 (W/m^2)
		Convection from air		Absorbed sun in pane		Conduction from pane 3		Longwave radiation to room

10 Conclusion

The aim of this study was to investigate the detailed energy transfer at an ambient wall including window. The investigation included both theoretic analysis and measurements performed under conditions close to the real situation with for example ambient climate.

10.1 Measurement and calculation techniques

From the verification of the experiment the following conclusions were drawn:

- It is possible to measure the continuous heat flow through a window from temperature sensors and solar radiation measurements. The accuracy at least for low angles of incidence of the solar radiation was estimated to +/- 10%

- Care must be taken when using measurements from a heat flow meter mounted on the inner gypsum board to verify a thermal model for a wall. Calculations showed that for a temperature variation on an inner surface with a period of 100 min or less, the heat flow meter reports 20% more heat flow variation than is transferred into the gypsum board. Even for a temperature variation of 18 h on the inner surface the heat flow meter reports 10% more heat flow variation than is transferred to the gypsum board.

- The absorption of solar radiation on the thin thermocouples (0.08 mm) glued to the window pane beneath a microscope cover glass was not a problem.

- To measure air temperatures in sunlit places thin (0.08 mm in this case) stripped thermocouples are the only alternative. With the thin thermocouples the measurement error was estimated to less than 0.5°C when exposed to 400 W/m^2 of solar radiation.

- When calculating the longwave radiation exchange in a room based on surface measurements care must be taken to have enough temperature sensors spread out in the room. In this study problems were noticed when the only floor thermocouple was sunlit and when the wall sensors were close to the radiator.

- The one-dimensional finite difference model for the heat transfer through the wall was acceptable. It was possible to calculate the heat flow through a wall from temperature sensors but some problems were noticed when the room was heated by a radiator making the surface temperature slowly increase 6°C.

- The one-dimensional dynamic heat transfer model for the window which included shortwave radiation was fairly good except for small temperature differences and high angles of incidence for solar radiation.

10.2 Conclusions about the convective heat transfer coefficient

Conclusions for the convective heat transfer coefficient were:

- It is possible to continuously measure the convective heat transfer coefficient on the inner surface of a wall or a window. The accuracy is not very good: at best +/-15% for the window and +/- 20% for the wall. Even with this low accuracy the effect of different heating and ventilation strategies on the inside could clearly be detected.

- The presented results show that the importance of the ventilation design and the position of the radiator is crucial. Local convective heat transfer coefficients can be more than 10 times the expected, due to ventilation or position of the radiator.

- It is not obvious how the results of this study should be generalized. But as a rough estimate, we suggest that the following formulae can be used:

$$h_c = f \cdot \begin{cases} 1.34(\Delta T / H)^{1/4} & \Delta T H^3 < 9.5\,\mathrm{m^3K} \\ 1.33\Delta T^{1/3} - 0.474 / H & \Delta T H^3 > 9.5\,\mathrm{m^3K} \end{cases}$$

h_c = the convective heat transfer coefficient ($W/m^2°C$)
ΔT = temperature difference between surface and air (°C)
H = height of the wall or window (m)

Radiator at back wall: f=0.7 for the window and f=1 for the wall.

Radiator below window: f=2.5 for the window with the radiator power on and f=0.7 with the radiator off and f=0.7 for the wall.

10.3 Future studies

With the already measured data comfort calculations will be performed. The importance of low U-value windows and comfort will be studied. The experimental setup also allows total heat transfer coefficients to be estimated with a furnished and occupied room.

The presented method was not entirely satisfying due to the low accuracy. Future studies will be focused on investigating the Mayer ladder technique, or more precisely to measure the temperature difference very close to a surface with thermocouple pairs in series. This study suggests that the measurement error of that type of technique could be less than 10% in the convective heat flow.

References

Arasteh, D., K., Reilly, M., S., and Rubin , M., D., A Versatile Procedure for Calculating Heat Transfer through Windows, *ASHRAE Trans.* Vol. 95, pp 755-756, 1989.

Anderlind G., *Dynamic Thermal Models Two dynamic models for estmating thermal resistance and heat capacity from in situ measurements*, Report A16:1996 ; Swedish Council for Building Research, ISBN 91-540-5767-1, Sweden, 1996.

Almadari F. and Hammond G. P., Improved data correlations for buoyancy-driven convection in rooms, *Building Services Engineering Research & Technology*, Vol.4, No. 3, 1983.

Blomberg, T., *Heat conduction in two and three dimensions, Computer modelling of building physics applications*, Dep. of Building Physics, Lund Institute of Technology, Report TVBH-1008, ISBN 91-88722-05-8, Lund Sweden, 1996.

Bejan, A., *Heat transfer*, Wiley & Sons, New York, USA, ISBN 0-471-50290-1, 1993.

Curchill S. W. and Chu H. S, Correlation equations for laminar and turbulent free convection from a vertical plate, *Int. J. Heat. Mass Transfer*, Vol. 18, pp. 1323-1329, 1975.

Curcija D., *Three-dimensional finite element model of overall, night time heat transfer through fenestration systems*, Dep. of Mechanical Engineering, Univer. of Massachuusetts, Thesis, 1992.

Delaforce, S. R., Hitchin E. R., Watson D. M. T., Convective Heat Transfer at Internal Surfaces, *Building and Environment*, Vol. 28, No. 2, pp 211-220, 1993.

ElSherbiny, S. M., Raithby, G. D. and Hollands, K. G. T., Heat Transfer by Natural Convection Across Vertical and Inclined Air Layers, *ASME Transactions,* Vol. 104, February, p.96, 1982.

Gross U., Spindler K. ans Hahne E., Shapefactor-equations for radiation heat transfer between plane rectangular surfaces of arbitrary position and size with parallel boundaries, *Letters in heat and mass transfer*, Vol. 8, pp 219-227, 1981.

Hatton, A. and Awbi, H. B., Convective heat transfer in rooms, *Building Simulartion '95, Fourth Int. Conf., Proceedings*, Madison Wisconsin, USA, 1995.

Håkansson, H. *Instrument for measuring the U-value of buildings*, Dep. of Building Physics, Lund Institute of Technology, TVBH-5020, Lund, Sweden, 1984, Master Thesis. (in Swedish).

Källblad, Kurt, *Thermal Models of Buildings, Determination of Temperatures, Heating and Cooling Loads. Theories, Models and Computer Programs.* Lund Institute of Technology, Dep. of Building Science, ISSN 1103-4467, ISRN LUTADL/TABK—1015—SE, 1998, Lund Sweden. (thesis)

Khalifa A. J. N., Marshall R. H., Validation of heat transfer coefficients on interior building surfaces using real-sized indoor test cell, *Int. J. of Heat and Mass Transfer*, Vol 33, No. 10, pp 2219-2236, (1990).

Klems, J.H, and Reilly, S., Window Nighttime U-values: A Comparison between Computer Calculations and MoWiTT Measurements, *Proceedings from ASHRAE winter meeting, Atlanta GA, February 11-14*, 1990.

Lindfors A, Christoffersson A., Model Based Frequency Domain Estimation of the Thermal Properties of Building Insulation, *J. Thermal Insul. and Bldg. Envs.*, Vol. 18, pp 229-260, 1995.

Min T. C. et al, Natural Convection and Radiation in a Panel heated Room, *ASHRAE Transactions* 62, 337-358, 1956.

McAdams W. H., *Heat Transmission*, McGraw-Hill, New-York, 3rd edn.,1954.

Mayer, E., Measurement of the convective surface coefficient of heat transfer of man, *Room Vent 87,* session 2b june 10th, Stockholm, Sweden, 1987.

Peng, S. and Peterson F., Convection from a cold window with simulated floor heating by means of transiently heated flat unit., *Energy and Buildings*, Vol 23., pp 95-103, 1995.

Roos, A., Optical characterization of coated glazings at oblique angles of incidence: measurements versus model calculations. *Journal of Non-Crystalline Solids*, 218, pp 247-255, 1997.

Siegel R. and Howell J.R., *Thermal radiation heat transfer,* Hemisphere Publishing Corp., ISBN 0-07-057316-6, 1981.

Shapiro, M. M., El Diasty Ramy, Fazio Paul, Transient Three-dimensional Window Thermal Effects, *Energy and Buildings*, Nr. 10, pp 89-98, 1987.

Wall, M., *Glazed courtyard at Tärnan, Thermal performance of the courtyard and surrounding residential buildings Measurements and calculations,* Swedish Council for Building Research, D7:91992, ISBN-91-540-5428-9, Sweden, 1992.

Wright, J. L. and Sullivan, H., F., A two dimensional numerical model for glazing system thermal analysis, *ASHRAE Transactions Symposia* pp 819-83, 1995.

Wright, J, L., A Correlation to Quantify Convective Heat Transfer Between Vertical Window Glazings, *ASHRAE Transaction Symposia,* pp 940-946, 1996.

Yuan X., Huber A., Schaelin A., Hachman P. and Moser A., New wall functions for numerical simulation of air flow pattern in rooms, *Roomvent 92, Air distribution in Rooms*, Third International Conference, Aalborg, Denmark, 1992.

ISSN 1103-4467
ISRN LUTADL/TABK--3051--SE